Die approbierte Originalversion dieser Diplom-/Masterarbeit ist an der Hauptbibliothek der Technischen Universität Wien aufgestellt (http://www.ub.tuwien.ac.at).

The approved original version of this diploma or master thesis is available at the main library of the Vienna University of Technology (http://www.ub.tuwien.ac.at/englweb/).

Unterschrift des Betreuers

TECHNISCHE UNIVERSITÄT WIEN

VIENNA UNIVERSITY OF TECHNOLOGY

DIPLOMARBEIT

SIMULATION OF POLARIZATION MODE AND CHROMATIC DISPERSION IN PHASE CODING QUANTUM CRYPTOGRAPHY

Ausgeführt am Institut für
Austrian Institute of Technology - AIT
und
Atominstitut der Österreichischen Universitäten
der Technischen Universität Wien

unter Anleitung von Univ.Doz. Dipl.-Ing. Dr.techn. Martin Suda

durch

Osman Akcatepe

Adelbert Stifterstrasse 12/28
1200 Wien
masterofalgebra@hotmail.com

11.08.2009

Unterschrift

Abstract

We present the analysis of the polarization mode dispersion and the chromatic dispersion for the quantum cryptography on the phase coding method in a double Mach-Zehnder interferometry set-up, through some crucial examples of simulations. In this interferometric set-up system, communication is provided through fiber optics. Because of unavoidableness of dispersion appearances in fiber optics in real life, they should be handled with in optimum way. Examples show that how polarization mode dispersion and chromatic dispersion arise in optic systems, in which cases they should be most correlated.

Kurzfassung

"Simulation des Einflusses der Polarisationsmodendispersion und der chromatischen Dispersion auf die photonischen Zustände bei der Phasenkodierung in der Quantenkryptographie"

Im Zusammenhang mit der quantenkryptographischen Phasenkodierung bei einer Anordnung zweier Mach-Zehnder Interferometer, die aus monomoden Glasfasern bestehen, wird eine Analyse sowohl der Orts- als auch der Impulsspektren hinsichtlich des Einflusses der Polarisationsmodendispersion (PMD) als auch der chromatischen Dispersion (CD) durchgeführt. PMD und CD wird in dieser Arbeit erklärt und diskutiert und ein mathematisches Simulationsmodell aufgestellt. Wegen solcher unvermeidbarer Dispersionseinflüsse ist eine derartige Untersuchung mit Hilfe eines MATLAB - Simulationsprogramms von großem Wert, was an einer Reihe von Beispielen demonstriert wird.

Acknowledgements

Foremost, I would like to thank my God, Allah, Who granted me whatever I possess without any repaying, even this diploma thesis.

Secondly, I am deeply grateful to my supervisor Martin Suda, who is principle scientist in Austrian Institute of Technology and professor in Vienna University of Technology as well as in Atomic Institute of the Austrian Universities. I improved my skills and benefited from his lectures, manuscripts, guidance and friendliness. He was extreme patient against my questions. His stimulating suggestions helped me in all the time of research for and writing this thesis.

I have furthermore to thank the former University of Vienna, current AIT research member Andreas Poppe, who has provided the first opportunity to initialize this thesis. I'd like to thank also another member of AIT, Momchil Peev, who was very helpful to me to gather this work.

My special thanks are toward my lovely father, mother and dear brother, who supported me during thesis as every time.

Contents

Introduction vii

Chapter 1: Motivation 1

A. Notation 1

B. Single-Mode Fibers 2

C. Mach-Zehnder Interferometer (Double) and Phase Coding 3

Chapter 2: Chromatic Dispersion 5

A. Dispersion Concept and Its Types 5

B. Chromatic Dispersion 9

Chapter 3: Polarization Mode Dispersion 16

A. Polarization of Light 16

B. What is Polarization? 17

C. Polarization Ellipse 18

D. Linearly Polarized Light 19

E. Circularly Polarized Light 19

F. Polarization and Polarization-Maintining Fibers 20

G. PMD and DGD 20

H. PMD Coefficient in Terms of Ordering 24

I. From PMD Cable to PMD Distance 26

J. PMD Link Design Value 26

K. PMD of Optical Devices 27

L. The Measurement of PMD 27

M. Time-Domain Representation and Other Representations 27

N. Summary and Outlook 28

Chapter 4: Comparison of Both Dispersions 29

Chapter 5: Calculations and Simulations on Polarization Mode Dispersion and Chromatic Dispersion 30

A. Determination of CD and PMD Parameters from Spectra Equations 30

B. Demonstration of CD and PMD Impacts into Position and Wavelength Spectra 33

Example 1.1.1 34

Example 1.1.2 39

Example 1.1.3 42

Example 1.2 45

Example 1.3 47

Example 2.1 50
Example 2.2 53

C. Results and Discussion 56

Chapter 6: Summary and Conclusion 59

Appendix: Main Parts of MATLAB GUI Source Code 60

Bibliography 69

Introduction

Today's one of the most crucial phenomenon is perhaps information. And this phenomenon's one of the most important component is its delivery, its transfer. Since 1960s, optical fibers have been fulfilling this task by an increasing significance. They are still being utilized as the most efficient media in order to convey the information in the world. Of course, everything encounters some problems in the development duration to be overcome. Optical fibers have been also encountering such problems due to environmental, structural, infrastructural conditions, such as **chromatic dispersion and polarization mode dispersion**. Handling with these problems come into prominence, individually if the topic would become information security, which must be provided through transmission process in optical fibers. Here, quantum cryptography comes into the scene.

Quantum cryptography (or quantum key distribution) has become an information security task to reach the niveau of mature technology, already convenient for commercialization. It aims at the creation of a secret key between authorized partners –these partners are going to be Alice and Bob in this thesis, who have been symbolized for exchanging encrypted and/or decrypted data in cryptography field usually- connected by a quantum channel and a classical authenticated channel. The security of the key can in principle be guaranteed without putting any restriction on the eavesdropper's power.

What we are going to investigate in general meaning is after giving background regarding relevant topic to reveal some calculations on chromatic dispersion and polarization mode dispersion in interferometers that can be established with single-mode optical fiber components for quantum cryptography using phase coding, and then to simulate in order to make them more understandable. Here, on which point to be careful is to record stationary interferences in order to hold the path difference stable, which is a kind of obligation in terms of quantum cryptography. By reason that each arm should be a number of tenth kilometres, holding the path difference is too uneasy.

- Therefore our calculations and simulations are based on 2 unbalanced Mach-Zehnder interferometers, which are connected in series by a single optical fiber. In chapter 1, after some essential definitions, terms, phrases are introduced, we will study characteristics of single-mode optical fibers, which are used for quantum channels and to show dispersion. Another topic is double Mach-Zehnder interferometer concept as a motivation for experimental quantum cryptographic field in order to make this work more profitable. Giving information concerning notation used for the entire thesis would be also very helpful. So, readers could reference notation section anytime in case of need.

- In chapter 2, we introduce the dispersion concept in general meaning, and then types of dispersions. After that, origin of chromatic dispersion, its properties, disadvantages, its effects in single-mode fibers. Is it compensatable or non-compensatable, if compensatable, how?... etc.

- Chapter 3 will illuminate polarization mode dispersion. To achieve that, we will need some introductory information such as what polarization is and then polarization types. Next, PMD will be given as well as its types in terms of 1st and 2nd order.

- In chapter 4, we compare the polarization mode dispersion and the chromatic dispersion. What are their advantages upon each other, which one is easier to overcome?... etc.

- In chapter 5, we will study some calculations concerning both kind of dispersions together and some characteristic simulations will be demonstrated.

- Chapter 6 will be the conclusion part of the thesis. We will summarize the important and difficult problems of impacts of polarization mode dispersion and chromatic dispersion in quantum cryptography, where the emphasis is more on the diversity of the issues than on formal details. Some futuristic views will be presented as well. The different parts of this thesis are written as much as possible in such a way that they can be read independently.

- In the Appendix: Source code (about 1500 lines) will be released which was developed for the simulation of CD and PMD in phase coding quantum cryptography to whom may want to implement examples based on the calculations in this thesis. To make the thesis not unnecessarily long, resembling parts of the source code have been skipped. They can be easily added to code by copying similar parts and then changing relevant names and words. In case of information need about code, please contact the author.

Chapter 1

Motivation

A. Notation
B. Single-Mode Fibers
C. Mach-Zehnder Interferometer (Double) and Phase Coding

A. Notation

Here we present a notation packet to be helpful, so that readers could refer it whenever they need.

λ: Wavelength. We will see that many quantities depend on this parameter.

λ_0: Mean wavelength.

υ: Group velocity is very important that affects pulse propagation in fiber glass, which is also to be examined whether it is dependent on the wavelength.

c_0: Speed of light in vacuum.

n: Refractive index. Note that $n = n(\lambda)$.

N: Group index. Sometimes it is "called group velocity index" and $N = N(\lambda)$.

$\Delta\tau$: PMD delay in picosecond (ps, one trillionth of a second).

T_{Bit}: Bit length.

l_i: Fiber length.

D_{λ_0}: Coefficient of CD.

D_{PMD}: Coefficient of PMD.

i = c, d, g, m, n: Indices for optical fibers.

a_i: Absorption factors.

P_i: Phase factors.

Δ_i: Phase shifts.

T_i: Transmission coefficients.

ε: Parameter for PMD.

κ : Parameter for CD.

σ_λ : Spectral width.

$\mathcal{E}(\mathbf{r}, t)$: Electric field vector.

$\delta\tau$: Differential group delay.

$\vec{\tau}_w$: PMD vector.

B. Single-Mode Fibers

The first propose to utilize small core optical fibers for high-capacity communications belongs to Kao and Hockham [1]. In most transmission systems single-mode fibers are very common currently.

Light travels in optical fibers due to the refractive index parameter n along the section of the fibers. For several years, many studies have been made to lower transmission penalty. At the beginning, it was a couple of dB in a kilometer, but today the attenuation is as low as 2 dB/km at 800-nm wavelength, 0.35 dB/km at 1310 nm, and 0.2 dB/km at 1550 nm. Therefore, an affirmative hit corresponds to a potential well in the refractive index. The section of the well is called the fiber core. If the core is vast, there are many layer modes in the fiber, corresponding to many guided modes. Such fibers are called multimode fibers, They usually have cores 50 μm in diameter.

The modes couple slighty, acting on the qubit like a non-isolated environment. Hence, multimode fibers are not convenient as quantum channels. Despite the fact this situation, if, the core is sufficiently narrow according to diameter in the unit wavelength, then a single spatial mode is delivered. These media are called **single-mode fibers**. The diameter of the single-mode fibers' core is generally 8 μm for the common transmission wavelengths 1.3 μm or 1.5 μm. Single-mode fibers are pretty fit to convey single quanta. For example, the optical phase at the output of a fiber is in a stable balance with the phase at the input, didn't make the fiber extended. Hence, fiber interferometers are convenient enough that became prevalent for a lot of optical devices.

Thus, a single-mode fiber with flawless geometry would oversupply a fit quantum channel. Unfortunately in real life, it is impossible to provide perfect symmetric fibers, that have the two polarization modes are no longer degenerate, but rather each mode has its own propagation constant. A cause also for this situation is birefringence. A well-known sample of this is calcite crystal, where it is possible to see the different paths if the crystal is placed on an image and then rotated [2].

Birefringence is in optical fibers a default of fiber material, where the effective index of refraction varies with the polarization state of the input light. The main causes of this birefringence are non-perfect concentricity and inhomogeneity of the optical fiber in manufacturing design, as well as external stresses applied on the fiber cabling, such as bends, or twist, see Figure 1. An analogous cause for that is chromatic dispersion, in which the group delay depends on the wavelength [3].

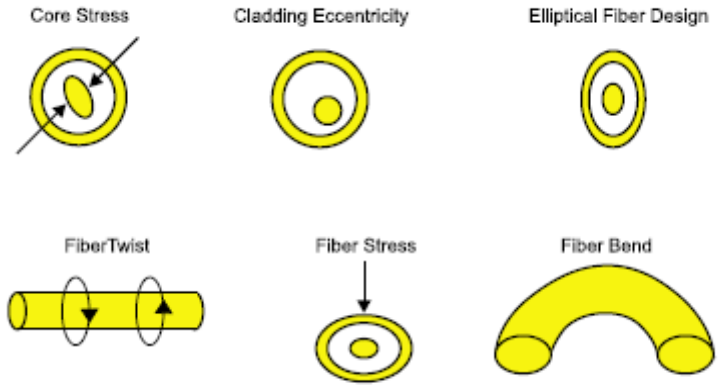

Figure 1: Main causes for birefringence are imperfect fiber design and external stress through a cross-section view.

There are numerous advantages of using single-mode fibers in lightwave communication systems. We can compile them as following:

- The modes of a multimode fiber travel at different group velocities so that a short-duration pulse of multimode light suffers a range of delays and therefore spreads in time. Besides that, in a single-mode fiber, there is only one mode with one group velocity, so that a short pulse of light arrives without delay distortion. Pulse spreading in single-mode fibers does result from other dispersive mechanisms, but these are significantly lower than modal dispersion.
- Moreover, the amount of power attenuation is smaller in a single-mode fiber than in a multimode fiber. This situation allows in a substantial manner higher data rates to be transmitted over single-mode fibers than over multimode fibers along with the smaller rate of pulse spreading.
- Another difficulty with multimode fibers stems from the random interference of the modes. Because of unmastered imperfections, strains and temperature variations, each mode suffers a random phase shift so that the sum of the complex amplitudes of the modes exhibits an intensity that is random in time and space. This phenomenon is known as modal noise or speckle. This effect is similar to the fading of radio signals resulting from multiple-path transmission. By reason that there is a single path in a single-mode fiber, there is no modal noise.
- As a result of their small size and small numerical apertures, single-mode fibers are more useful with integrated-optics technology. But these features make single-mode fibers more costly to manufacture [4].

B. Mach-Zehnder Interferometer and Phase Coding

In chapter 5, we will study some models and simulations which are based on the result data of a 2 unbalanced Mach-Zehnder interformeters (MZ) set-up for quantum cryptography, implemented by M. Suda et al. [5,6].

Phase coding method in quantum cryptography is something, which makes the optic play a crucial role. Application and use of system are therefore applied with interferometers, which can be realized with single-mode optical fiber components. Consequently, phase modulators are placed in each arm of the 2 MZ.

These 2 MZ are connected one after another by a single-mode optical fiber (fiber g), see Figure 2. The first MZ indicates Alice (A) and the second indicates Bob (B). One pulse is input (input a) by Alice and decomposed into two. The two pulses is guided in series through the fiber g. The following short path is indicated by S and the following long path is indicated by L. If the path distances are different in both MZ, four pulses occur after passing through 2. MZ. But if the path distances aren't different, just 3 pulses occur. So, there are four possible ways to follow: SS (short-short), LL (long-long), SL (short-long) and LS (long-short). SS and LL are not fit, when they don't show any interference. For the SL and LS possibilities, the middle higher pulse refers to interference and hence the behaviour of indistinguishableness.

The determination of the phase shifts between A and B corresponds to encoding-decoding. We mention this topic shortly in the following subsection. Note that the path distances in each interferometer should be smaller than the path g. Because both positions of the photons could be affected by environmental perturbations. Here, as a result of these perturbations, chromatic dispersion (CD) and polarization mode dispersion (PMD) come into the scene, that we have to handle with them seriously. Because they intervene pulses like displacing or enlarging peaks. And such problems affect our quantum channel in negative manner [6].

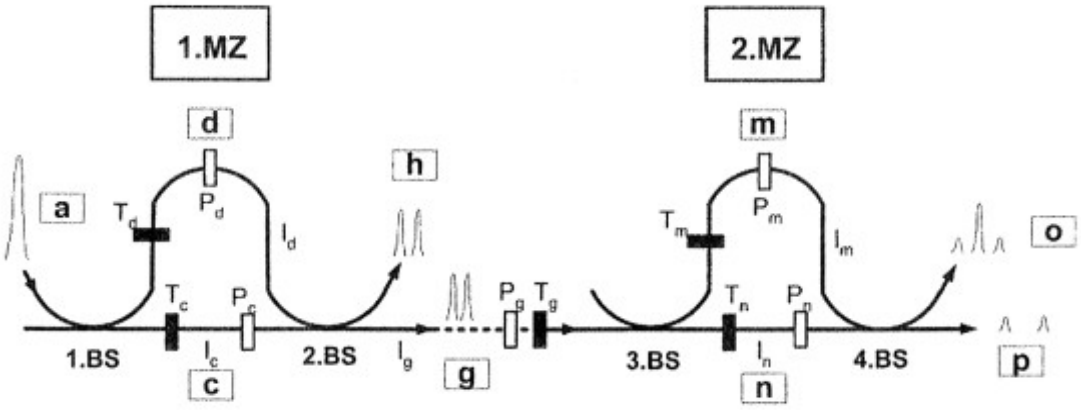

Figure 2: Two MZ interferometers in series: 1 input a, 3 outputs h, o, p, 4 beam splitters (BS), 5 optical optical fibers (i = c, d, g, m, n), fiber lengths l_i , phase factors P_i =exp{ $\iota . k . l_i . \Delta_i$ }, Δ_i are phase shifters, transmission coefficients T_i =exp{ $-2 . l_i . a_i$ } (a_i are absorption factors); position distributions (or time pulses) are drawn.

Chapter 2

Chromatic Dispersion

A. Dispersion Concept and Its Types

I. What is Dispersion?
II. Types of Dispersion
III. Modal Dispersion
IV. Material Dispersion
V. Waveguide Dispersion
VI. Nonlinear Dispersion
VII. A Remark for Dispersion, CD and PMD

B. Chromatic Dispersion

I. Parametric Elements of Chromatic Dispersion
II. Chromatic Dispersion as a Combination of the Material and Waveguide Dispersion
III. Pulse Propagation Undergoing Chromatic Dispersion
IV. Group Velocity
V. Normal and Anomalous Chromatic Dispersion
VI. Summary and Outlook

A. Dispersion Concept and Its Types

I. What is Dispersion?

Dispersion is one of the two performance limiting factors of the optical fiber medium. Other is attenuation so that associated with losses of various kinds, it limits the magnitude of the optical power transmitted, whereas dispersion limits the rate at which data may be transmitted through the fiber, since it governs the temporal spreading of the optical pulses carrying the data.

In fact, dispersion is the time domain spreading or broadening of the transmission signal light pulses as they travel through and because of the dispersive media, the fiber, by a frequency-dependent (and therefore wavelength-dependent) susceptibility. Since the speed of light is variable according to frequency in dispersive media, every frequency component constitutes a short pulse of light, which sustains a different time delay. If the length of propagation is long through the

medium (e.g. light transmission through optical fibers), the pulse is dispersed in time and its width broadens, see Figure 3a and 3b.

Figure 3a: Variation of the signal light pulses.

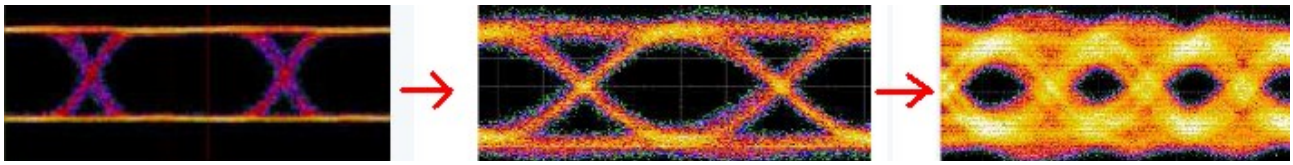

Figure 3b: Change of phases of an optical pulse.

II. Types of dispersion

A short pulse of light becomes **dispersed** with time as it travels through an optical fiber so that the pulse spans into a larger time interval. There are five principal sources of dispersion in optical fibers:

- Modal dispersion
- Material dispersion
- Waveguide dispersion
- Polarization-mode dispersion
- Nonlinear dispersion

As we will see, chromatic dispersion is the combination of material and waveguide dispersion. By reason that our main topics are chromatic dispersion and polarization-mode dispersion, here we will take a look at them just briefly, skip most parts as other dispersion types and leave them next studies.

III. Modal Dispersion

Modal dispersion appears in multimode fibers because of the differences in the group velocities of the different modes. When a single impulse of light introduce in an M-mode fiber at z =0 and then

departs into M pulses whose differential delay ascends as a function of z. For a fiber of length L, the time delays produced through the various velocities are $\tau_q = L/v_q$, $q=1,...,M$, where v_q is the group velocity of mode q. If v_{min} and v_{max} are the smallest and the largest group velocities, respectively, the obtained pulse spreads over a time interval $L/v_{min} - L/v_{max}$. Because of the modes' unequal excitedness, general view of the obtained pulse has a slight envelope, see Figure 4. An estimate of the overall pulse duration (assuming a triangular envelope and using the FWHM definition of the width) is $\sigma_\tau = \frac{1}{2}(L/v_{min} - L/v_{max})$, which symbolizes the modal-dispersion response time of the fiber [4].

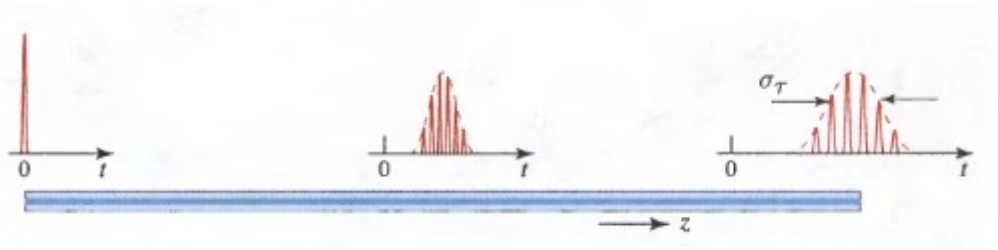

Figure 4: Modal dispersion causes pulse spreading.

IV. Material Dispersion

An optical pulse is delivered, in a dispersive medium (e.g. made of glass) of refractive index n through a group velocity $v = c_o/N$, where $N = n - \lambda_0 dn/d\lambda_0$. By reason that pulse is a wavepacket, including a bundle of constituents of various wavelengths, every travelling at a group velocity, its width spreads. The time duration of an optical impulse of spectral width σ_λ (nm), after passing a length L through dispersive medium, is $\sigma_\tau = |(d/d\lambda_0)(L/v)|\sigma_\lambda = |(d/d\lambda_0)(LN/c_0)|\sigma_\lambda$. This guides to a response time

$$\sigma_\tau = |D_\lambda| \sigma_\lambda L, \qquad (1)$$

where the material dispersion coefficient D_λ is

$$D_\lambda = -\frac{\lambda_0}{c_0}\frac{d^2 n}{d\lambda_0^2}. \qquad (2)$$

The response time rises linearly proportional to the length L. Generally, L is measured in km, σ_τ in ps, and σ_λ nm, so that D_λ has units of ps/km.nm. This type of dispersion is called **material dispersion**.

For a silica-glass fiber at wavelengths smaller that 1300 nm the dispersion coefficient is negative, so that wavepackets of long wavelength travel faster than those of short wavelength, due to the wavelength dependence of the dispersion coefficient D_λ. At a wavelength λ_0 = 870 nm, e.g. the dispersion coefficient D_λ is about -80 ps/km.nm. At λ_0 = 1550 nm, on the other hand, $D_\lambda \approx +17$ ps/km.nm. $\lambda_0 \approx 1312$ nm the dispersion coefficient disappears, so that σ_τ in *(1)* disappears. A more exact estimation for σ_τ that incorporates the dispersion of the spectral width σ_λ about $\lambda_0 = 1312$ gives a very little, but nonzero, width, see Figure 5, [4].

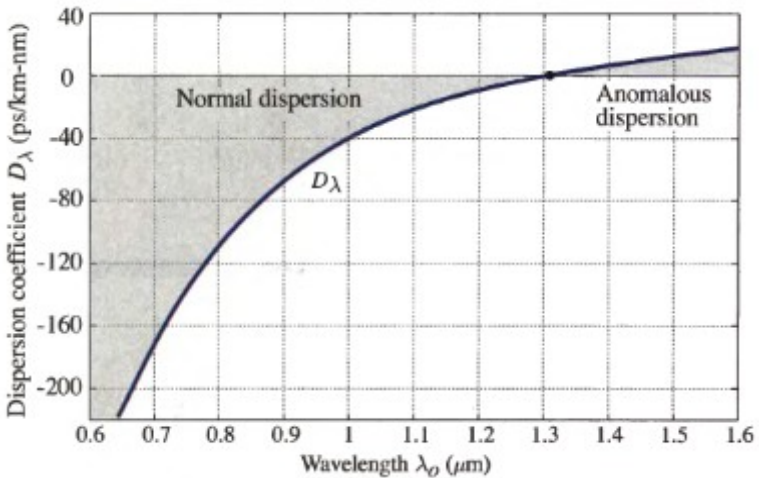

Figure 5: Dispersion coefficient D_λ for a silica-glass fiber as a function of wavelength λ_0 . The result is similar to, but distinct from, that of fused silica.

V. Waveguide Dispersion

Even if material dispersion is ignorable, the group velocities of the modes in a waveguide travels in accordance with the wavelength. This waveguide dispersion is stems from the dependence of the field distribution in the fiber on the ratio of the core radius to the wavelength (a/λ_0). Therefore, in the core and cladding, the relative parts of optical power possess λ_0 dependence. The group velocity of the mode is changed, for the reason that the phase velocities in the core and cladding vary. In case of non-existence of modal dispersion, and at wavelengths for which material dispersion is small (about λ_0 =1300 nm in silica glass), waveguide dispersion is particularly important in single-mode fibers, because it then dominates [4].

VI. Nonlinear Dispersion

As the intensity of light in the core of the fiber is sufficiently high, another dispersion effect arises because the refractive index then starts to depend on intensity and the material demonstrates nonlinear behavior. Because of proportionality of the phase to the refractive index, the high-intensity components of an optical pulse suffer phase shifts different from the low-intensity components, resulting in instantaneous frequencies shifted by different amounts. This nonlinear effect is known as self-phase modulation (SPM), causes to pulse spreading. Under certain conditions, SPM can compensate the group velocity dispersion associated with material dispersion, and the pulse can travel without altering its temporal structure. Such a guided wave is known as a soliton [4].

VII. A Remark For Dispersion, CD and PMD.

All forms of dispersion degrade a light wave signal, reducing the data carrying capacity through pulse-broadening. The dominating dispersion art in the single-mode optical fiber is the chromatic dispersion. It results from the sum of material dispersion and waveguide dispersion, see Figure 6. To the realization of a high bit transmission with 2.5 GBit/s, 10 GBit/s or 40 GBit/s over large distance lengths, it is required to reduce the impulse distribution as a result of chromatic dispersion in the single-mode optical fibers. That becomes by use of an optical fiber possible, whose parameter of chromatic dispersion is small as we will see in chapter 5.

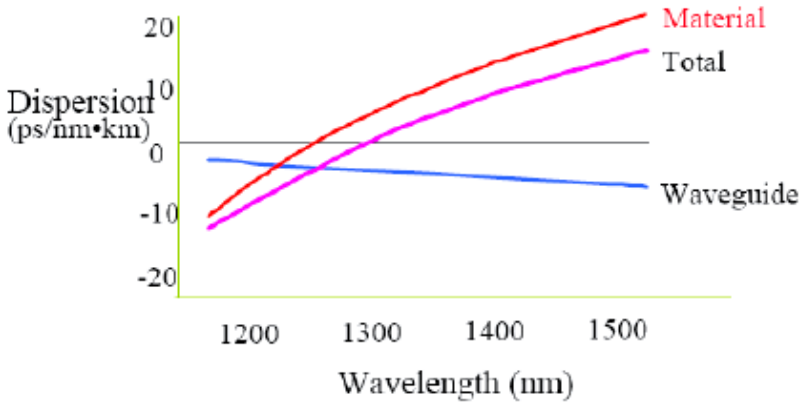

Figure 6: CD's structure in terms of its components, e.g. material dispersion and waveguide dispersion.

A succession for use of an extreme narrow band transmitter is possible only by achieving large bandwidth products in single-mode transmission systems. In order to achieve large bandwidth products, a distributed feedback laser with a dominating single-mode is utilized, whose half-power bandwidth lies in the order of 4-10 nm and rare modes strongly are suppressed, comes for example. Such lasers are used especially in wavelength-division multiplexing (DWDM) systems. In DWDM systems, the case comes along, that the wave lengths of the single transmitter have a slight distance –about ~0,8nm- and may influence itself mutually [7]. The general conditions are selected now so that the chromatic dispersion strongly is suppressed, the effects of the polarization mode dispersion become apparent and considerably can restrict the range of optical transmission distances in high bit rates. In all other use cases, the PMD is clearly smaller than the impulse distribution as a result of chromatic dispersion and consequently negligible.

B. Chromatic Dispersion

Chromatic dispersion is the combination of material dispersion and waveguide dispersion. We may simply review CD as a function of wavelength. It may be determined through comprising the wavelength dependence of the refractive indices, n_1 and n_2 and hence Numerical Aperture ($\sin\theta_\alpha \approx n_0 a\alpha$, a radius, θ_α angle), when finding out $d\beta/d\omega$ from the characteristic equation. Although generally smaller than material dispersion, waveguide dispersion shifts the wavelength at which the total chromatic dispersion is minimum.

I. Parametric Elements of Chromatic Dispersion

The angular dispersion $d\theta_\alpha/d\lambda_0 = (d\theta_\alpha/dn)(dn/d\lambda_0)$ is a product of the material dispersion factor $dn/d\lambda_0$ and a factor $d\theta_\alpha/dn$, which depends on the geometry and refractive index.

The first and second derivatives $dn/d\lambda_0$ and $d^2n/d\lambda_0^2$ govern the effect of material dispersion on pulse propagation. A pulse of light of free-space wavelength λ_0 travels with the group velocity ($v = c_0/N$ and N is group index, $N = n - \lambda_0 dn/d\lambda_0$). The pulse gets broadened at a rate $|D_\lambda|\sigma_\lambda$ seconds per unit distance, because of the dependence of the group velocity itself on the wavelength. Here σ_λ is the spectral width of the light and $D_\lambda = -(\lambda_0/c_0)d^2n/d\lambda_0^2$ is CD coefficient in ps/km-nm (picoseconds of temporal speed per kilometer of optical fiber length per nanometer of spectral width) [4].

II. Chromatic Dispersion as a Combination of the Material and Waveguide Dispersion

The phenomena of the material dispersion and the waveguide dispersion arise, because the characteristic of optical signals that exhibit finite spectral width, and several spectral constituents will be guided at different speeds through the length of the fiber. The refractive index of the fiber core shows different characteristics for different wavelengths and this situation causes that velocity difference. As we saw before, this is the material dispersion, and it is the weighted part of chromatic dispersion in single-mode fibers. Another factor of chromatic dispersion is: The cross-sectional distribution of light within the fiber changes for different wavelengths as well. In the fiber core, the smaller wavelengths are more layered bounded during a bigger part of the optical force at longer wavelengths propagates in the cladding. Since the index of the core is greater than the index of the cladding, this case causes a change in propagation velocity for spatial distribution. And this is the waveguide dispersion, see Figure 7.

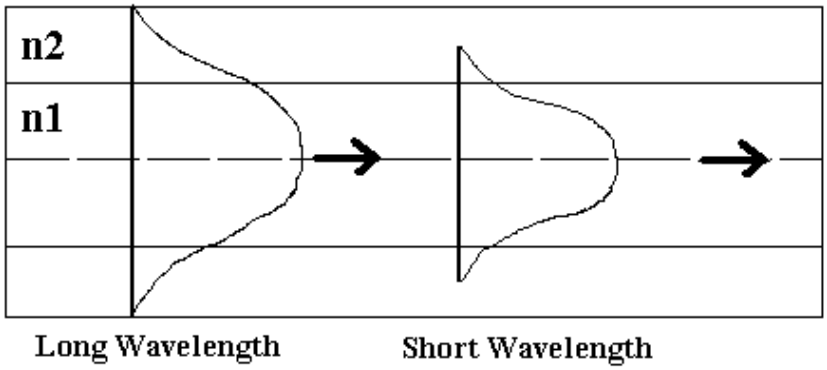

Figure 7: Different wavelengths show different refractive indices.

It is dramatically worth mentioning that chromatic dispersion in a component is significantly different than chromatic dispersion in long length optical fiber. Chromatic dispersion can remain constant over the bandwidth of a communications channel for long lengths of fiber. If it tends to vary, then it varies over the bandwidth of the channel in optical components. As a result, chromatic dispersion is not that sufficient predictor of component performance in a communications system.

Since chromatic dispersion lowers the capacity of single-mode fibers, more developed fiber designs aim at reducing this effect by using graded-index cores through refractive index profiles selected such that the wavelength at which waveguide dispersion is shifted to the wavelength at which the fiber is to be used. Dispersion-shifted fibers have been produced by using a linearly tapered core refractive index and a reduced core radius. This technique can be used to shift the zero-chromatic-dispersion wavelength from 1300 nm to 1550 nm, where the fiber has its most limited situation. However, because of use of dopants, process of index grading itself causes losses. In order to make the chromatic dispersion disappear at two wavelengths and reduce for wavelengths between, other grading profiles have been developed. These fibers, called dispersion-flattened, have been implemented by using a quadruple-clad layered grading [4].

Chromatic dispersion can cause bit errors in digital communications or distortion and a higher noise floor in analog communications. If it would not be determined absolutely and taken into a compensation,it can cause a significant problem in high-bit-rate communications, see Figure 8a, 8b, 8c.

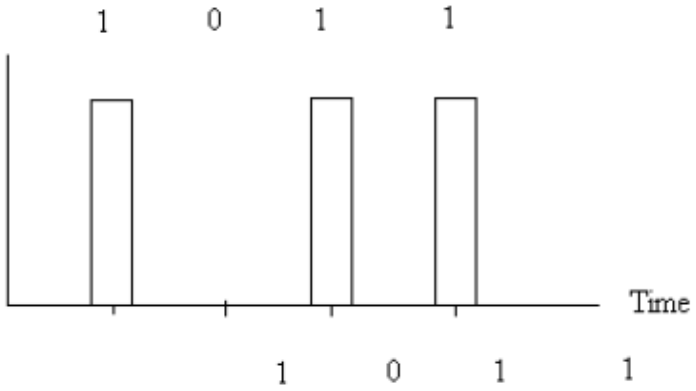

Figure 8a: Broadening of return to zero (RZ) format pulses due to CD.

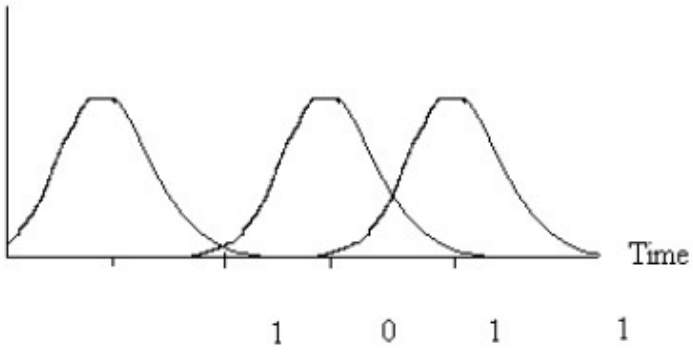

Figure 8b: Distinguishable pulses due to CD.

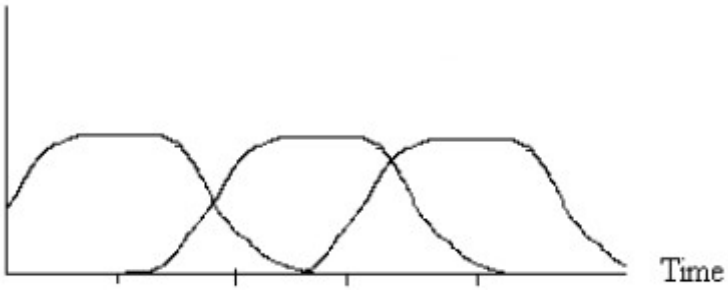

Figure 8c: Indistinguishable pulses due to CD.

III. Pulse Propagation Undergoing Chromatic Dispersion

A dispersion medium consists of refractive index (frequency dependent), absorption coefficient and phase velocity. Consequently, monochromatic waves of different frequencies travel in the medium at different velocities and experience different attenuations. Since a pulse of light includes a sum of many monochromatic waves, each of which is modified differently, the pulse is delayed and broadened; its shape is also altered.

IV. Group Velocity

Let a pulsed plane wave travel in the z direction through a lossless dispersive medium with refractive index n(ω). Assume that the initial complex wavefunction at z=0 is $U(0,t) = \mathcal{A}(t)\exp(j\omega_0 t)$, where ω_0 is the central angular frequency and $\mathcal{A}(t)$ is the complex envelope of the wave. If the dispersion is weak, i.e., if n varies slowly within the spectral bandwidth of the wave, then the complex wavefunction at a distance z is approximately $U(z,t) = \mathcal{A}(t)\exp[j\omega_0(t - z/c)]$, where $c = c_0/n(\omega_0)$ is the speed of light in the medium at the central frequency, and v is the velocity at which the envelope travels, see Figure 9.

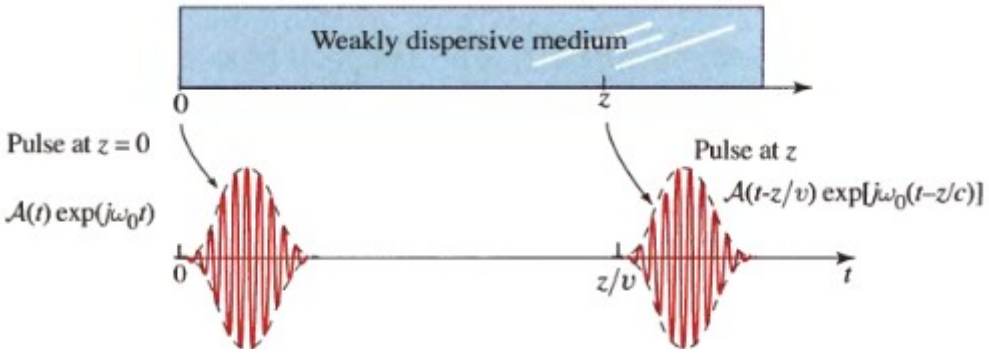

Figure 9: An optical pulse travelling in a dispersive medium that is weak enough so that its group velocity is frequency independent. The envelope with group velocity u, while the underlying wave travels with phase velocity c.

One can get v as group velocity by

$$\frac{1}{v} = \beta' = \frac{d\beta}{d\omega}, \qquad (3)$$

where $\beta = \omega n(\omega)/c_0$ is the frequency-dependent propagation constant and the derivative, which is often denoted β', is evaluated at the central frequency ω_0. The group velocity is a characteristic of the dispersive medium, and generally varies with the central frequency. The corresponding time delay $\tau_d = z/v$ is group delay.

Since the phase factor exp[$j\omega_0(t - z/c)$] is a function of $t - z/c$, the speed of light c, given by $\beta = \omega n(\omega)/c_0$, is often called the phase velocity. In an ideal (nondispersive) medium, $\beta(\omega) = \omega/c$ whereupon $v = c$ and the group and phase velocities are identical.

Since the index of refraction of most materials is typically measured and tabulated as a function of optical wavelength rather than frequency, it is convenient to express the group velocity v in terms of $n(\lambda)$. Using the relations $\beta = \omega n(\lambda_0)/c_0 = 2\pi n(\lambda_0)/\lambda_0$ and $\beta = \omega n(\omega)/c_0$, along with the chain rule $d\beta/d\omega = (d\beta/d\lambda)(d\lambda/d\omega)$, provides

$$v = \frac{c_0}{N}, \qquad N = n - \lambda_0 \frac{dn}{d\lambda_0}, \qquad (4)$$

where N is the group index.

By reason that the group velocity $v = 1/(d\beta/d\omega)$ is itself often frequency dependent, different frequency components of the pulse suffer different delays $\tau_d = z/v$. Consequently, the pulse spreads in time. To estimate the spread with associated dispersive group velocity it suffices to note that, upon travelling a distance z, two identical pulses of central frequencies ν and $\nu + \delta\nu$ undergo

a differential group delay

$$\delta\tau = \frac{d\tau_d}{d\nu}\delta\nu = \frac{d}{d\nu}\left(\frac{z}{v}\right) = D_\nu z\,\delta\nu, \qquad (5)$$

where the quantity

$$D_\nu = \frac{d}{d\nu}\left(\frac{1}{v}\right) = 2\pi\beta'', \qquad (6)$$

is dispersion coefficient and $\beta'' \equiv d^2\beta/d\omega^2$. This effect is actually associated with the higher-order terms in the Taylor series expansion of $\beta(\omega)$ that were neglected in the derivation of the group velocity carried out above.

If the pulse has an initial spectral width σ_ν (Hz), in accordance with *(5)* a good estimate of its temporal spread is then provided by

$$\sigma_\tau = |D_\nu|\sigma_\nu z. \qquad (7)$$

The dispersion coefficient D_ν is a measure of the pulse-time broadening per unit distance per unit spectral width (s/m-Hz). See Figure 10 for this temporal broadening process. If the refractive index is specified in terms of the wavelength, $n(\lambda_0)$, then *(4)* and *(6)* give dispersion coefficient

$$D_\nu = \frac{\lambda_0^3}{c_0^2}\frac{d^2 n}{d\lambda_0^2}. \qquad (8)$$

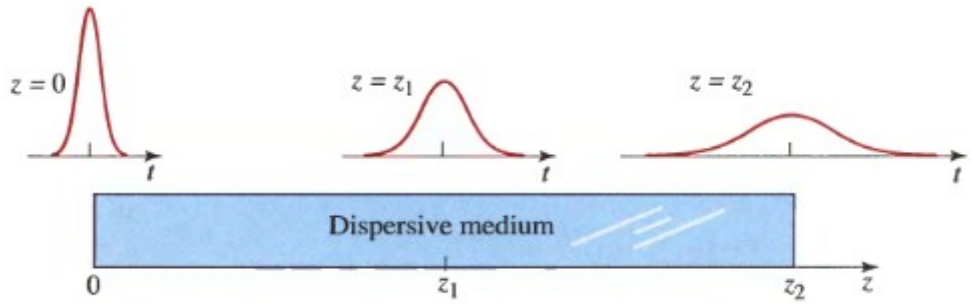

Figure 10: An optical pulse travelling in a dispersive medium is broadened at a rate proportional to the product of the dispersion coefficient D_ν, the spectral width σ_ν, and the distance traveled z.

It is also common to define a CD coefficient D_λ in terms of the wavelength instead of the frequency. Using $D_\nu d\lambda = D_\nu d_\nu$ yields $D_\lambda = D_\nu d_\nu/d\lambda_0 = D_\nu(-c_0/\lambda_0^2)$, which leads to directly to

$$D_\nu = \frac{\lambda_0^3}{c_0^2}\frac{d^2 n}{d\lambda_0^2} \qquad (9)$$

In analogy with *(6)*, for a source of spectral width σ_λ the temporal broadening of a pulse of light is

$$\sigma_\tau = |D_\lambda|\sigma_\lambda z. \qquad (10)$$

In fiber optics applications, D_λ is usually specified in units of ps/km.nm: the pulse broadening is measured in picoseconds, the length of the medium in kilometers, and the source spectral width in nanometers [4].

V. Normal and Anomalous Chromatic Dispersion

Although D_λ does not affect the pulse-broadening rate, it does affect the phase of the complex envelope of the optical pulse. As such, the sign can play an important role in pulse propagation through media consisting of cascades of materials with different dispersion properties. If $D_\nu > 0 \, (D_\lambda < 0),$ the medium exhibits normal CD. In this case, the travel time for higher-frequency components is greater than the travel time for lower-frequency components so that shorter-wavelength components of the pulse arrive later than longer-wavelength components, see Figure 11. If $D_\nu < 0 \, (D_\lambda > 0),$ the medium exhibits anomalous CD, in which case the shorter-wavelength components travel faster and arrive earlier. Most glasses exhibit normal CD in the visible region of the spectrum; at longer wavelengths, however, the dispersion often becomes anomalous, which is the case we study in this work [4].

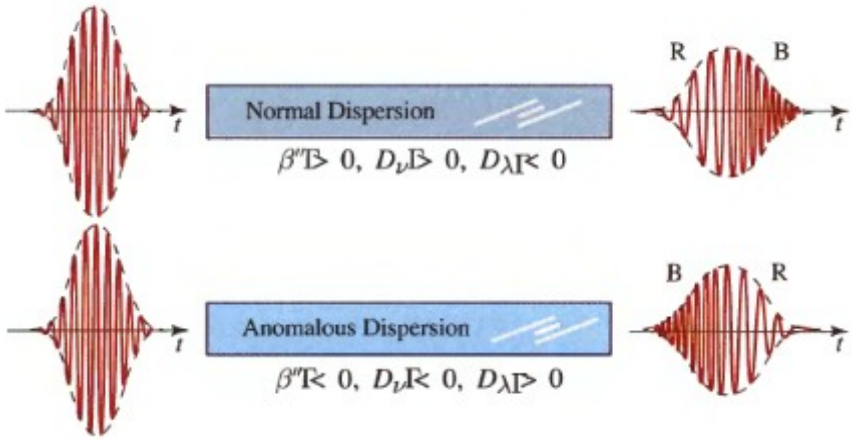

Figure 11: Propagation of an optical pulse through media with normal and anomalous CD. In a medium with normal CD, the shorter-wavelength components of the pulse (B) arrive later that those with longer wavelength (R). A medium with anomalous CD exhibits the opposite behaviour. The pulses are chirped since the instantaneous frequency is time varying.

VI. Summary and Outlook

In a multimode fiber, modal dispersion dominates and the width of the pulse received at the terminus of the fiber. It is governed by the disparity in the group delays of the individual modes.

In a single-mode fiber, there is no modal dispersion and the transmission of optical pulses is limited by combined material and waveguide dispersion (called chromatic dispersion) The width of the output pulse is governed by group velocity dispersion.

Pulse propagation in long single-mode fibers for which chromatic dispersion is negligible is dominated by polarization mode dispersion (PMD). Small anisotropic changes in the fiber, caused, for example, by environmental conditions, alter the polarization modes so that the input pulse travels in two polarization modes with different group indexes. This differential group delay (DGD) results in a small pulse spread.

In addition to polarization effects, which we will see in the next chapter, chromatic dispersion can also cause problems for quantum cryptography. For example, methods applying phase coding based on photons arriving at well-defined times, namely, on photons well placed in space.

However, in optical fibers, different group velocities behave as a noisy effect on the positioning of the photon as well as on the phase obtaining in an interferometer. Therefore the broadening of

photons featuring non-zero bandwidth, that is, the coupling between frequency and position, must be manipulated or even controlled. Hence, working with photons of small bandwidth, or, as long as the bandwidth is not too large, operating close to the wavelength λ_0 at which chromatic dispersion is zero, that is, for standard fibers around 1312 - 1310 nm. Fortunately, fiber losses are relatively small at this wavelength and amount to ~0.35 dB/km [8].

Material dispersion is usually much stronger than waveguide dispersion. However, at wavelengths where material dispersion is small, waveguide dispersion becomes important. Fibers with special index profiles may then be used to alter the chromatic dispersion characteristics, creating dispersion-flattened, dispersion-shifted, and dispersion-compensating fibers such that the chromatic dispersion goes to zero around 1550 nm, where the attenuation is minimal [7].

In opposition to birefringence, the chromatic dispersion does not need active and continuous compensation. Because the chromatic dispersion properties of optical fibers do not change with time. Therefore the chromatic dispersion results that phase is especially suited to transmission for long paths in optical fibers. Thus, the nonlinear impact decohering the qubit ‘‘energy’’ are totally insignificant, and chromatic dispersion effects existing on the position can be avoided or compensated in many cases.

Under certain conditions an intense pulse, called an optical soliton, can render a fiber nonlinear and travel through it without broadening. This results from a balance between material dispersion and self-phase modulation (the dependence of the refractive index on the light intensity).

Chapter 3

Polarization Mode Dispersion

A. Polarization of Light
B. What is Polarization?
C. Polarization Ellipse
D. Linearly Polarized Light
E. Circularly Polarized Light
F. Polarization and Polarization-Maintaining Fibers
G. PMD and DGD
H. PMD Coefficient In Terms of Ordering
I. From PMD Cable to PMD Distance
J. PMD Link Design Value
K. PMD of Optical Devices
L. The Measurement of PMD
M. Time-Domain Representation and Other Representations
N. Summary and Outlook

A. Polarization of Light

The polarization of light at a fixed position is determined by the time course of the electric-field vector $\mathcal{E}(\mathbf{r}, t)$. In a simple medium, this vector lies in a plane tangential to the wavefront at that position. For monochromatic light, any two orthogonal components of the complex-amplitude vector $\mathbf{E}(\mathbf{r})$ in that plane vary sinusoidally with time, with amplitudes and phases that are generally different, so that the endpoint of the vector $\mathbf{E}(\mathbf{r})$ traces an ellipse. Since the wavefront generally has different directions at different positions, the plane, the orientation, and the shape of the ellipse also vary with position, see Figure 12a.

For a plane wave, however, the wavefronts are parallel transverse planes and the polarization ellipses are the same everywhere, see Figure 12b, although the field vectors are not necessarily parallel at any given time. The plane wave is therefore described by a single ellipse and becomes elliptically polarized. The orientation and ellipticity of the polarization ellipse determine the state of polarization of the plane wave, whereas the size of the ellipse is found by the optical intensity. When the ellipse distorted into a straight line or a circle, then this polarization known as linearly or circularly, respectively.

In paraxial optics, light propagates along directions that lie within a narrow cone centered about the optical axis (the z axis). Waves are approximately in transverse planes, and have negligible axial components. From the perspective of polarization, paraxial waves may be approximated by plane waves and described by a single polarization ellipse (or circle or line).

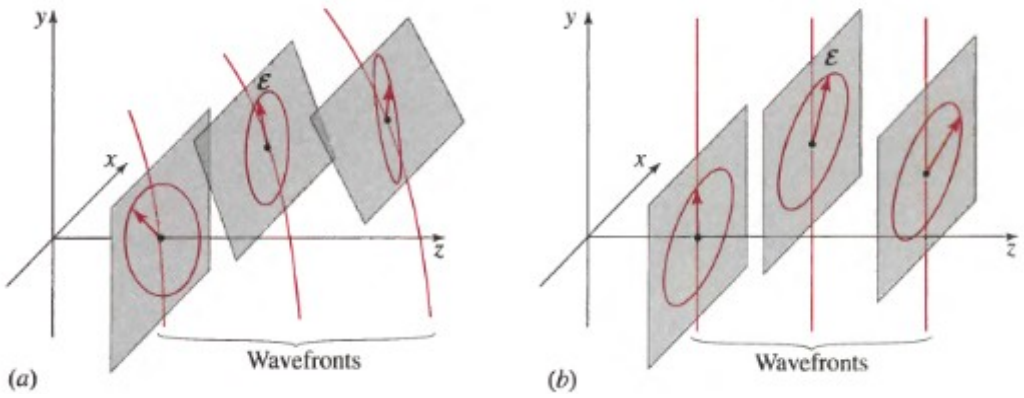

Figure 12: Time course of electric field vector of monochromatic light at several positions: (a) arbitrary wave; (b) plane wave or paraxial wave travelling in the z direction.

These are the examples in which the interaction of light with matter is witnessed:

- The polarization of the incident wave play an important role for the amount of the light at during reflection at the boundary between two materials.
- The sum of the light that is absorbed by given materials is dependent on polarization.
- The radiant light from matter is usually susceptible for polarization.
- Anisotropic materials' refractive index is polarization dependent. Waves with different polarizations travels at different velocities and suffers different phase shifts. In fact, the ellipticity of the polarization is altered when the wave goes forward. For example, linearly polarized light can turn into circularly polarized light. This is also useful for the design of optical devices.
- The polarization plane of linearly polarized light is rotated by passage through certain media, including those that are optically active, liquid crystals, and certain substances in the presence of an external magnetic field [4].

B. What is Polarization?

Suppose that a monochromatic plane wave of frequency ν and angular frequency $\omega = 2\pi\nu$ travelling in the z with velocity c. The electric field lies in the x-y plane and is generally described by

$$\mathcal{E}(\mathbf{r}, t) = Re\{\mathbf{A}\ \exp[j\omega(t - \frac{z}{c})]\}, \qquad (11)$$

where the complex envelope

$$\mathbf{A} = A_x\ \hat{\boldsymbol{x}} + A_y\ \hat{\boldsymbol{y}}, \qquad (12)$$

is a vector with complex components A_x and A_y. In order to determine the polarization of this wave, we trace the endpoint of the vector $\mathcal{E}(z, t)$ at each position z as a function of time [4].

C. Polarization Ellipse

Describing A_x and A_y in terms of their magnitudes and phases, $A_x = a_x \exp(j\varphi_x)$ and $A_y = a_y \exp(j\varphi_y)$, and substituting into *(12)* and *(11)* we get

$$\mathcal{E}(z,t) = \mathcal{E}_x\,\hat{\boldsymbol{x}} + \mathcal{E}_y\,\hat{\boldsymbol{y}}, \qquad (13)$$

where

$$\mathcal{E}_x = a_x \cos[\omega(t-\frac{z}{c})+\varphi_x] \qquad (14a)$$

$$\mathcal{E}_y = a_y \cos[\omega(t-\frac{z}{c})+\varphi_y] \qquad (14b)$$

are the x and y components of the electric-field vector $\mathcal{E}(z,t)$. They are also oscillating periodic functions of t-z/c at frequency ν and the parametric equations of the ellipse

$$\frac{\mathcal{E}_x^{\,2}}{a_x^{\,2}} + \frac{\mathcal{E}_y^{\,2}}{a_y^{\,2}} - 2\cos\varphi\,\frac{\mathcal{E}_x\mathcal{E}_y}{a_x a_y} = \sin^2\varphi, \qquad (15)$$

where $\varphi = \varphi_y - \varphi_x$ is the phase difference.

If we fix z, the tip of the electric-field vector rotates periodically in the x-y plane and draws an ellipse. If we fix t, the locus of the tip of the electric-field vector lines a helical trajectory and wraps around the surface of an elliptical cylinder, see Figure 13. The electric field moves periodically for each distance with the equation $\lambda = c/\nu$.

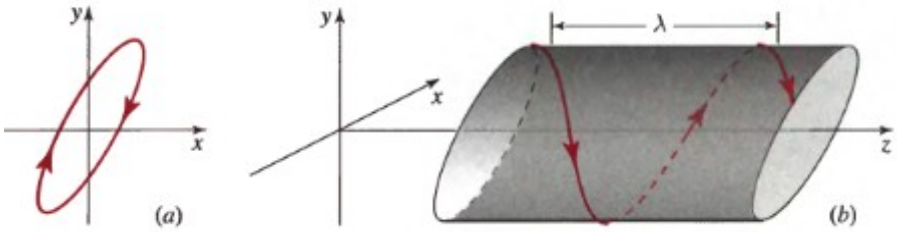

Figure 13: (a) Rotation of the endpoint of the electric-field vector in the x-y coordinates at a fixed position z. (b) A view from trajectory of the endpoint as time paremeter t is fixed.

The state of polarization of the wave is determined by the orientation and shape of the polarization ellipse, which is characterized by the two angles, see Figure 14. The angle Ψ determines the direction of the major axis, whereas the angle χ determines the ellipticity, namely the ratio of the minor to major axes of the ellipse b/c. These angles depend on the ratio of the magnitudes $r = a_y/a_x$, and on the phase difference $\varphi = \varphi_y - \varphi_x$ in accordance with the following relations: $\tan 2\psi = \frac{2r}{1-r^2}\cos\varphi$, $r = \frac{a_y}{a_x}$; $\sin 2\chi = \frac{2r}{1+r^2}\sin\varphi$, $\varphi = \varphi_y - \varphi_x$. These equations may be derived

by finding the angle Ψ that achieves a transformation of the coordinate system of $\mathcal{E}_x$ and $\mathcal{E}_y$ in *(13)* such that the rotated ellipse has no cross term. The size of the ellipse is determined by the intensity of the wave, which is proportional to $|A_x|^2+|A_y|^2=a_x{}^2+a_y{}^2$ [4].

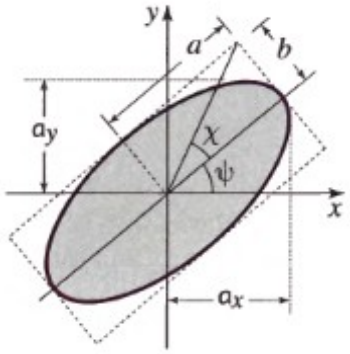

Figure 14: Polarization ellipse.

D. Linearly Polarized Light

In polarization ellipse, if one of the constituents doesn't exist (e.g. $a_x=0$), the light is linearly polarized in the direction of the other constituent (the y direction). The wave is also linearly polarized if the phase discrepancy $\varphi=0$ or π due to *(14),* $\mathcal{E}_y = \pm(a_y/a_x)\ \mathcal{E}_x$. Accordingly, the elliptical cylinder in Figure 15b transforms into a plane, see Figure 15. Hence, the wave gets the shape of planar polarization [4].

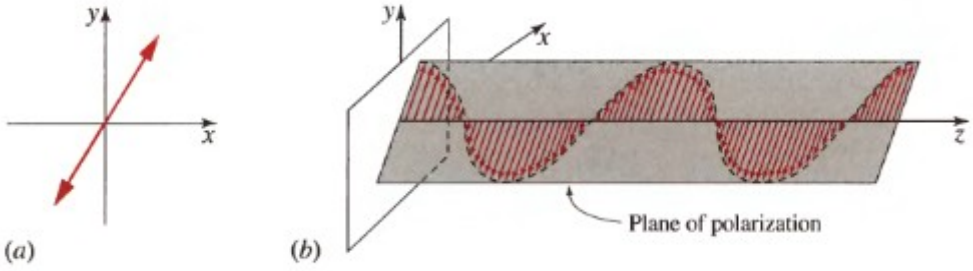

Figure 15: Plane (linearly) polarized light. (a) Route of time at a fixed position *z*. (b) A snapshot (fixed time *t*).

E. Circularly Polarized Light

In the case $\varphi=\pm\pi/2$ and $a_x=a_y=a_0$, according to *(14),*one can find $\mathcal{E}_x = a_0\cos[\omega(t-z/c)+\varphi_x]$ and $\mathcal{E}_y = \mp a_0\sin[\omega(t-z/c)+\varphi_x]$, from which $\mathcal{E}_x{}^2 + \mathcal{E}_y{}^2 = a_0^2$ (circle equation). In Figure *(12b),* the elliptical cylinder transforms into circular cylinder and becomes circularly polarized. If $\varphi=+\pi/2$, the electric field at a fixed position *z* rotates in a clockwise direction when observed from the direction toward which the wave is approaching. In this case light becomes right

circularly polarized; if $\varphi = \pi/2$, then rotation gets counterclockwise direction and then light becomes left circularly polarized, see Figure 16 [4].

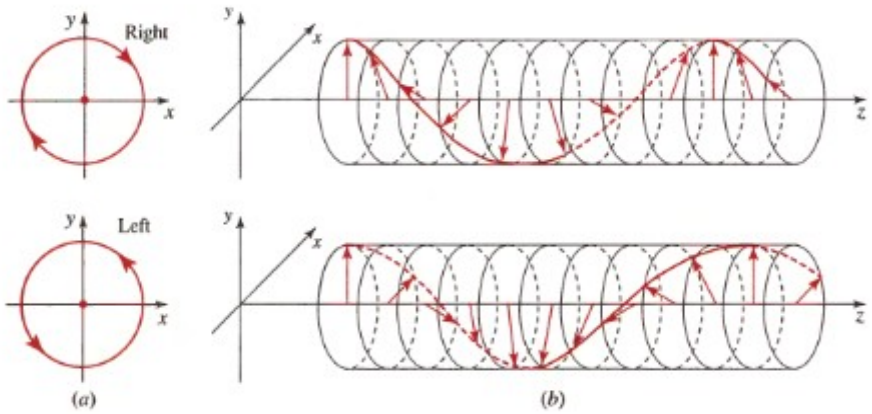

Figure 16: (a) Time course at a fixed position z. (b) A view from a fixed time *t*.

F. Polarization and Polarization-Maintaining Fibers

In a fiber with circular cross-section, every mode has two detached polarization states with equal proceeding constant. Consequently, the principle linear polarization mode in a single-mode which leads slenderly, may be polarized in the x or y; therefore the two orthogonal polarizations have the same propagation constant and the same group speed.

Essentially, there should be no exchange of the power between the two polarization constituents. If the power of the light source is delivered exclusively into a polarization, the power is to be kept in that polarization state. Despite the theory, in practice, weakly casual impediments and the distension, which are to be overcome, in the fiber cause in random power transfer between the two polarizations. These kind of intercourse becomes possible because the two polarizations have the same propagation constant and their phases are therefore matched. In fact, at the fiber input, linearly polarized light is usually distorted into elliptically polarized light at the fiber output. Despite the fact that the total optical power remains fixed, the ellipticity of the received light varies randomly with time as a result of fluctuations in the fiber extensions and temperature, and of the source wavelength. In case the object should just deliver light power, provided that the total power is collected, the mixture of the power division demonstrates no difficulty between the two polarization states.

Indeed, in several fields that fiber optics is utilized, e.g., in a quantum cryptography channel based on interferometric techniques, and coherent light sources, the fiber must deliver the complex amplitude (magnitude and phase) of a specific polarization. Polarization-maintaining fibers are necessary for such applications. The circular symmetry of the traditional fiber must be ignored, in order to build a polarization-maintaining fiber, e.g. through using fibers with elliptical cross section or stress-induced anisotropy of the refractive index. This destroys the polarization degeneracy, thereby making the propagation constants of the two polarizations independent. The introduction of such phase mismatch serves to reduce the coupling efficiency [4].

G. PMD and DGD

As indicated earlier, the fundamental spatial mode (linearly polarization mode) of an optical fiber has two polarization modes, say linearly polarized in the x and y directions. If the fiber has perfect

circular symmetry about its axis, and its material is perfectly isotropic, then the two polarization modes are degenerate, i.e., they travel with the same velocity. However, fibers exposed to real environmental conditions exhibit a small birefringence that varies randomly along their length. This is caused by slight variations in the refractive indexes and fiber cross-section ellipticity. Although the effects of such inhomogeneities and anisotropies on the polarization modes, and on the dispersion of optical pulses, are generally difficult to assess, it is generally useful to consider these effects in terms of simple models.

In addition to chromatic effects, the polarization mode dispersion (PMD) in the fiber optic components plays also an increasingly critical role as linear electromagnetic phenomena and statistical treatment in the optical transmission technology, especially if it would be taken into account for phase coding in quantum cryptography through interferometric systems. PMD's testing is becoming essential in the fiber characteristic process, but still one of the most difficult to test, due its sensitivity to a number of environmental constraints, as we will see in the following parts of this chapter.

The polarization mode dispersion leads in digital optical systems as chromatic dispersion to impulse distortion and therewith to an increase of the bit error rate. That restricts the range, especially of transmission distances with high bit rate, considerably. As a cause for these disturbing effects, variations of the propagation speed are in a single-mode optical fiber used for quantum cryptography in our case. For example, the variations of the group velocity υ as a result of refractive index fluctuations $N(\lambda)$ along the optical fiber; then $\upsilon = c_0 / N(\lambda)$.

The refractive index arises however also diagonally to the propagation direction, i.e. the refractive index is inhomogeneous over the cross-section. As a consequence therefrom the fundamental mode is subject to swing vertically to the propagation direction. It now oscillates in two orthogonal direction with two different propagation velocities (birefringence) and therewith a time delay difference; the fundamental mode is split into two modes in two axes (fast and slow axes). The mean time delay difference is called **PMD delay**, see Figure 17.

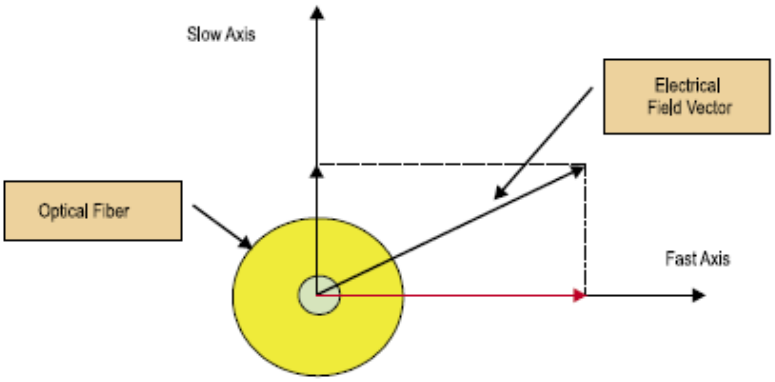

Figure 17 The decomposition of two axes for two polarization modes.

Because of geometric asymmetries and photo elastic effective, as a rule, even further delays accrue, which show explicit impacts on long intervals and in high data rates: In practice, an intrinsic birefringence is caused by the manufacturer evoked by geometry mistake or internal tensions and an extrinsic birefringence by the placing, for example through external tension, bend, torsion or extension of the fiber. In part, these mechanisms vary along the optical fiber and are moreover locally different. Correspondingly, the propagation speeds of both modes change permanently. The one mode can hurry ahead and can make up the other mode later. They start to spread and overlap each other. To summarize, a light pulse transmitted through a polarization maintaining fiber could be defined as the decomposition of the pulse into 2 orthogonal pulses, travelling at different, but constant speed.

Therefore it is resulted in contrast to chromatic dispersion that the impulse distribution is here not steady and proportional to the length, but rather it is statistical and depends fewer strongly on the length. Its stochastic behaviour resembles **random walk** in mathematical point of view [9]. It is in principle conceivable also that if the PMD delay could be compensated totally at the end of the distance, so there would be no measurable PMD delay. Moreover, the optical fibers show a strong tie-in between the polarization modes for the telecommunication. Mode coupling places emerge at splice, tensions, in the fiber or for example phase overlaps. So it comes between the modes to a further reduction of the time delay difference.

Consider first a fiber modeled as a homogeneous anisotropic medium with principal axes in the x and y directions and principal refractive indexes n_x and n_y. The third principal axis lies, of course, along the fiber axis (the z direction). The fiber material is assumed to be dispersive so that n_x and n_y are frequency dependent, but the principal axes are taken to be frequency independent within the spectral band of interest. If the input pulse is linearly polarized in the x direction, over a length of fiber L, it will undergo a group delay $\tau_x = N_x L / c_0$; if it is linearly polarized in the y direction, the group delay will be $\tau_y = N_y L / c_0$. Here, N_x and N_y are the group indices associated with n_x and n_y. A pulse in a polarization state that includes both linear polarizations will undergo a **differential group delay (DGD)** $\delta\tau = |\tau_y - \tau_x|$ given by

$$\delta\tau = \Delta N L / c_0, \qquad (16)$$

where $\Delta N = |N_y - N_x|$, therefore designated as the time delay difference between both part modes, that depends on the wave length. Upon propagation, therefore, the pulse will split into two orthogonally polarized components whose centers will separate in time as the pulses travel, see Figure 18. And then, it seems as arrival time difference at the output of the media, see Figure 19.

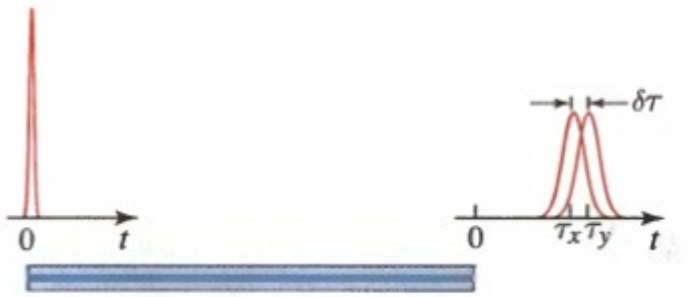

Figure 18: Differential group delay (DGD) associated with polarization mode dispersion (PMD).

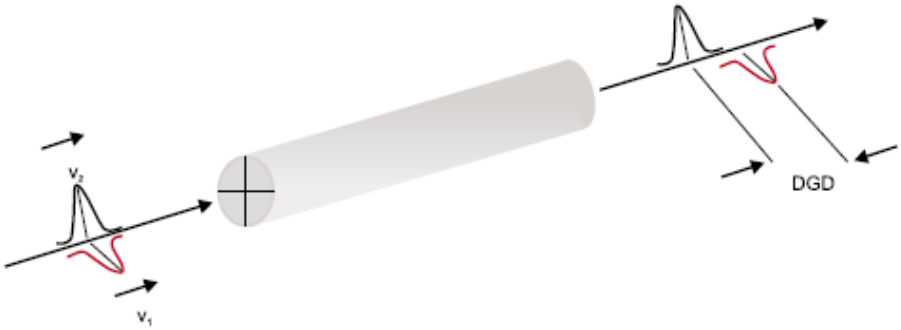

Figure 19: Differential group delay.

DGD has a statistical character (Maxwell Distribution) because of the totally irregular connection between fiber position and refractive index, see Figure 20. The PMD delay also appears on an averaged value of the DGD through certain wavelength range.

The DGD corresponds to polarization mode dispersion (PMD) that increases linearly with the fiber length at the rate $\Delta N / c_0$, which is usually expressed in units of ps/km.

This quotation could be very useful for understanding DGD in terms of Maxwellian distribution: "From [the] data. DGD varies slowly over time but rapidly over wavelength…data showed good agreement with a Maxwellian distribution. The frequency averaged mean DGD [emphasis added] varied about 10% or less during periods that showed significant temperature swings."[9]

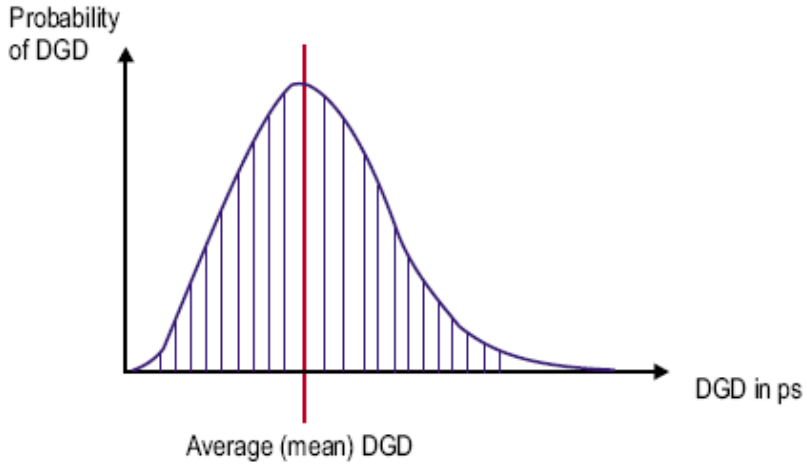

Figure 20: A Maxwellian distribution of the differential group delay.

The PMD coefficient defined as the fiber parameter D_{PMD} has the measure unit of ps / $\sqrt{km}$, i.e. the PMD doesn't rise linearly, but only by the root of the distance length:

$$\Delta \tau = D_{PMD} / \sqrt{L} \qquad (17)$$

In digital transmission, the maximally allowable PMD delay may amount to tenth of the bit length T_{Bit} :

$$\Delta \tau_{max} \leq T_{Bit} / 10 \qquad (18)$$

If one sets T_{Bit} =1/B, whereby B called the bit rate, one receives out of equation *(17)* and *(18)* a relation between the realizable distance length, the bit rate and PMD coefficient:

$$L \leq 1 \frac{1}{100.\mathrm{B}^2 . D_{PMD}^2} \qquad (19)$$

Hence, the relation between bit rate, bit length, PMD delay and PMD coefficient according to equation *(17)* evidently results that the bridgeable length diminishes reciprocally proportionally to the square of the bit rate. A quadrupling of the data rate caused therefore a reduction of the realizable distance length through PMD effects to 1/16. Thus, it can come to considerable restrictions for the transition from 2,5 Gbit/s to 10 Gbit/s by reason of the PMD.

H. PMD Coefficient In Terms of Ordering

By reason that between distance length and PMD coefficient, a strong dependence exists, this parameter is used recently for the specification of the optical fibers. At older optical fibers, PMD coefficient is however usually not well known and it can include comparatively large values. Moreover it is subject to very strong variations.

One must carry out a PMD measurement for older fibers if the data rate should be transmitted by 10 GBit/s or more highly. It is not sufficient to measure single fibers within the cable randomly. Because the PMD coefficients can vary strongly between the fibers of a cable. In modern fibers, one minimizes PMD delay through suitable manufacture procedures. Through turning of the preform or of the fiber during the drawing process, ovality of the preform are balanced. So it is averaged over the geometric deviations therewith reached an improvement of the values reached.

In the meantime modern fibers are specified with respect to the PMD coefficient. While standardization bends recommend a maximum value for the PMD coefficient of 0.5 ps / $\sqrt{km}$, the manufacturers specify their fibers already partially with 0.2 ps / $\sqrt{km}$ or even 0.8 ps / $\sqrt{km}$ as a PMD link design value.

In the previously discussed PMD coefficient, it concerns exactly taken the 1. order PMD coefficient. It is also possible that more complicated pulse distortions appear when the PMD spectrum fluctuates over the bandwidth of the signal. For the same PMD, the higher the data rate the wider the signal spectrum. For this reason, each spectral portion can be studied conventionally, but then the interference between these portions must be taken into account. A measure of pulse-degeneration complexity can be determined by the level of PMD difference over a signal bandwidth. When the PMD changes little, then only “first-order” PMD affects the pulse. If the PMD changes a lot, then “higher-order” PMD affects become pronounced. The higher-order PMD effects engender sophisticated pulse disruptions.

One higher-order effect that points out much is second-order PMD. Second-order PMD is a vector engendered by a first-order transformation of the PMD vector with frequency, see Figure 21. Generally, the PMD vector τ is different for different frequencies. Let $\vec{\tau}(w_1)$ and $\vec{\tau}(w_2)$ be two vectors particularly, where the difference of $w_2 - w_1$ is small. The vector discrepancy is the second-order PMD vector, denoted with $\vec{\tau}_w$. As other vectors, $\vec{\tau}_w$ has a length and a pointing direction. Usually, the pointing direction shouldn't be parallel or perpendicular to either first-order PMD vector, and the length is zero only when τ pirouettes about itself or when there is only one birefringent element. The length of the second-order PMD vector in relation to the DGD resolves the significance of the second-order vector.

The second-order PMD vector can be determined onto two components called the depolarization component and the polarization-dependent chromatic dispersion component, see Figure 21b. The

depolarization component lies perpendicular to $\vec{\tau}(w_1)$ and indicates the rate which the pointing direction of the PMD vector changes. The polarization-dependent chromatic dispersion component lies parallel to $\vec{\tau}(w_1)$ and indicates the difference of DGD with frequency. The length of the polarization-dependent chromatic dispersion component is in fact the frequency derivative of the DGD spectrum at w_1.

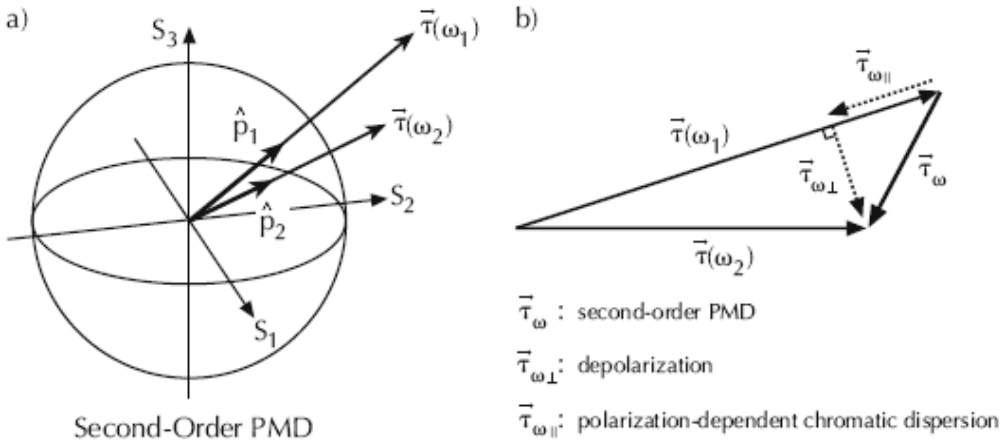

Figure 21: Definition of the second-order PMD vector $\vec{\tau}_{\omega}$. a) PMD vectors $\vec{\tau}(w_1)$ and $\vec{\tau}(w_2)$. The vectors have differential distances and pointing directions. b) Second-order PMD is the vector difference $\vec{\tau}_{\omega}=(\vec{\tau}(w_2)-\vec{\tau}(w_1))/\Delta\omega$ as $w_2 - w_1 \rightarrow 0$. The second-order PMD vector is found on the $\vec{\tau}(w_1)$ axis into perpendicular and parallel constituents. The perpendicular constituent is called depolarization and the parallel component is called polarization-dependent chromatic dispersion.

The term “depolarization” has an inferred meaning in the time domain, so why does the second-order PMD, best described in the frequency domain, have a depolarization component? The change in pointing rotation of the PMD vector with frequency spreads a fixed input polarization into many states at the output. Every frequency has one output state. When the signal is inverse Fourier changed to the time domain, the spread output polarizations are folded into the time-domain signal so that each time interval contains many polarizations. A time average over these states reduces the degree-of-polarization as compared to the input; that is, the input state is depolarized by the PMD.

The second-order PMD is the frequency derivative of the PMD vector such as $\vec{\tau}_w=\tau_w\hat{p}+\tau\hat{p}_w$, where the first vector component corresponds to the polarization-dependent chromatic dispersion component, and the second one corresponds to depolarization component, which are orthogonal to each other [10].

On the other hand, the 2nd order PMD coefficient is also utilized as a measure for the wavelength dependence of the differential group delay; that is a measure how strongly the PMD fluctuates, which is dependent upon the wavelength.

The 2nd order PMD coefficient has that immediately unit of measure such as the chromatic dispersion and makes itself calculate 1st order in strong coupling optical fiber out of PMD coefficient. Out of 0.5 ps / $\sqrt{km}$ a 2nd order PMD coefficient of 0,15/ps(nm.km) arises. Because the 1st order PMD is proportionally to the root of the distance length, also the 2nd order PMD can play a role in very large distance lengths under circumstances.

I. From PMD Cable to PMD Distance

PMD coefficient of the distance can be influenced yet through further factors by the cable PMD except through environment influences and installation deficiencies: As above mentioned, PMD firstly causes disturbing effects in very large distances. This distance consists in general of many fractions, because the pull-in lengths are limited usually from two to six kilometers.

If one wonders, how large PMD of the entire distance is, as the single sections have different PMD coefficients, investigations showed that PMD delay of the distance $\Delta\tau$ (in strong mode coupling) does not correspond to the sum of PMD delays of the cable sections $\Delta\tau_i$, but rather results from the sum of the squares:

$$\Delta\tau = \sqrt{\sum_i (\Delta\tau_i)^2} \qquad (20)$$

From the equations *(18)* and *(19)* a connection follows between PMD coefficient of the entire distance $D_{PMD_{total}}$ and PMD coefficient D_{PMD_i} of the distance sections with the lengths L_i:

$$D_{PMD_i} = \frac{\sqrt{\sum_i [L_i \cdot (D_{PMD_i})^2]}}{\sqrt{L}} \qquad (21)$$

One can calculate PMD coefficient of the total distance therefore in well known PMD coefficient and the distance of the sections. Corresponding to equation *(19)* out of this quadratic dependence follows however also that a single cable section significantly can influence the PMD coefficient of the entire distance.

An example: Let the entire distance be composed of the length of ten equal intervals. Nine intervals with $D_{PMD_{1...9}}$ =0,008 ps / $\sqrt{km}$, one interval with $D_{PMD_{10}}$ = 4 ps / $\sqrt{km}$. Hence, it implies with the equation *(17)*: $D_{PMD_{total}}$ =1,27 ps / $\sqrt{km}$. This shows that a mixture of old and modern fibers requires a PMD measuring unconditionally.

J. PMD Link Design Value

In principle, the equation *(21)* is not necessary only for PMD delay, but also for all values of the statistical distribution of the differential group delay. That is, a statistical distribution of PMD distance can be calculated, out of the statistical distributions of the PMD cable. Through the squaring down, very small and/or very large values disappear. The narrower the statistical distribution, the more cable pieces of the entire distance form.

The demand corresponding to equation *(20)* results from the acceptance that the triple value of PMD delay enables just another transmission with an achievement loss at the receiver with 1dB. This triple value results out of the statistical distribution of the differential group delay and steps with a probability of 4,5 up. For comparison, that corresponds 21 minutes per year. If many cable

pieces of the entire distance form, the probability is slighter for the occurrence of outliers. Therefore, in comparable probability, if a certain value is exceeded, the maximal value is to be considered smaller. It lies now more closely to the average.

That leads to the definition of PMD link design value D_{PMD_Q}. One can understand the PMD coefficient, that is kept by 99.99 percent of all distances. Accordingly, a fictional transmission distance of at least 20 homogeneous fibers underlie. The distance planning can take place consequently by means of a more favorable (smaller) value. The cable manufacturers specify as a typical PMD link design value as $D_{PMD_Q} \sim 0{,}008 \text{ps} / \sqrt{km}$.

K. PMD of Optical Devices

PMD delays of all distance elements should be balanced for a dependable planning. In fact, optical fibers and optical devices are to be considered compatible with each other. Correspondingly, in contrast to long optical fiber distance with strong mode coupling in short mode coupling distance is negligible and PMD delay rises proportionally to the length of the distance. The corresponding PMD coefficient has the measure unit ps/km. PMD of optical devices is indicated in ps [11].

L. The Measurement of PMD

In PMD measurement, the polarization conditions of the light and respectively its variations during passing through of the optical fibers are to be determined. The polarization condition of the light cannot be registered by the naked eye. Because the eye does not recognize the light amplitude, but rather the light intensity, then the sum square of the complex amplitude. Just as, usual optical test receivers function. Likewise, these register only intensities. Contrived methods are therefore required in order to make the polarization condition visibly and to register therefore its variations. There are a couple of measuring methods for PMD like interferometric methods [12, 13, 14, 15]. But to make it brief, we won't go into the detail here.

M. Time-Domain Representation and Other Representations

So far, we mentioned PMD in terms of the frequency domain which is an inartificial result of the frequency-centric definition of the PMD vector. However, the parallel representation is the PMD impulse response in the time domain. Despite the fact that it is more complicated to compute the impulse response, more different and more plenty points of views are obtained from the real time relations and interactions between these two domains.

Between the extremes of sine-wave response and impulse response lies the signal response of a communications channel, especially the deformation imparted on a signal due to PMD. The signal response is fundamentally the convolution of the input waveform with the impulse response. What makes the calculation tricky is that co-polarized signal-image components that result from the convolution interfere coherently; the temporal location of the impulses matter to within a fraction of a wave. When in one case two co-polarized signal images are in phase and add constructively, a dephasing by π leads to destructive interference between the signal images. When the impulse weights differ with changes in mode mixing, the temporal locations of the impulse response change only when the composition of the PMD concatenation changes. This implies that for a specific concatenation, the impulse response may extend well into the duration of a signal pulse; how the signal is distorted depends on which co-polarized signal images make constructive interference

and which make destructive interference. In some cases the signal will look undistorted while in others it will look quite distorted. How the PMD impacts the signal depends on the expression of this coherent interference.

As a result, there are three main components to refer in polarization mode dispersion for practical systems and design: propagation length, optical frequency, and time. In each case a statistical process must be defined to characterize the evolution on a microscopic level. The ergodic structure of PMD makes “length” replaced by “optical frequency” in the density functions and “long length” is replaced by “wide bandwidth.” Due to statistical calculations of the PMD, it is possible to connect the length and the frequency regimes. There is, however, no definite process for the time evolution. For example, submarine cable changes at a slow rate while aerial fiber changes in the millisecond range. Moreover, there is likely no spatial homogeneity to the temporal changes – for instance, a train may cross a cable at a particular location – so one cannot expect a neat answer [10, 16].

N. Summary and Outlook

All fiber-based implementations of quantum cryptography have to face problem of PMD. As the bit rate in optical fiber transmission approaches 40 Gbit/s per wavelength division multiplexed channel and beyond, impairments of second order polarization mode dispersion has been becoming increasingly important [17, 18]. It is therefore necessary to compensate for both the first- and second-order PMD in such systems [19]. This is clearly true for polarization-based systems, but it is equally a concern for phase-based systems, since interference visibility depends on the polarization states.

There are no simple theoretical predictors of installed cable PMD, but PMD is more critical with older fibers that were manufactured with less geometrical control than today. PMD measurements are required at old fibers from data rates of 10 Gbit/s in every case. For fibers with minimized coefficient, the necessity of the measurement depends on the data rate, the distance length, the specified coefficient and the security factor introduced above. Especially for older optical fibers, the compensation is beneficial similar to the PMD delay compensation. Unfortunately the compensation technique is quite costly. Because the signal is subject to statistical variations. First PMD compensators are however already available.

PMD remains the dominant bit rate-limiting effect in long single-mode fibers, when chromatic dispersion is reduced by state-of-the-art techniques like compensated fibers or chirped gratings. PMD has to be measured in order to characterize the fiber dedicated to this transmission speed.

Chapter 4

Comparison of Both Dispersions

Both CD and PMD reason temporal spreading of the optical bits as they propagate along the fiber, see Figure 22 [20]. As briefly,

- chromatic dispersion is caused by different wavelengths of light traveling at different speeds, and is a combination of material and waveguide dispersion,
- CD can cause adjacent bits to smear into each other in a signal, because the signal actually contains a small range of wavelengths,
- Advanced fiber types can be used to compensate for chromatic dispersion,
- Polarization mode dispersion is caused by the lightwave's different principal states traveling at different speeds,
- PMD is caused by imperfections in fiber symmetry and fluctuating fiber stresses, which make it a random effect.

To summarize:

CD is deterministic, PMD is stochastic; CD is linear, PMD is nonlinear; CD is not affected by environmental conditions, PMD is affected by environmental conditions; CD can be compensated, PMD cannot be compensated thoroughly; CD depends on L, PMD does not depend on L (but depends on $\sqrt{L}$); CD depends on bandwidth ($\delta\lambda$), PMD does not depend on bandwidth.

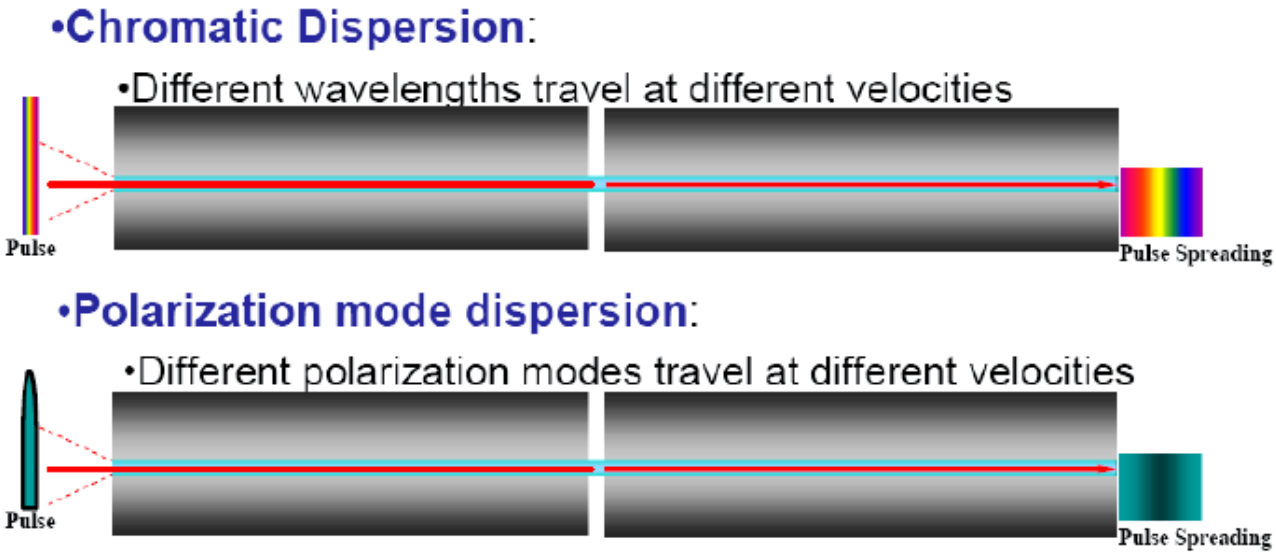

Figure 22: One of the differences between CD and PMD is the wavelength dependence.

Chapter 5

Calculations and Simulations on Polarization Mode Dispersion and Chromatic Dispersion

A. Determination of CD and PMD Parameters from Spectra Equations
B. Demonstration of CD and PMD Impacts into Position and Wavelength Spectra
C. Results and Discussion

A. Determination of CD and PMD Parameters from Spectra Equations

There have been multitudinous calculations of academic researches regarding polarization mode dispersion and chromatic dispersion since they appeared. Complex differential equations, stochastic partial differential equations, statistical calculus, vectoral calculus in terms of Jones and Stokes vectors are only a couple of them. Instead of detailled calculations, some useful notes will be utilized from Professor Suda's manuscripts and [5], which will lead us to simulations. These simulations were made through MATLAB GUI* programming techniques. Readers could also refer to "Appendix: Source code of simulation of chromatic and polarization mode dispersion in phase coding quantum cryptography" for detailed information.

There are two arms c, d in the first Mach-Zehnder interferometer and two outputs g, h. Suppose for the beginning a MZ in vacuum. The beam paths c and d are characterized by the path lengths l_c and l_d increasing phase factors exp{ $-\imath . k.l_c$ } and exp{ $-\imath . k.l_d$ } respectively. Besides that, phase shifts Δ_c and Δ_d produce phase factors P_c =exp{ $\imath . k. \Delta_c$ } and P_d =exp{ $\imath . k. \Delta_d$ }. And then, when needed, absorption factors a_c and a_d involve transmission coefficients T_c =exp{ $-2.1_c . a_c$ } and T_d =exp{ $-2.1_d . a_d$ }, see Figure 2.

Some of the most main factors affecting pulse propagation in dispersive media are CD coefficient D_{λ_0} with parameter κ ; and the PMD coefficient D_{PMD} with parameter ε . One can also examine those's dependence on the wavelength with the group velocity υ:

$$\upsilon = \frac{c_0}{N}, \quad N = n - \lambda \frac{dn}{d\lambda} . \qquad (22)$$

* My personal suggestion for who wants to use MATLAB GUI is to use low level GUI programming techniques instead of using GUIDE. Although GUIDE seems easier than low level programming from outside, low level programming is very flexible and provides more facilities in order to manipulate user face, see Figure 23.

As in realistic schemes, if we take CD into account in the length $l\,(=l_g)$ of a single-mode fiber, then the phase factor exp{ $-\iota\,.\,k.l$ } has to be substituted by exp{ $-\iota\,(N_0 k-\kappa\,k^2)\,l$ }, where $N_0=N(\lambda_0)$ is the group index for the mean wavelength λ_0 and $\kappa=-D_{\lambda_0}\lambda_0^2 c_0/(4\pi)$. Caused by CD, the exponential function is extended by an expression which is proportional to k^2 . Thereby the dispersion coefficient is defined through

$$D_{\lambda_0}=-\frac{\lambda_0}{c_0}\frac{\partial^2 n}{\partial\,\lambda^2}\,. \qquad (23)$$

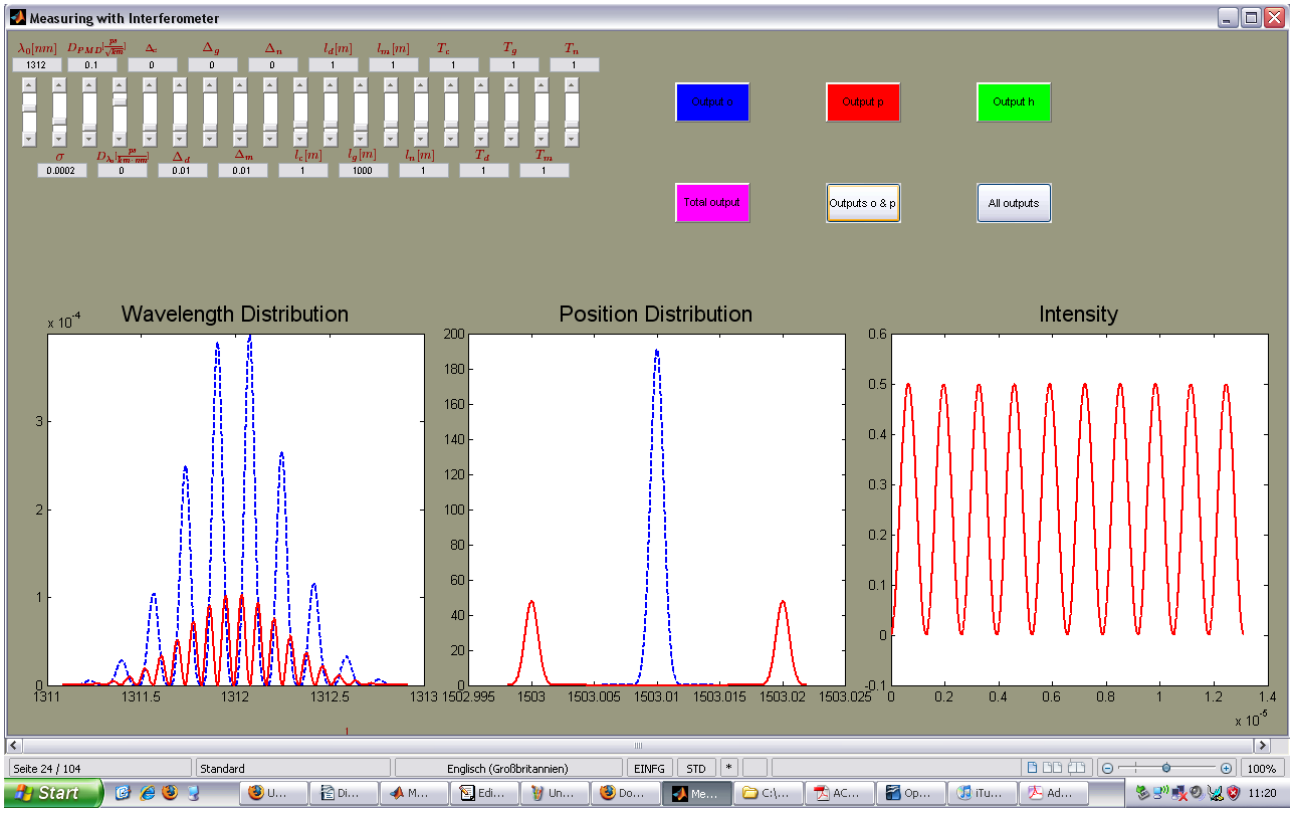

Figure 23: A view from GUI application for determination of output spectra in quantum cryptography.

Ansatz:

$$\omega_{total}=1+16\pi^2\left(\frac{c_o}{\lambda_0}\right)^2\sigma^2\left[(\Delta\tau_{CD})^2+(\Delta\tau_{PMD})^2\right], \qquad (24)$$

where the ω_{total} is total distribution of time pulses, the PMD delay $\Delta\tau_{PMD}=D_{PMD}\sqrt{l}$ is independent from ($\delta\lambda$), and the CD delay $\Delta\tau_{CD}=(\delta\lambda)\,D_{\lambda_0}l$ depends on ($\delta\lambda$). According to [5] we can write the ω_{total} into the form

$$\omega_{total}=1+16(\delta k)^4 B_{total}^2=1+16\,\sigma^4 k_0^4 B_{total}^2\,, \qquad (25)$$

and we therefore get through the necessary substitutions

$$\omega_{total} = 1 + 16\pi^2 \left(\frac{c_0}{\lambda_0}\right)^2 \sigma^2 [\sigma^2 \lambda^2 D_{\lambda_0}^2 l] . \qquad (26)$$

Due to [5] one can equate:

$$\sigma^2 k_0^2 B_{total}^2 = \pi^2 \left(\frac{c_0}{\lambda_0}\right)^2 \sigma^2 [\sigma^2 \lambda^2 D_{\lambda_0}^2 l] . \qquad (27)$$

Consequently, we obtain

$$B_{total}^2 = \pi^2 \left(\frac{c_0}{\lambda_0}\right)^2 \frac{\lambda_0^2 D_{\lambda_0}^2 l^2}{k_0^4} + \pi^2 \left(\frac{c_0}{\lambda_0}\right)^2 \frac{D_{PMD}^2 l}{k_0^4 \sigma^2}$$

$$= B_{CD}^2 + B_{PMD}^2 . \qquad (28)$$

As from now, B_{total} can be examined separately according to CD and PMD, and reduced respectively:

$$B_{CD}^2 = \pi^2 \frac{\lambda_0^2 \kappa^2 (4\pi)^2}{\lambda_0^4 c_0^2} l^2 \left(\frac{c_0}{\lambda_0}\right)^2 \left(\frac{\lambda_0}{2\pi}\right)^2$$

$$= \kappa^2 l^2 \frac{\pi^2 16\pi^2}{16\pi^4} = (\kappa . l)^2 . \qquad (29)$$

$$B_{PMD}^2 = \pi^2 \left(\frac{c_0}{\lambda_0}\right)^2 \frac{D_{PMD}^2 l}{\sigma^2 16\pi^4} \lambda_0^4$$

$$\frac{c_0^2 \lambda_0^2}{16\pi^2} \frac{D_{PMD}^2}{\sigma^2} l = \left(\frac{c_0 \lambda_0}{4\pi}\right)^2 \left(\frac{D_{PMD}^2}{\sigma}\right)^2 l$$

$$= \frac{1}{\sigma^2} \left(c_0 \lambda_0 \frac{D_{PMD}}{4\pi}\right)^2 l = \varepsilon^2 \frac{l}{\sigma^2} \qquad (30)$$

If we could bring the two individual CD and PMD parameters together:

$$B_{total}^2 = \sqrt{B_{CD}^2 + B_{PMD}^2} = \sqrt{(\kappa l)^2 + \frac{\epsilon^2 l}{\sigma^2}} , \qquad (31)$$

and finally unique parameters are gained:

$$\kappa = -\frac{c_0 \lambda_0^2 D_{\lambda_0}}{4\pi}, \qquad \varepsilon = \frac{c_0 \lambda_0 D_{PMD}}{4\pi} . \qquad (32)$$

This is the most useful form that we can benefit from the equations above. Because the position and the wavelength spectra just take value through these last two parameters.

B. Demonstration of CD and PMD Impacts into Position and Wavelength Spectra

Here we wil study varying parameters within 2 main examples including several examples into each other, in order to determine which parameters in optimum niveau for keeping interference according to peaks. The first one is for l = 50 km and the second one is for l = 100 km. The arms of the two interferometers for both examples have equal lengths of 1 m each and in arm d and m equal values of phase shifts $\Delta_d = \Delta_m = 1$ cm entail phase factors P_d =exp{ $\iota . k . \Delta_d$ } and P_m =exp{ $\iota . k . \Delta_m$ }, respectively. These phase shifts are enough to produce separated wave packets in space (or time pulses) behind the two interferometers.

A Couple of Remarks:

(1) In the following examples, the four main parameters variations will be demonstrated: $\sigma , \lambda_{0,} D_{PMD} , D_{\lambda_0}$. Other parameters (e.g. ε , κ) which depend on these 4 parameters will of course take their values accordingly. But independent values (e.g. Δ_d , Δ_m) other than these 4 parameters will stay constant.

(2) The PMD coefficient D_{PMD} will vary in interval [0,1]. This means, it is graded between 0 and 1. "0" is the fiber without PMD (perfect, however not possible today). "1" is the worst state of the fiber for any data transfer.

(3) The values that we used for parameters in the examples below are realistic according to the table in the following [4]:

$\lambda_0 [nm]$	$D_{\lambda_0} \frac{ps}{km.nm}$	κ [nm]
870	-80	1.4456
1312	0	0
1550	17	-0.9750

(4) Below, the blue output distribution lines will indicate for output o, reds will indicate p, greens will indicate h, and the pinks will indicate sum of all outputs.

(5) Here it would be very helpful to index shortly in advance again, in order to comprehend the following examples comfortably. Therefore, instead of looking for our individual desired example, whatever we look for, we can choose from the index below and reach it punctually due to this index. Another alternative for usefulness of the simulations is that reader could foremost skip simulations and take a look at the section of **Results and Discussion**, and then get back on the simulations with a precognition. So, simulations could be understood more consciously which one indicates what.

Our sub-samples are within the first example (l = 50 km):

1.1.1. $\sigma = 2.10^{-4}$, $\lambda_0 = 870\,nm$, $D_{PMD} = 0 \frac{ps}{\sqrt{km}}$, $D_{\lambda_0} = -80 \frac{ps}{km.nm}$ (p. 34-38),

1.1.2. $\sigma = 2.10^{-4}$, $\lambda_0 = 1312\,nm$, $D_{PMD} = 0{,}2\frac{ps}{\sqrt{km}}$, $D_{\lambda_0} = 0\frac{ps}{km.nm}$ (p. 39-41),

1.1.3. $\sigma = 2.10^{-4}$, $\lambda_0 = 1550\,nm$, $D_{PMD} = 0{,}9\frac{ps}{\sqrt{km}}$, $D_{\lambda_0} = 17\frac{ps}{km.nm}$ (p. 42-44),

1.2. $\sigma = 10^{-3}$, $\lambda_0 = 870\,nm$, $D_{PMD} = 0{,}5\frac{ps}{\sqrt{km}}$, $D_{\lambda_0} = -80\frac{ps}{km.nm}$ (p. 45-57),

1.3. $\sigma = 10^{-5}$, $\lambda_0 = 1312\,nm$, $D_{PMD} = 0{,}6\frac{ps}{\sqrt{km}}$, $D_{\lambda_0} = 0\frac{ps}{km.nm}$ (p. 47-50),

Sub-samples for within the second example (l = 100 km):

2.1. $\sigma = 2.10^{-4}$, $\lambda_0 = 1312\,nm$, $D_{PMD} = 0\frac{ps}{\sqrt{km}}$, $D_{\lambda_0} = 0\frac{ps}{km.nm}$ (p. 50-53)

2.2. $\sigma = 10^{-5}$, $\lambda_0 = 1550\,nm$, $D_{PMD} = 0{,}7\frac{ps}{\sqrt{km}}$, $D_{\lambda_0} = 17\frac{ps}{km.nm}$ (p. 53-55)

Example 1: $l = 50$ km

1.1.1. $\sigma = 2.10^{-4}$, $\lambda_0 = 870\,nm$, $D_{PMD} = 0\frac{ps}{\sqrt{km}}$, $D_{\lambda_0} = -80\frac{ps}{km.nm}$

Spectra for output o:

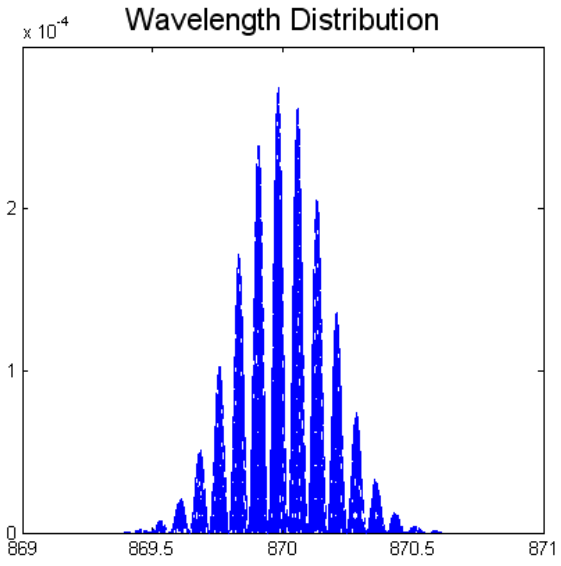

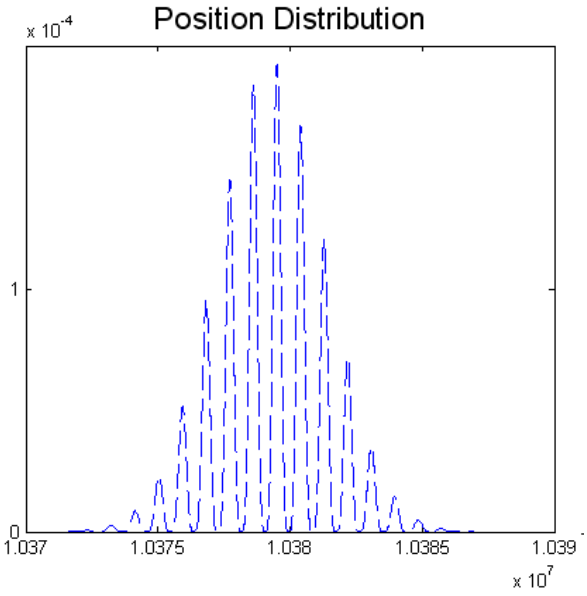

Spectra for output p:

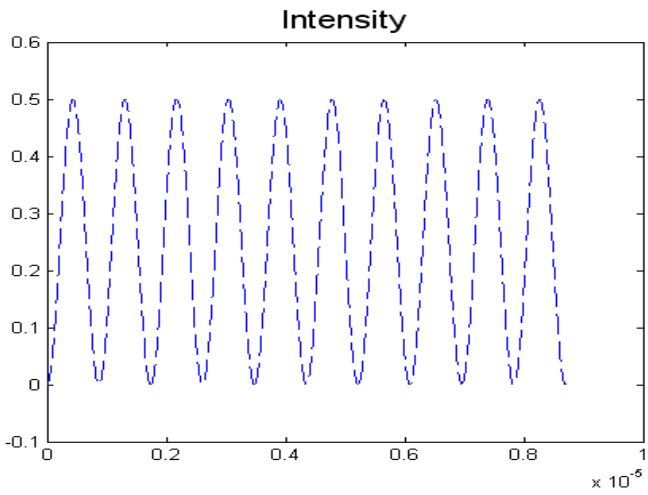

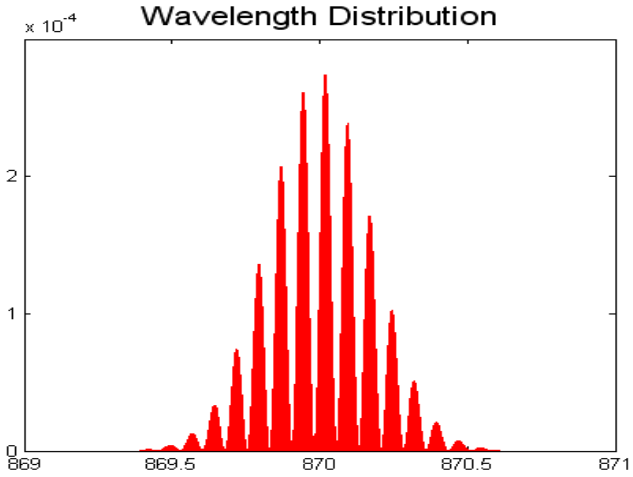

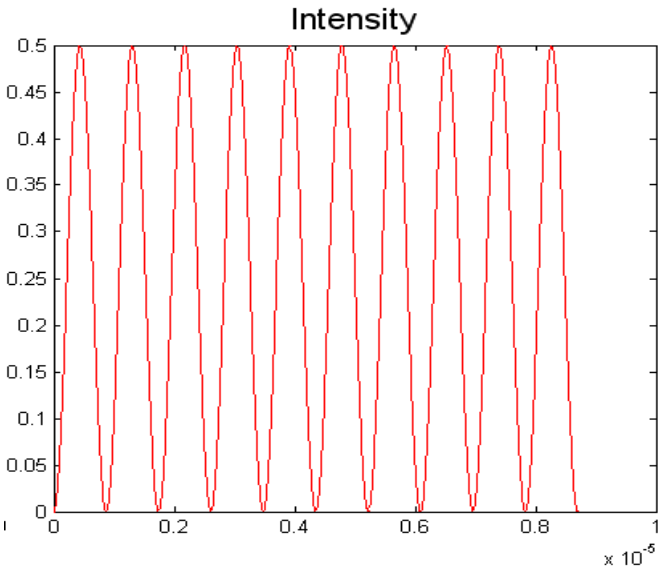

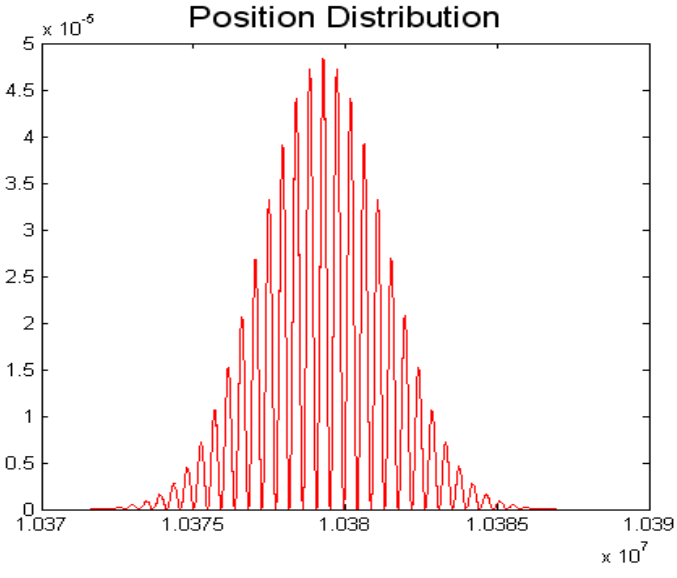

Spectra for output h:

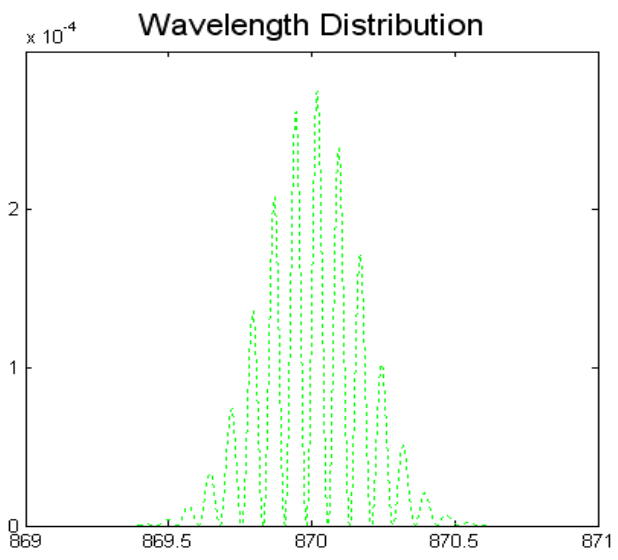

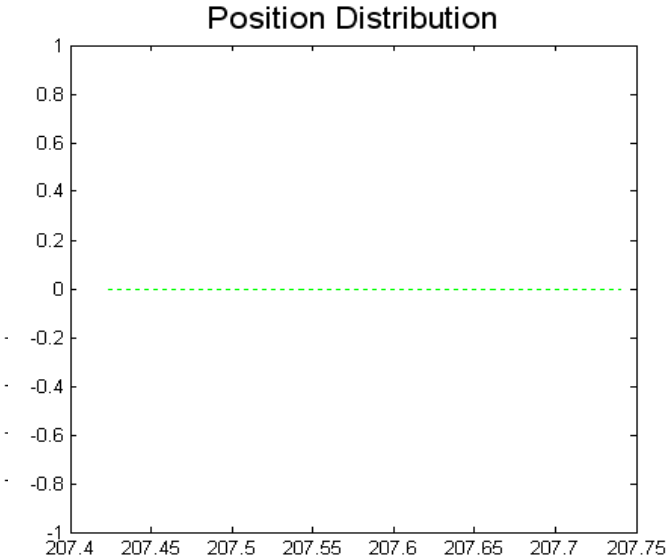

Sum of all output spectra:

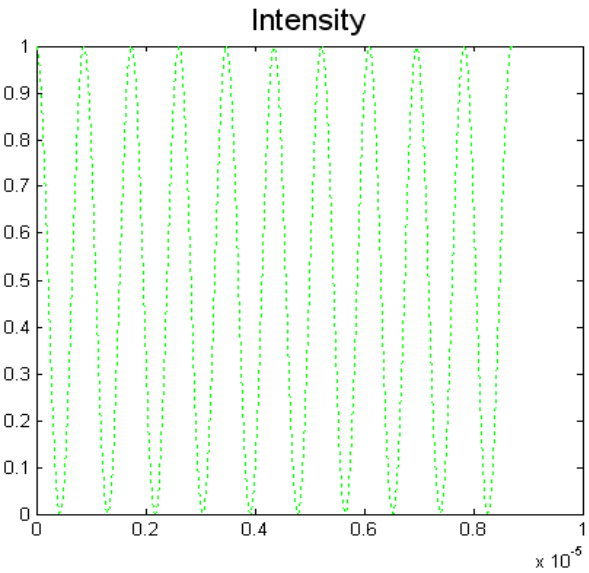

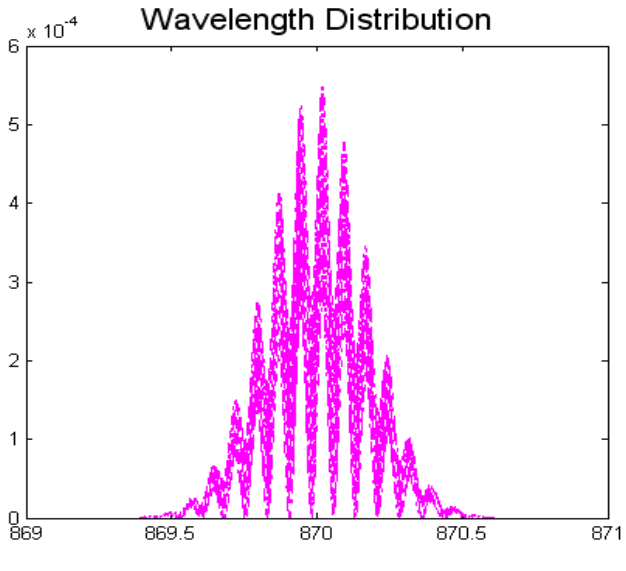

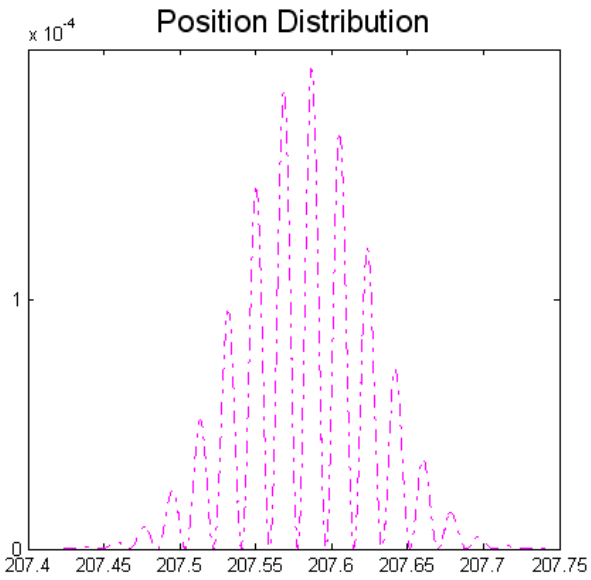

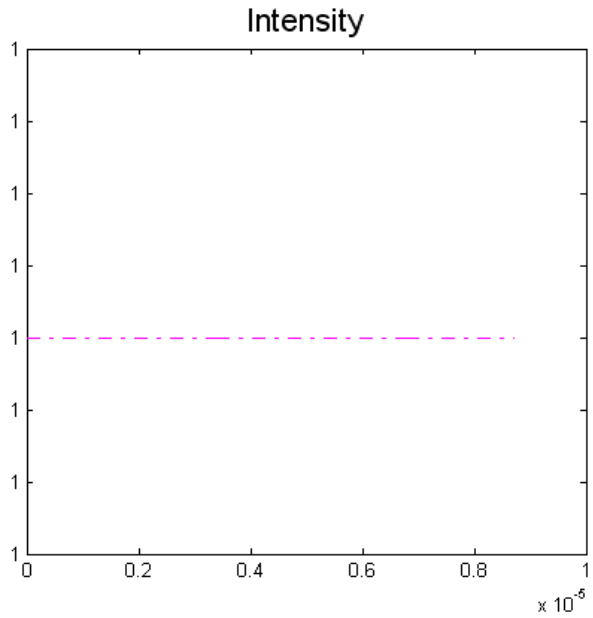

Comparison of output o & p:

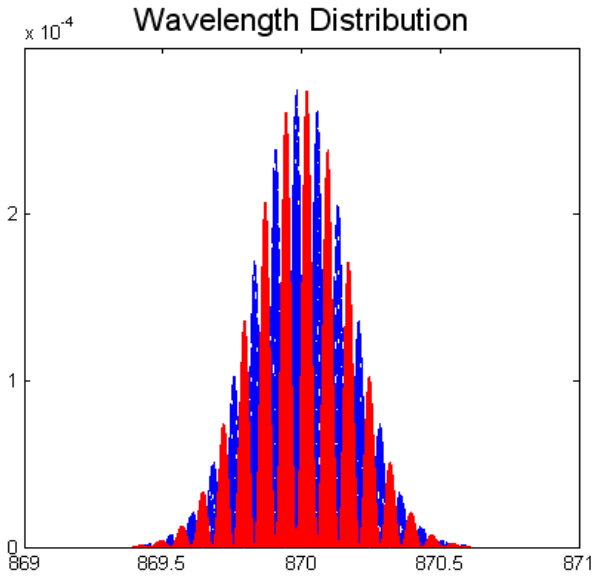

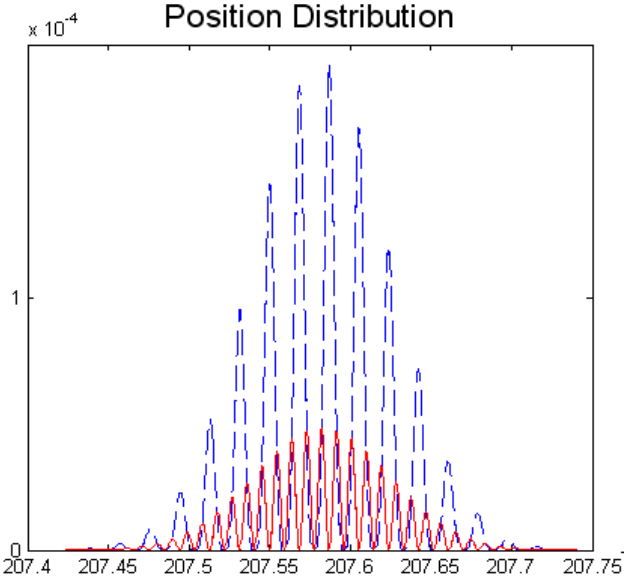

Comparison of all outputs (o & p & h & sum):

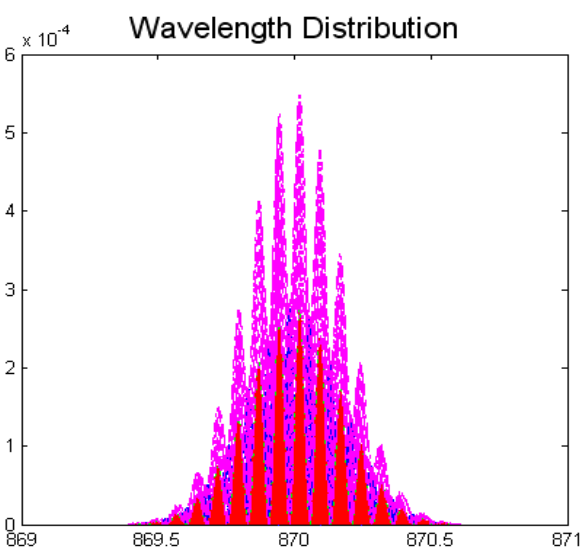

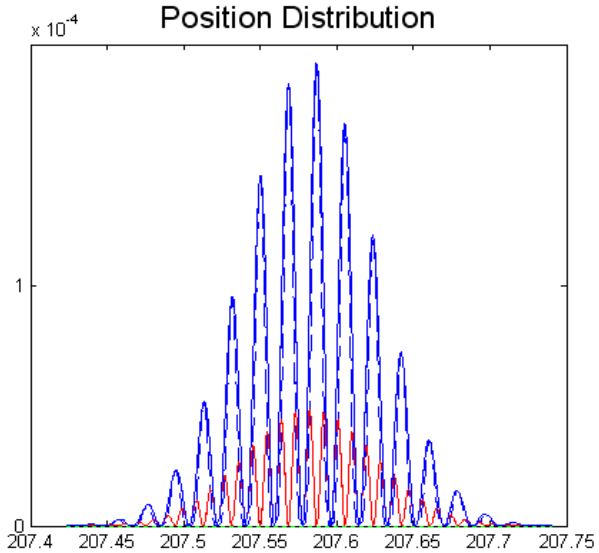

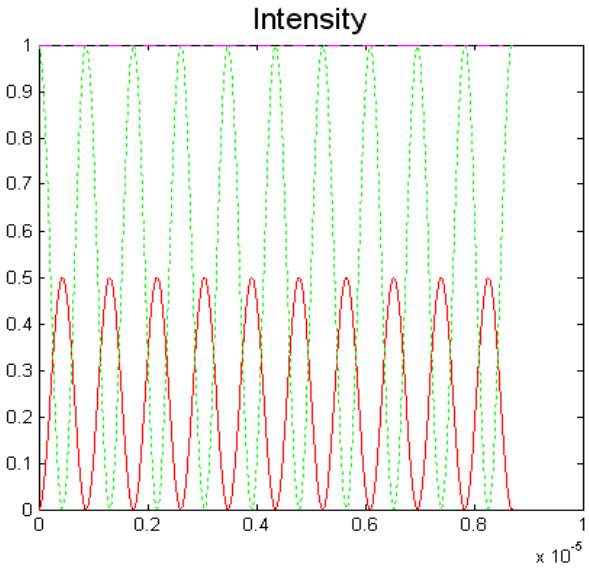

1.1.2. $\sigma = 2.10^{-4}$, $\lambda_0 = 1312\,nm$, $D_{PMD} = 0{,}2\frac{ps}{\sqrt{km}}$, $D_{\lambda_0} = 0\frac{ps}{km.nm}$

Spectra for output o:

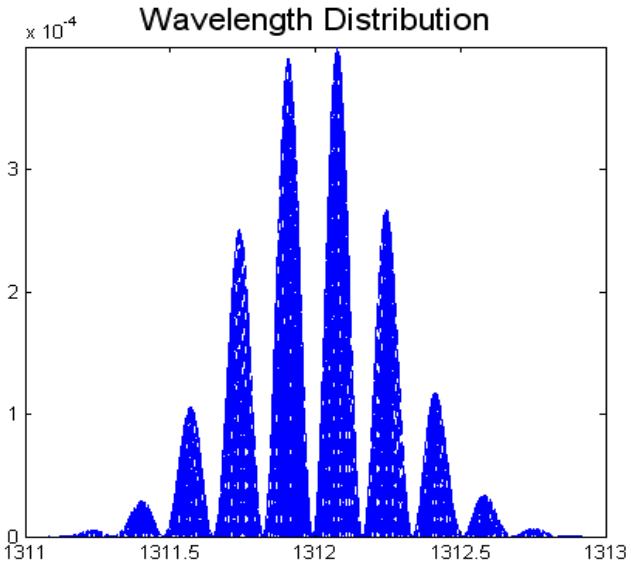

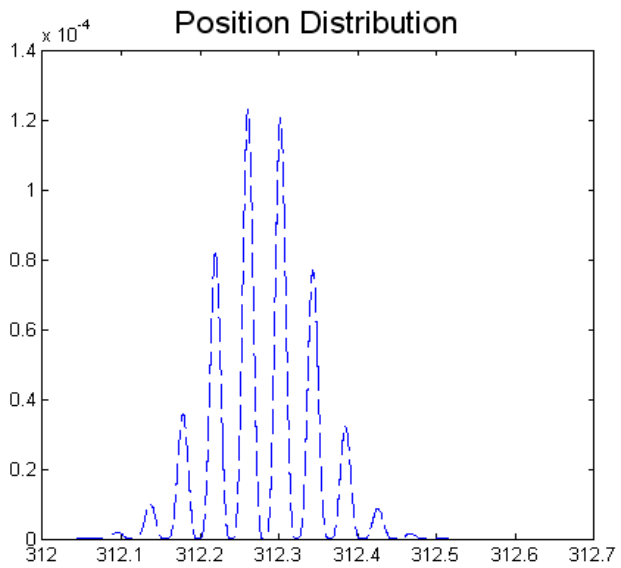

Spectra for output p:

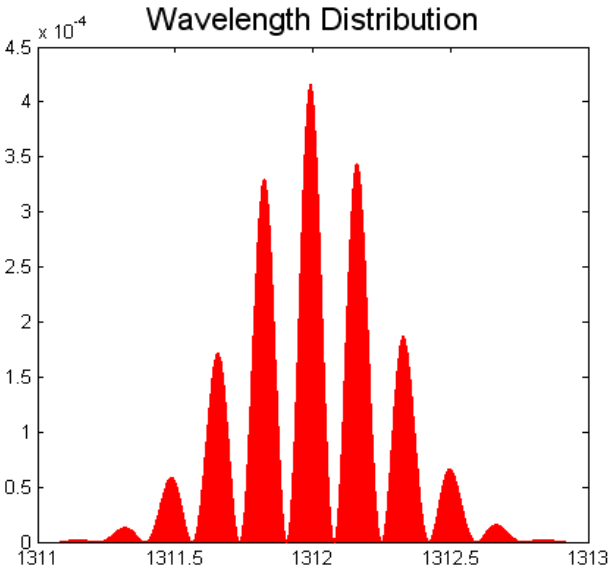

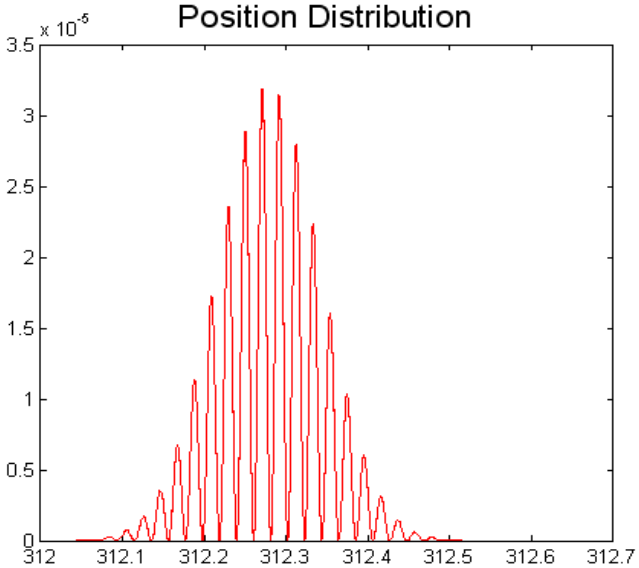

Spectra for output h:

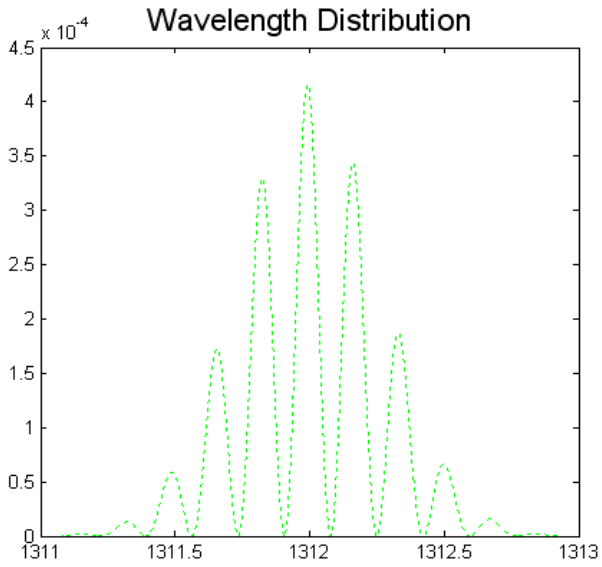

Sum of all outputs:

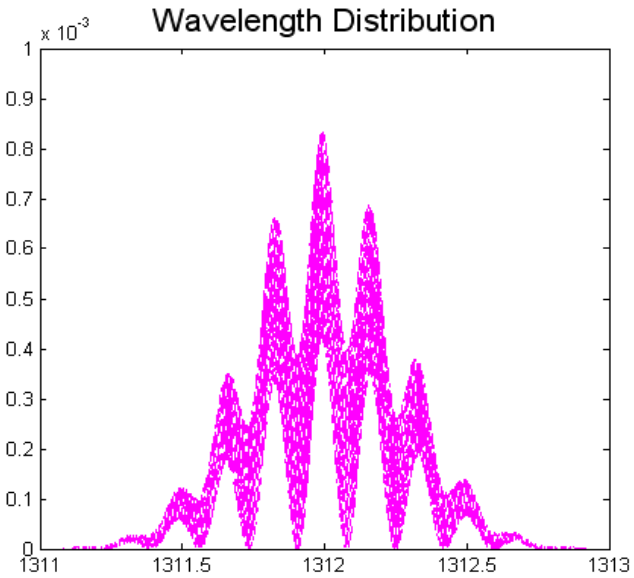

Comparison of outputs o & p:

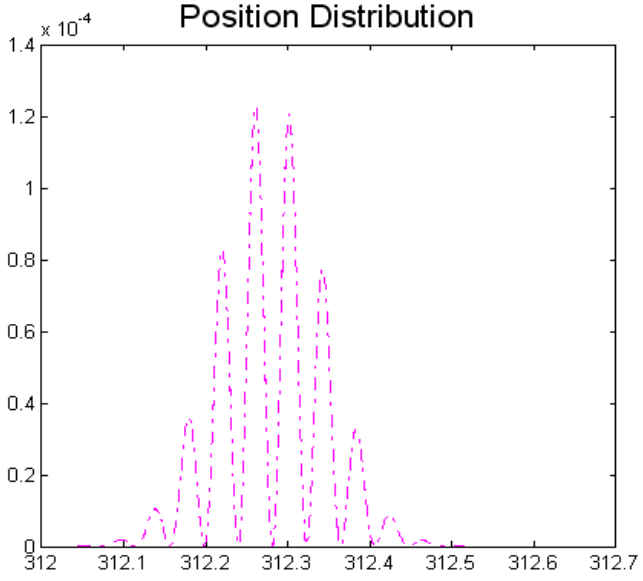

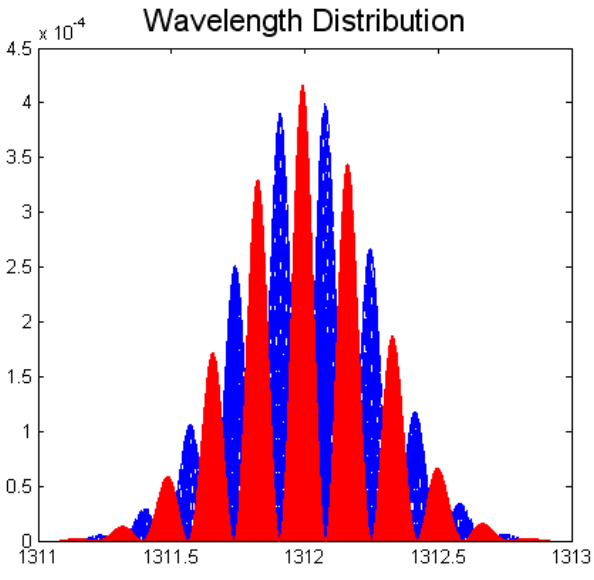

Comparison of all spectra (sum spectra is also included):

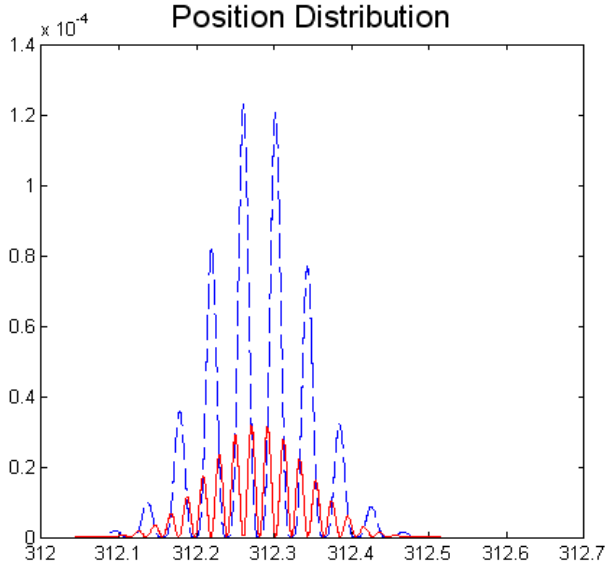

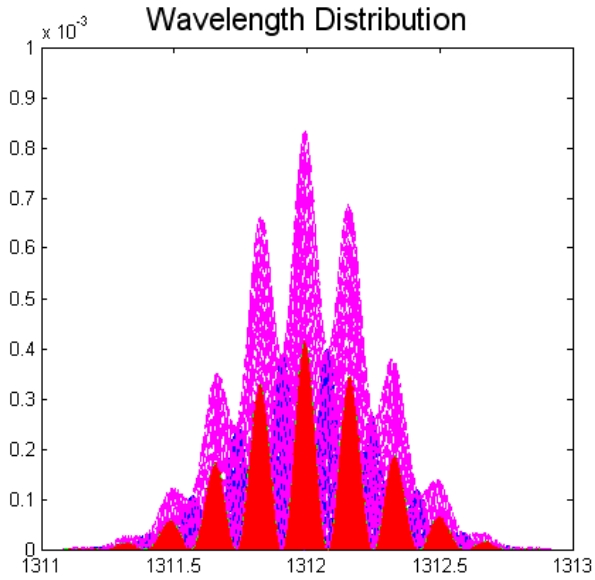

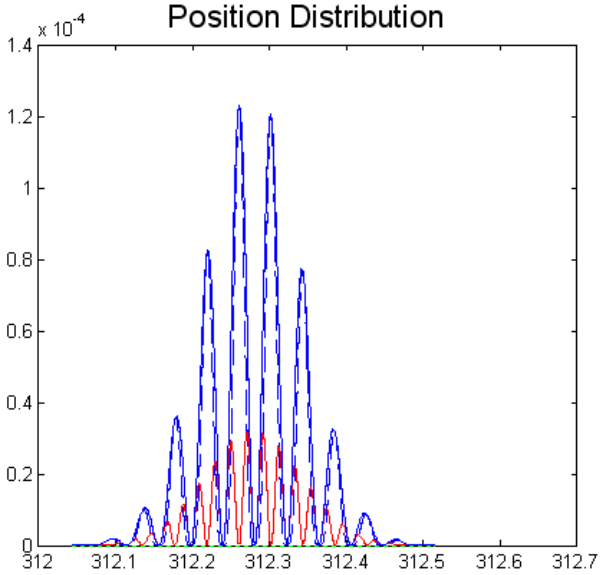

1.1.3. $\sigma = 2.10^{-4}$, $\lambda_0 = 1550\,nm$, $D_{PMD} = 0{,}9\frac{ps}{\sqrt{km}}$, $D_{\lambda_0} = 17\frac{ps}{km.nm}$

Spectra for output o:

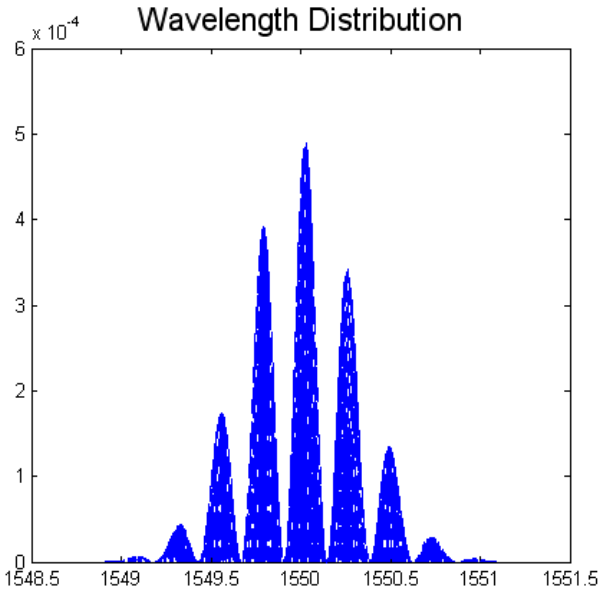

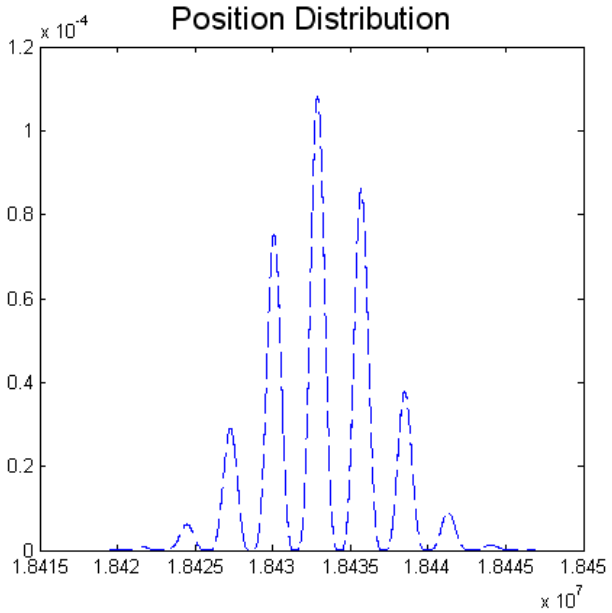

Spectra for output p:

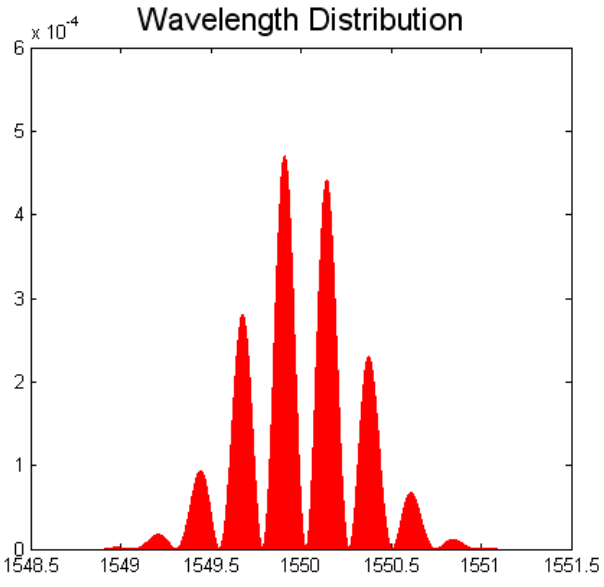

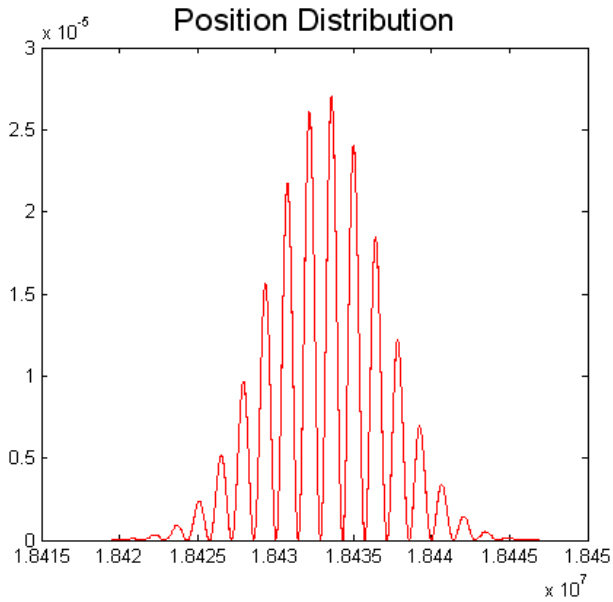

Spectra for output h:

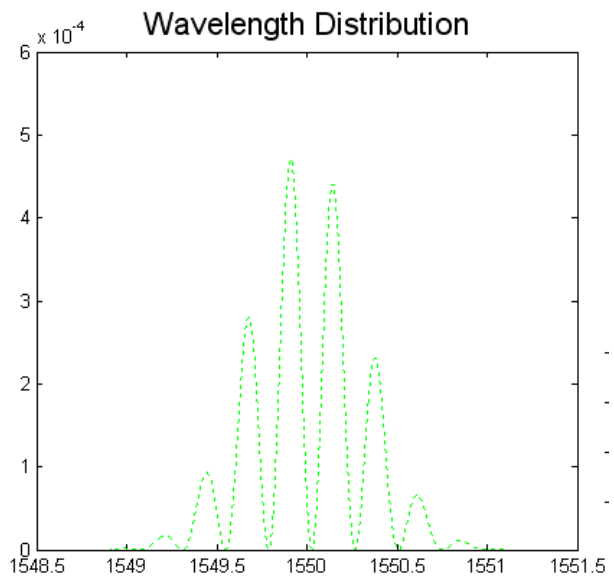

Sum of output spectra:

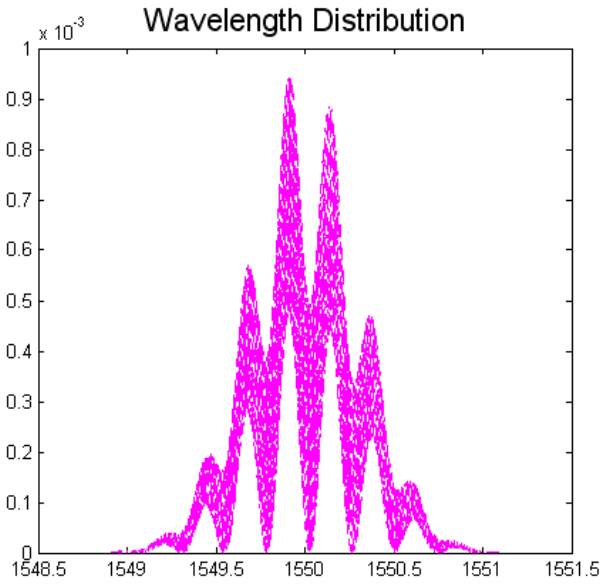

Comparison of outputs o and p:

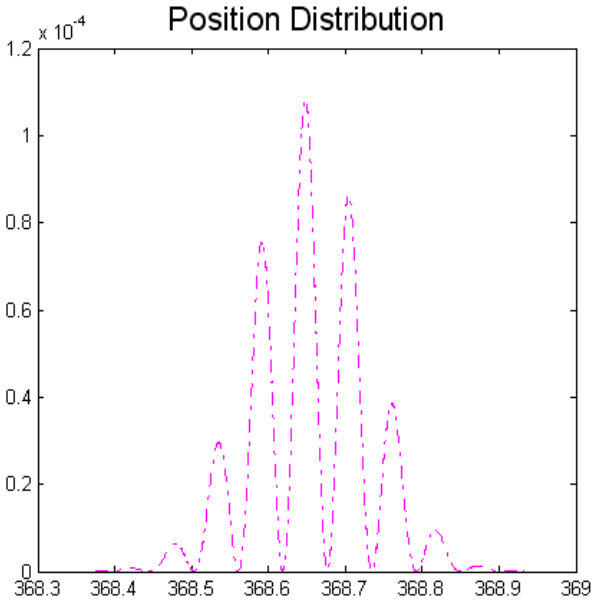

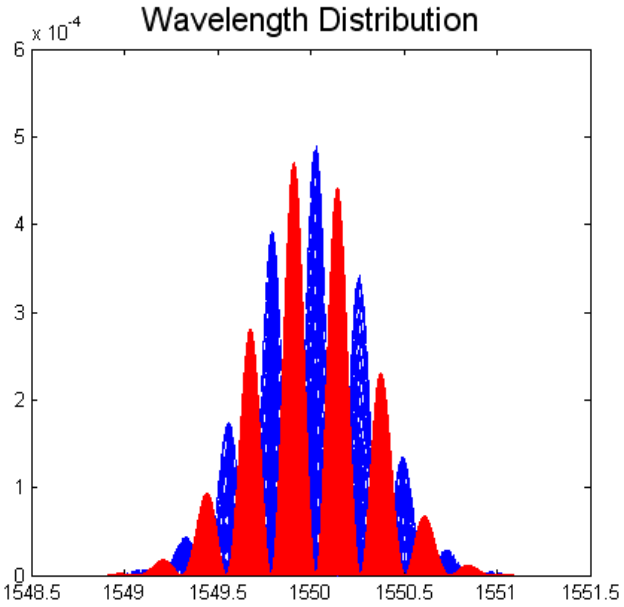

Comparison of all outputs (sum is also included):

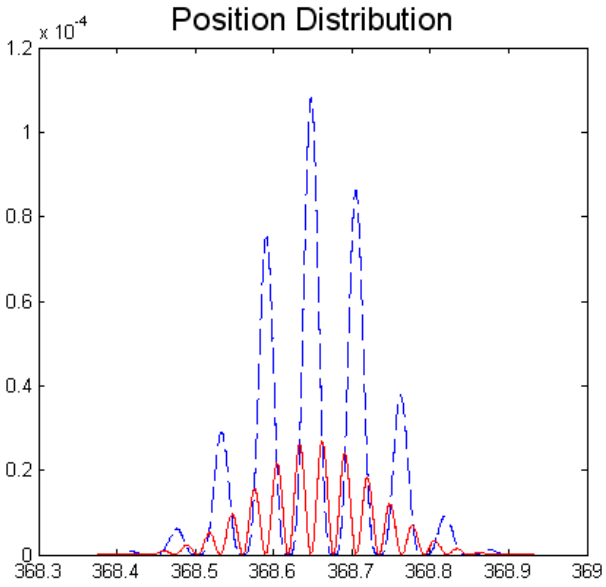

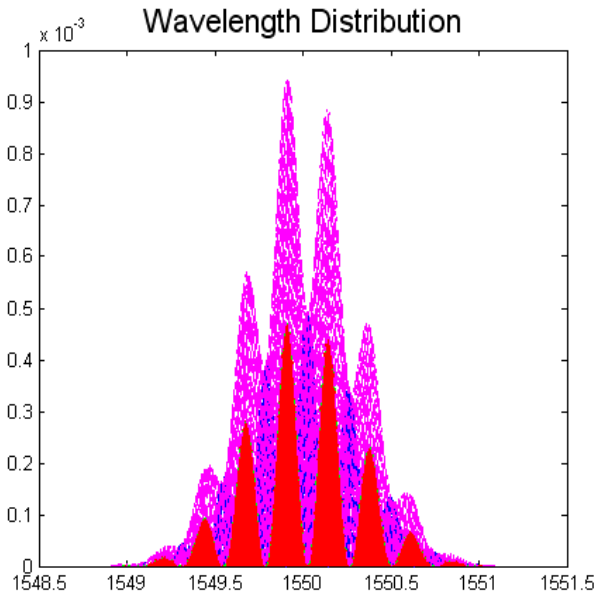

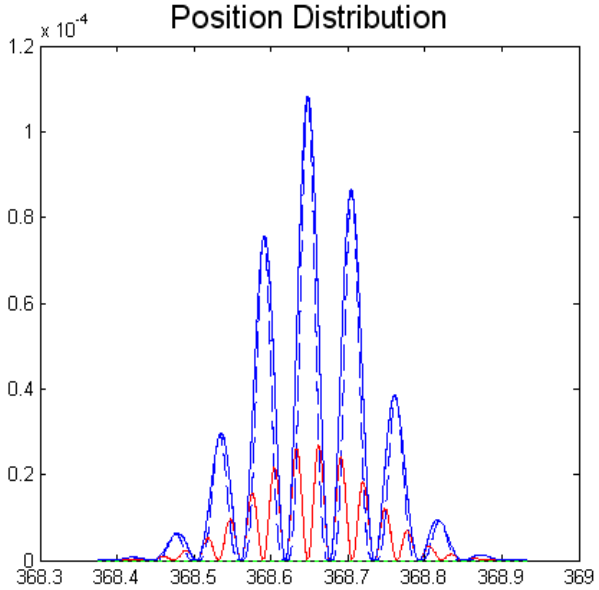

1.2. $\sigma = 10^{-3}$, $\lambda_0 = 870\,nm$, $D_{PMD} = 0{,}5\frac{ps}{\sqrt{km}}$, $D_{\lambda_0} = -80\frac{ps}{km.nm}$

Spectra for output o:

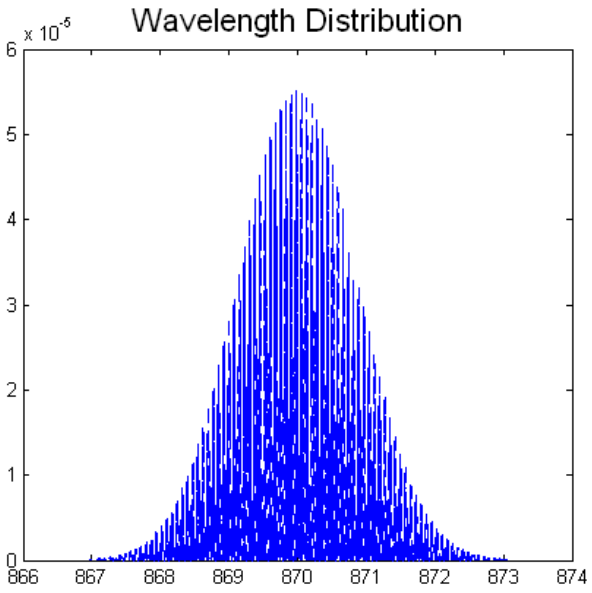

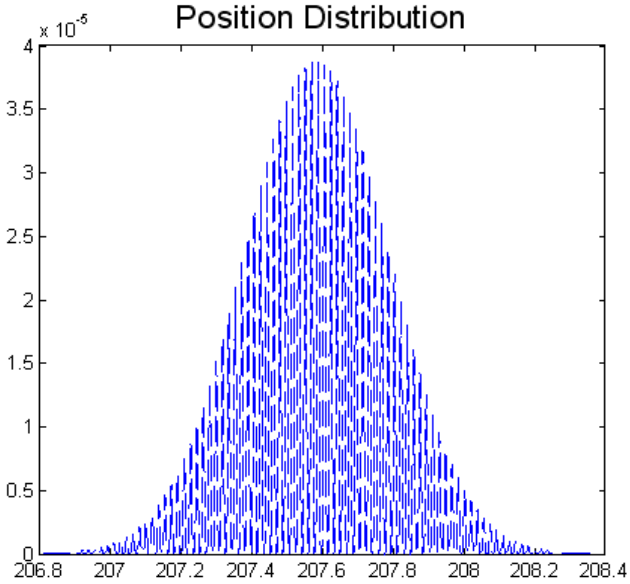

Spectra for output p:

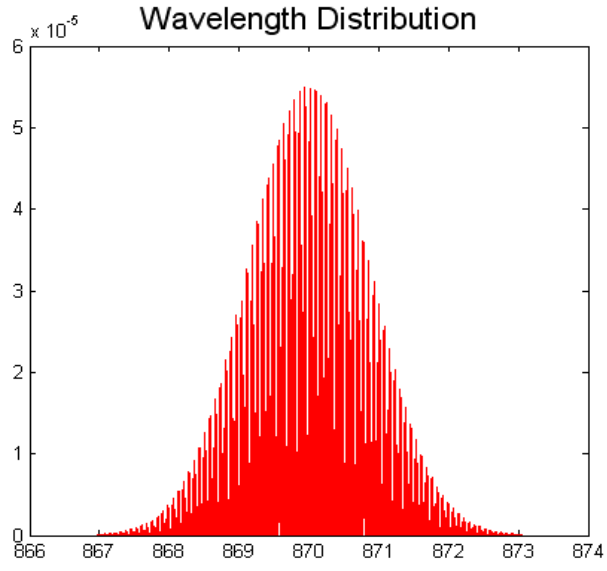

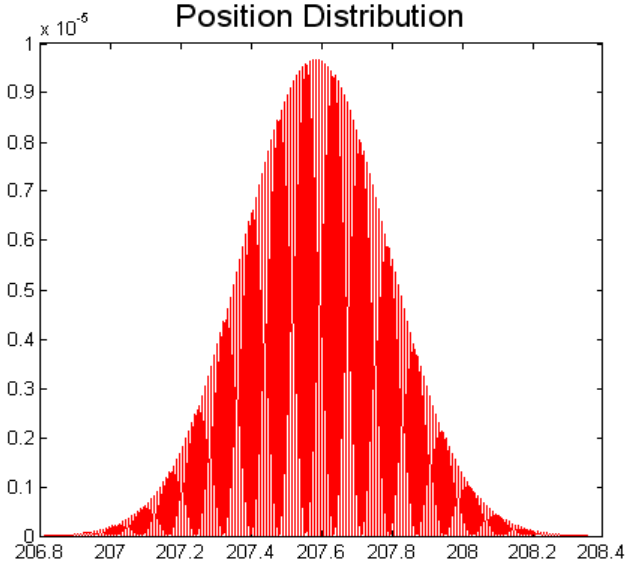

Spectra for output h:

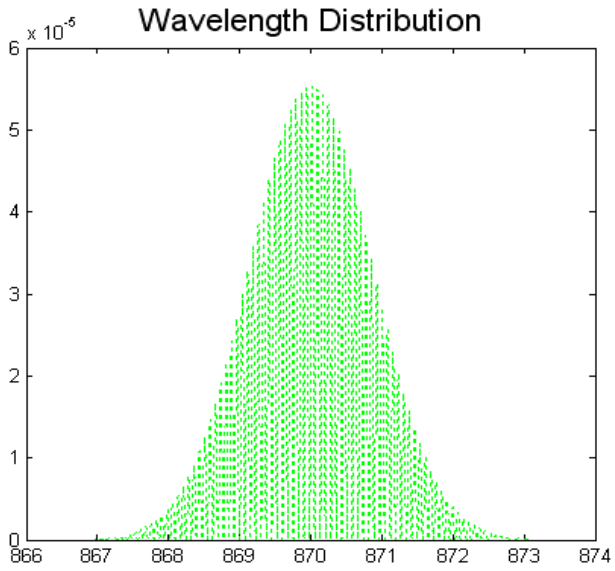

Spectra for sum of all outputs (o & p & h):

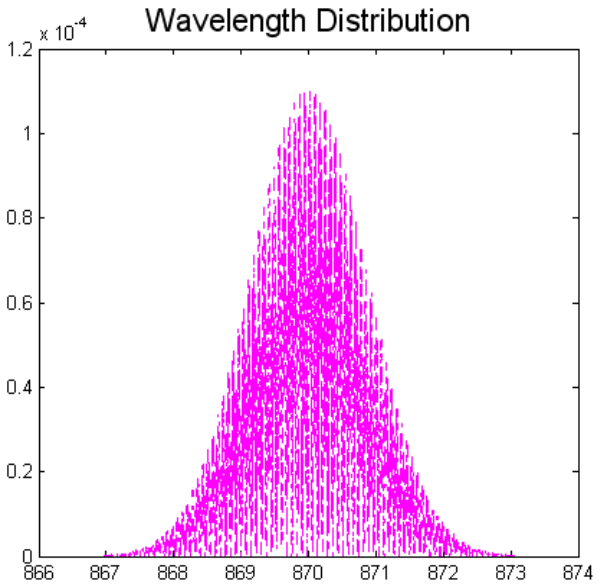

Comparison of all spectra (o & p & h & sum):

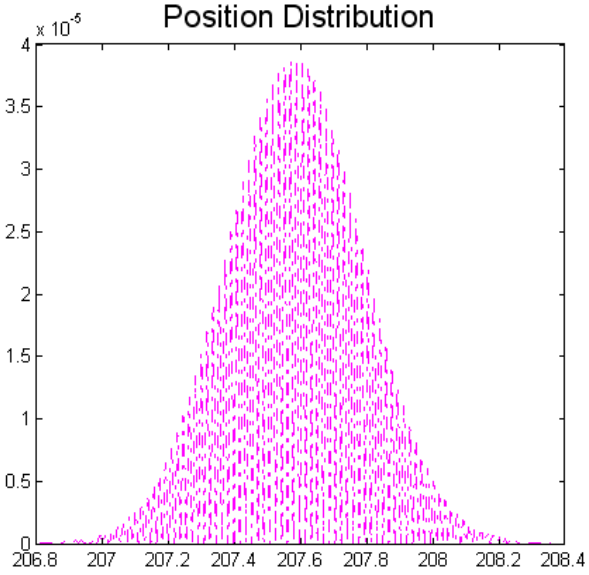

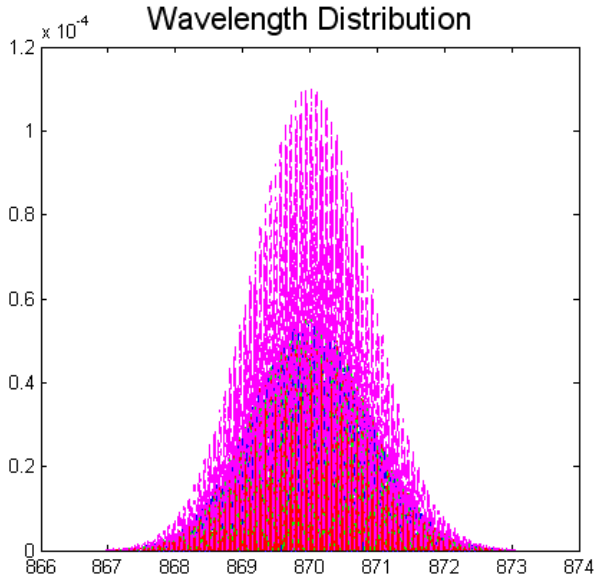

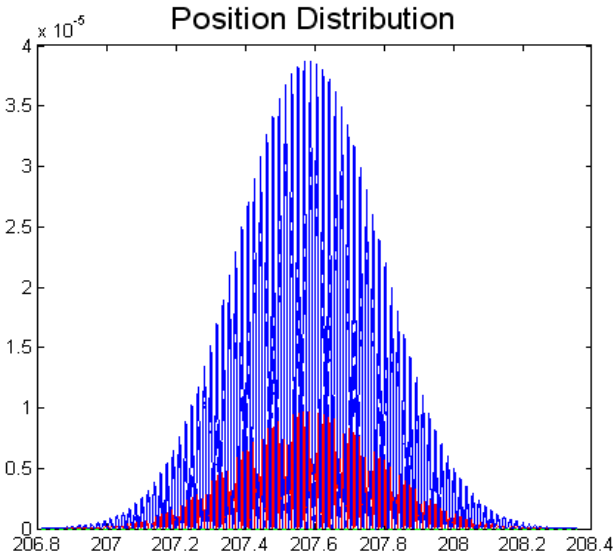

1.3. $\sigma = 10^{-5}$, $\lambda_0 = 1312\,nm$, $D_{PMD} = 0{,}6\frac{ps}{\sqrt{km}}$, $D_{\lambda_0} = 0\frac{ps}{km.nm}$

Spectra for output o:

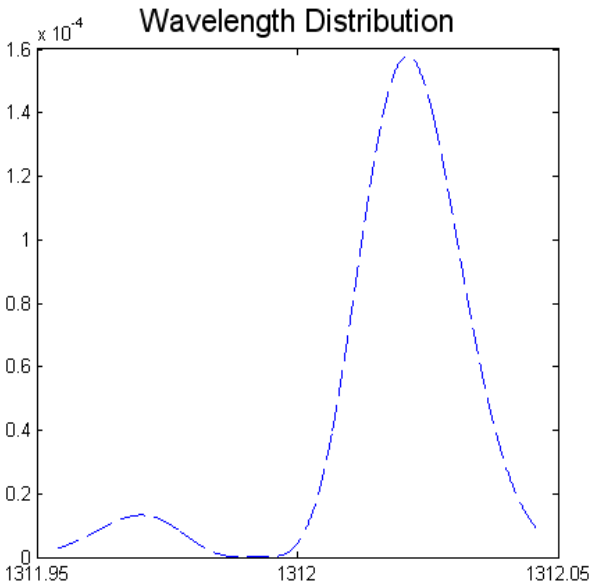

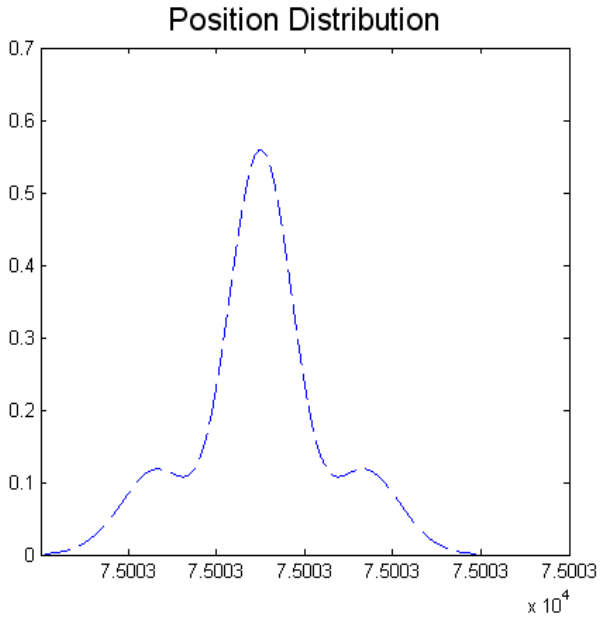

Spectra for output p:

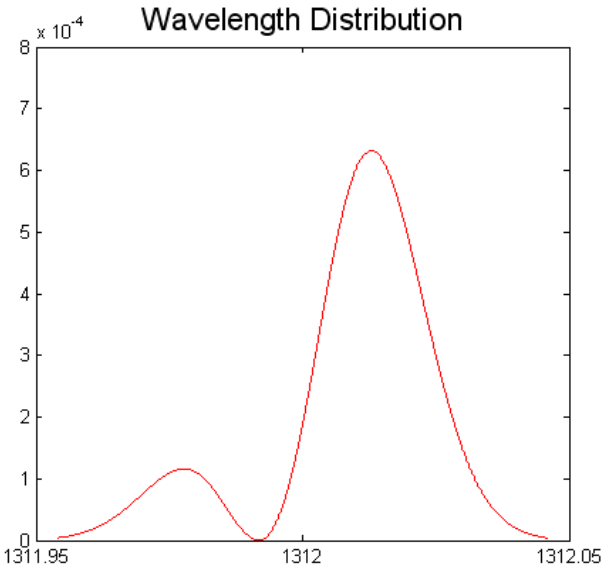

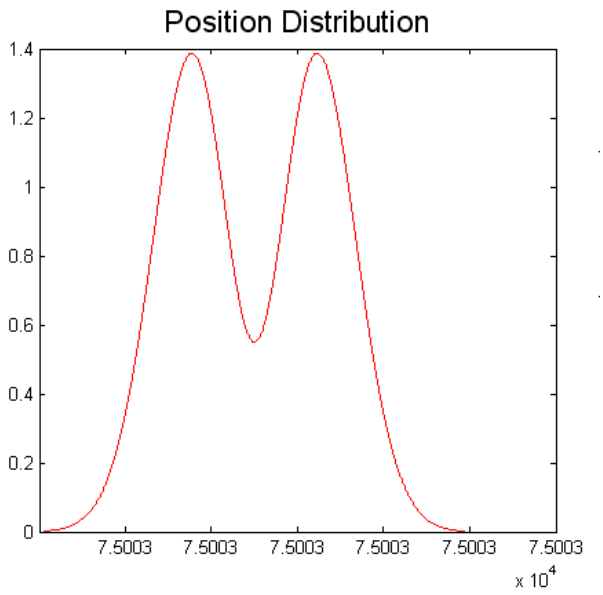

Spectra for output h:

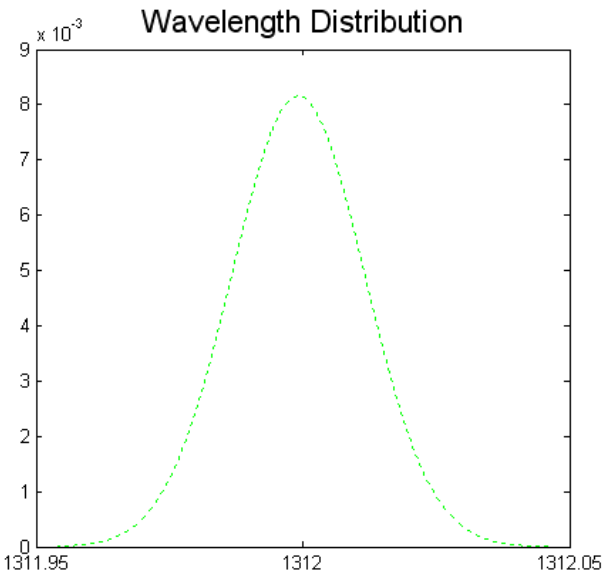

Spectra for sum of all outputs:

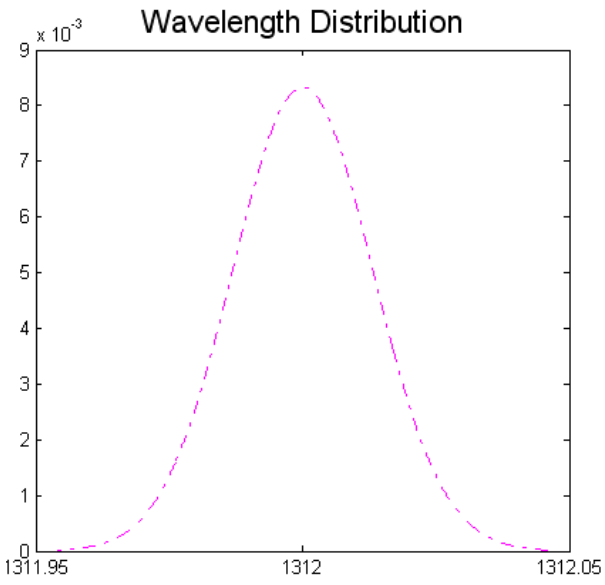

Comparison of outputs o & p:

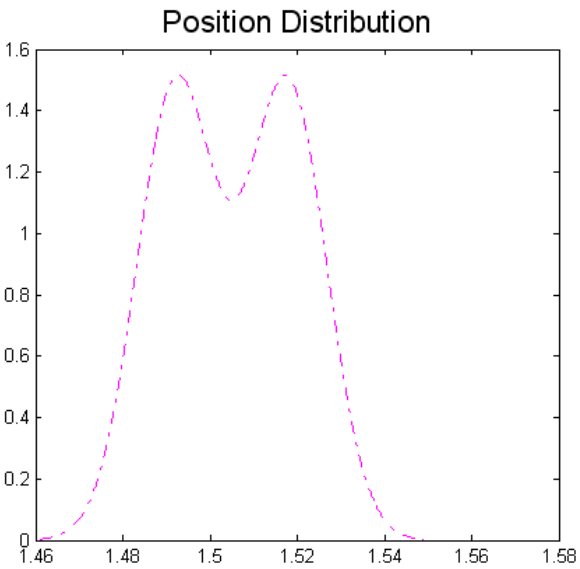

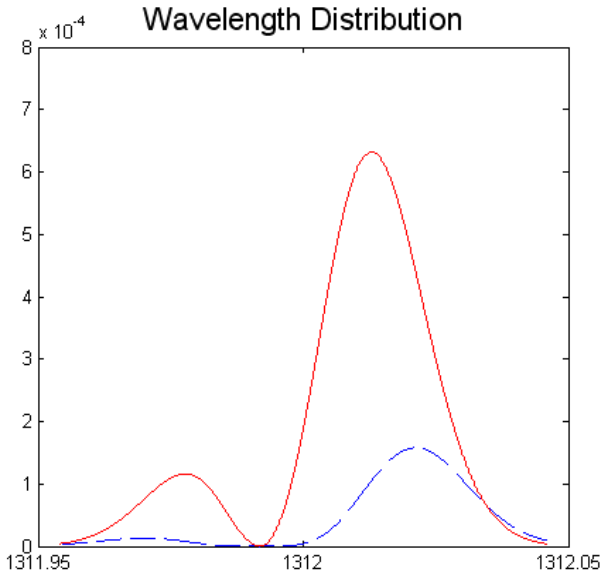

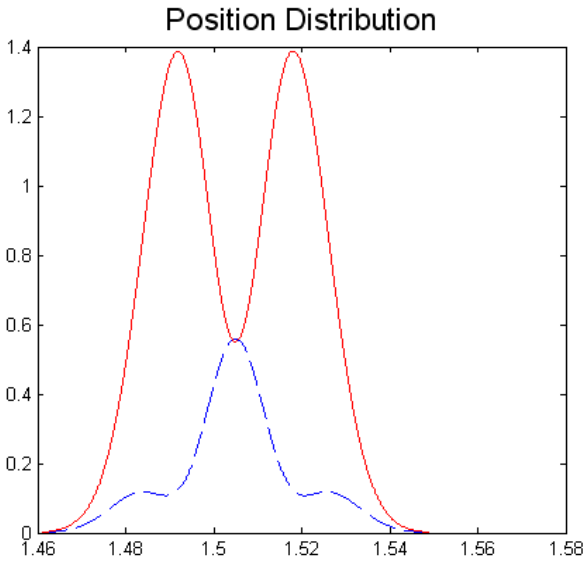

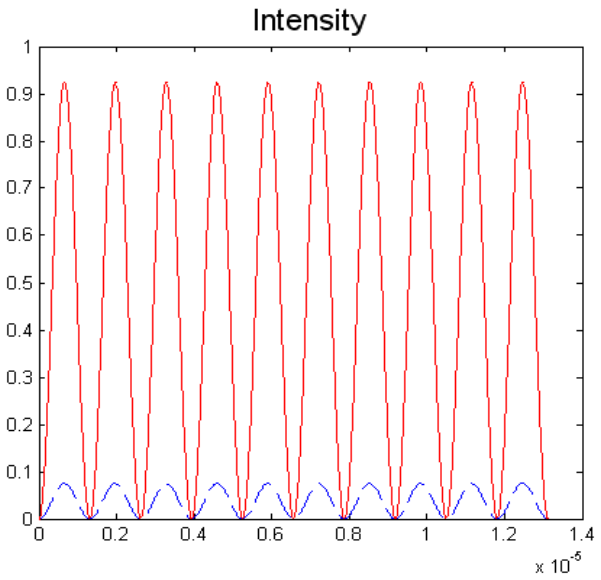

Comparison of all outputs (o & p & h & sum):

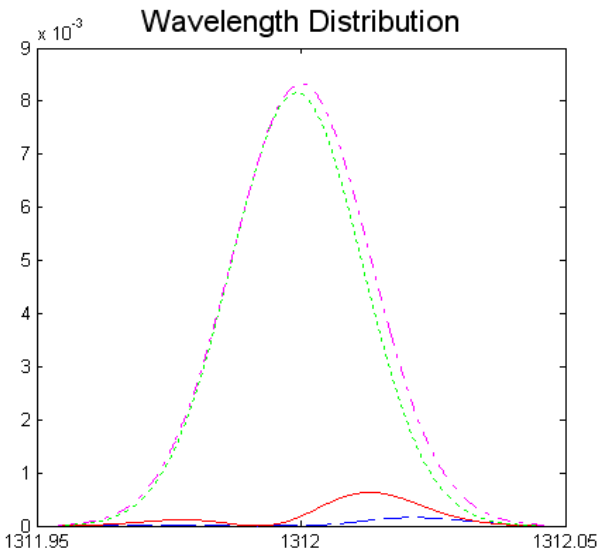

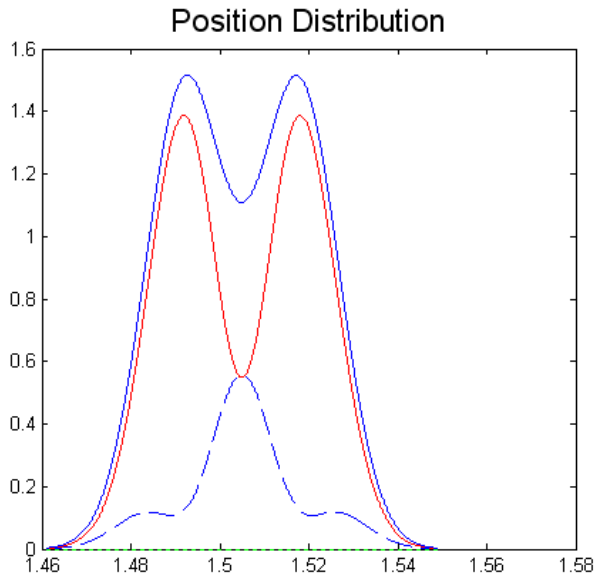

Example 2: $l = 100\ \mathrm{km}$

2.1. $\sigma = 2.10^{-4}$, $\lambda_0 = 1312\,nm$, $D_{PMD} = 0\frac{ps}{\sqrt{km}}$, $D_{\lambda_0} = 0\frac{ps}{km.nm}$

Spectra for output o:

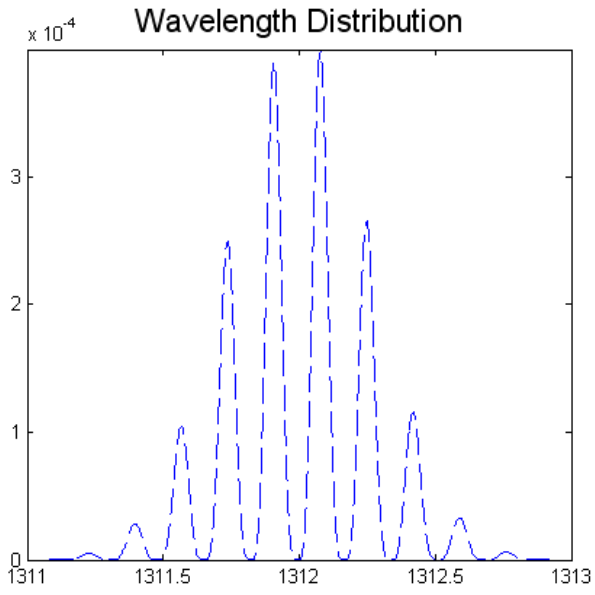

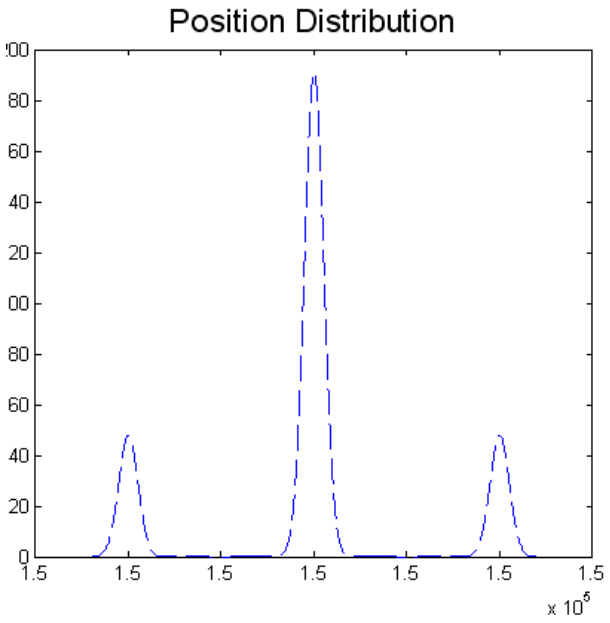

Spectra for output p:

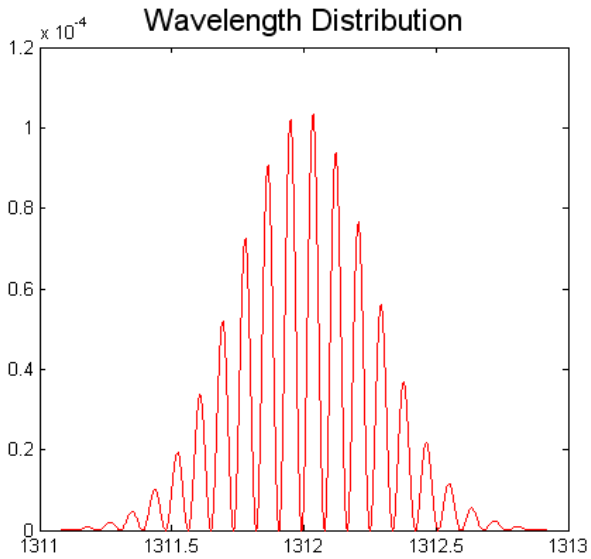

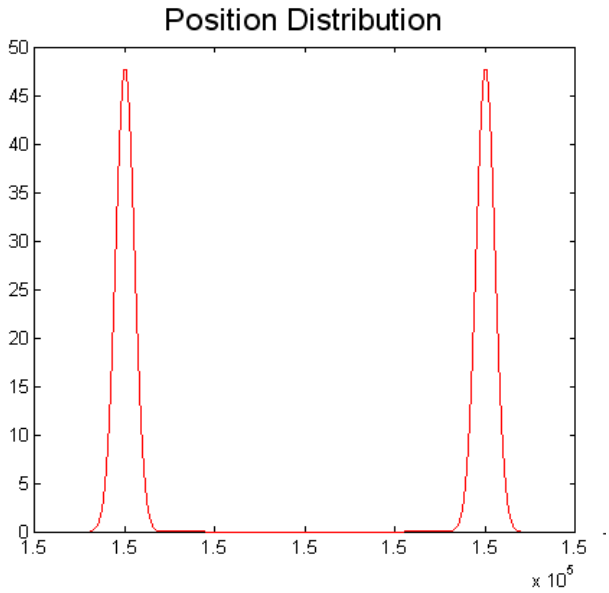

Spectra for output h:

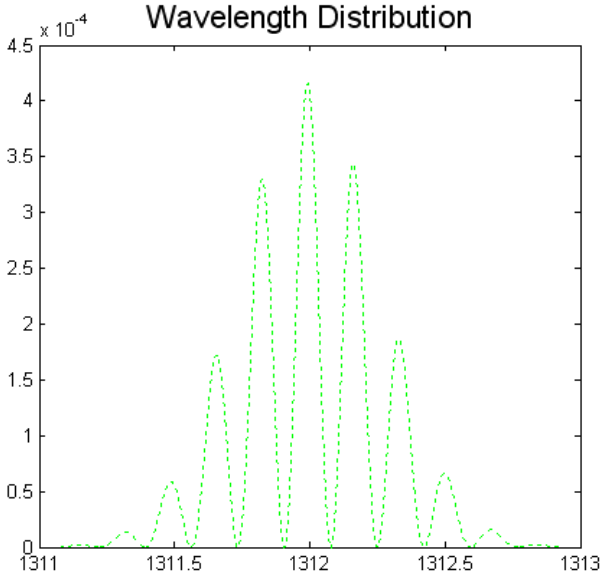

Spectra for sum of all outputs:

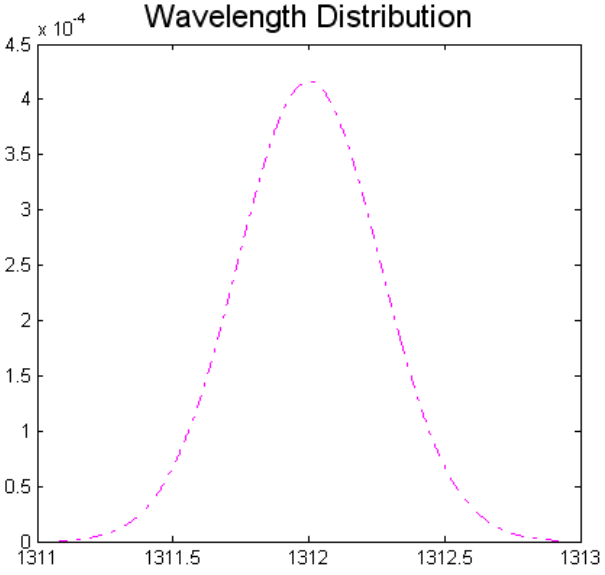

Comparison of o & p:

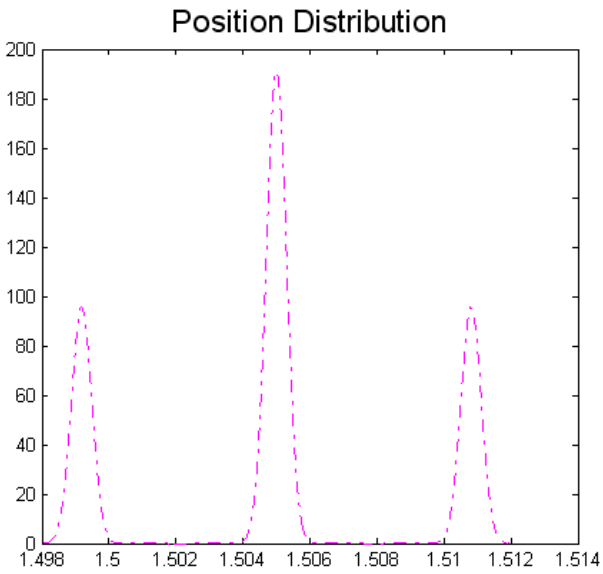

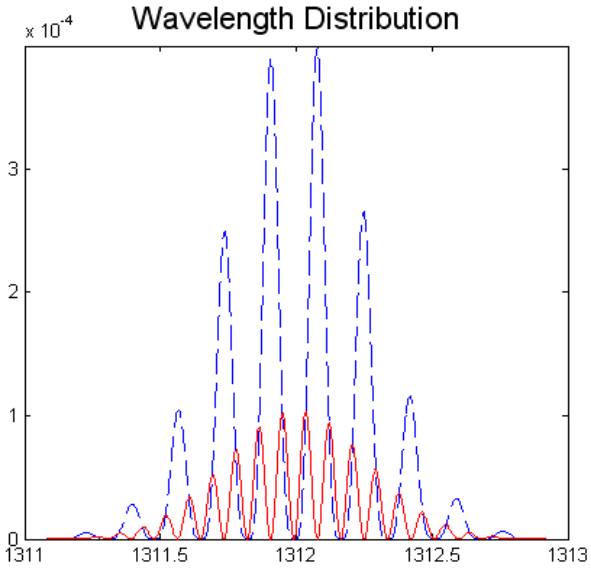

Comparison of all spectra (h & o & p & sum):

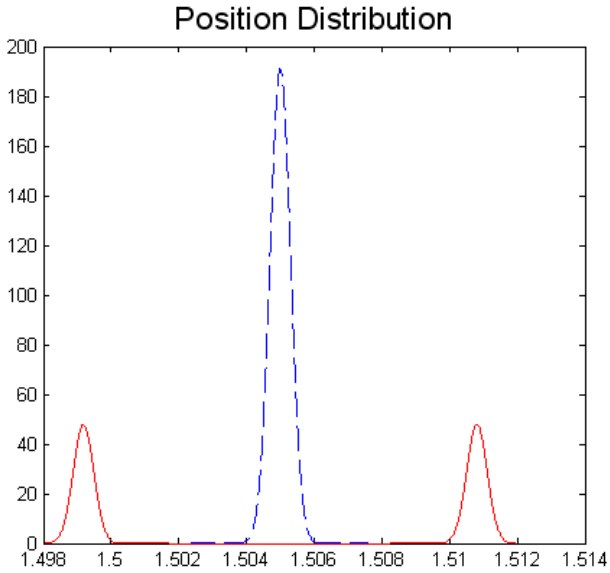

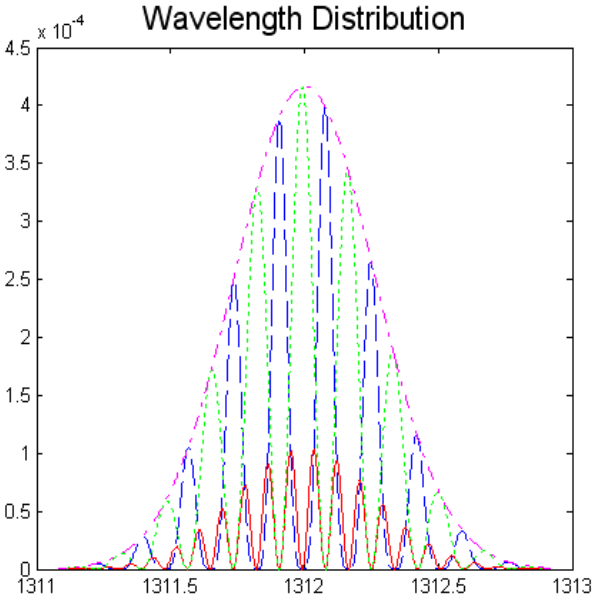

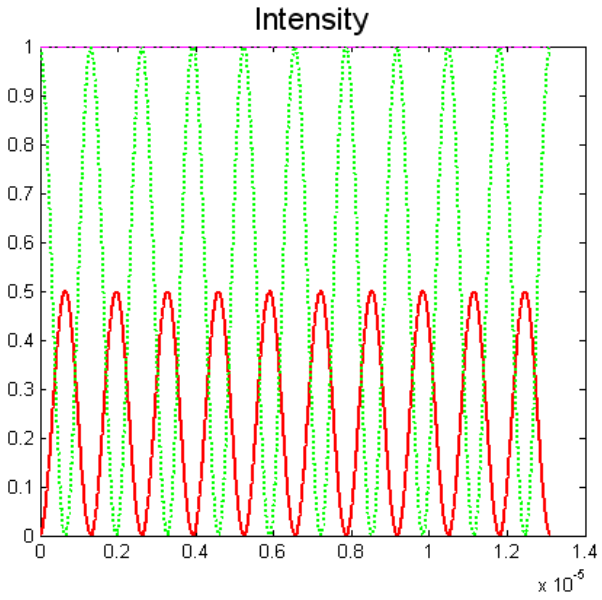

2.2. $\sigma = 10^{-5}$, $\lambda_0 = 1550\,nm$, $D_{PMD} = 0{,}7\frac{ps}{\sqrt{km}}$, $D_{\lambda_0} = 17\frac{ps}{km.nm}$

Spectra for output o:

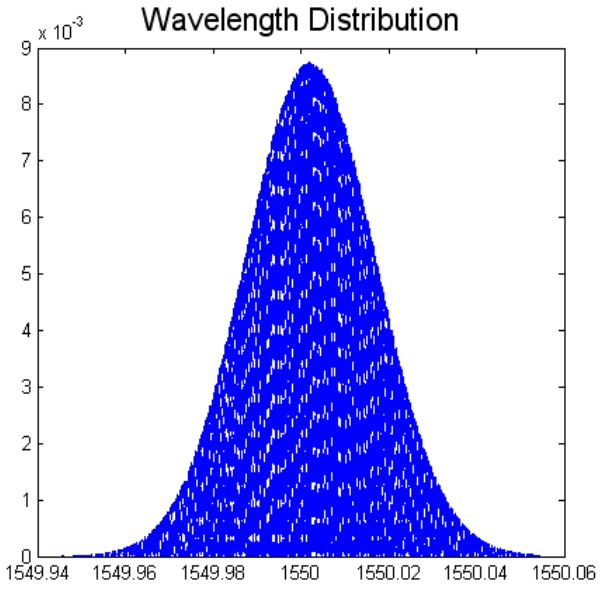

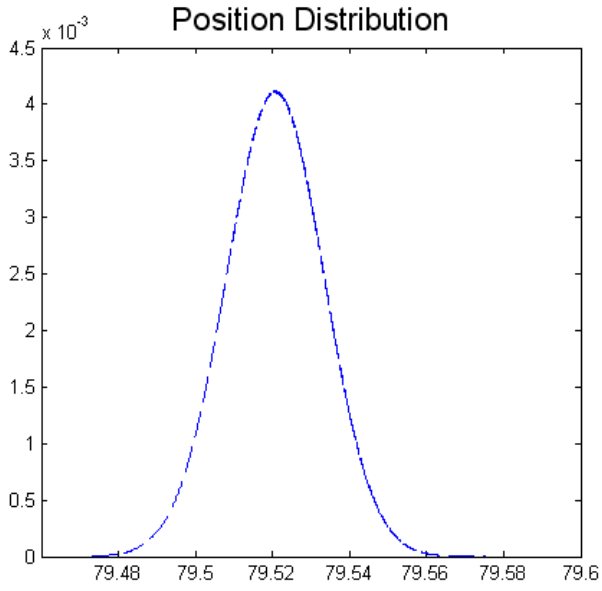

Spectra for output p:

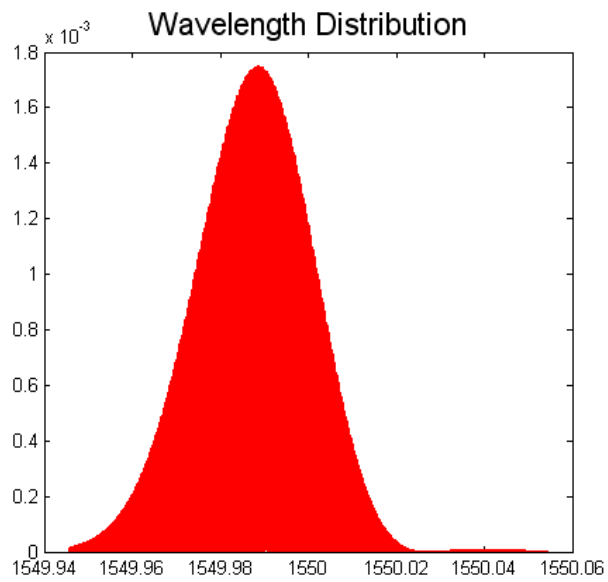

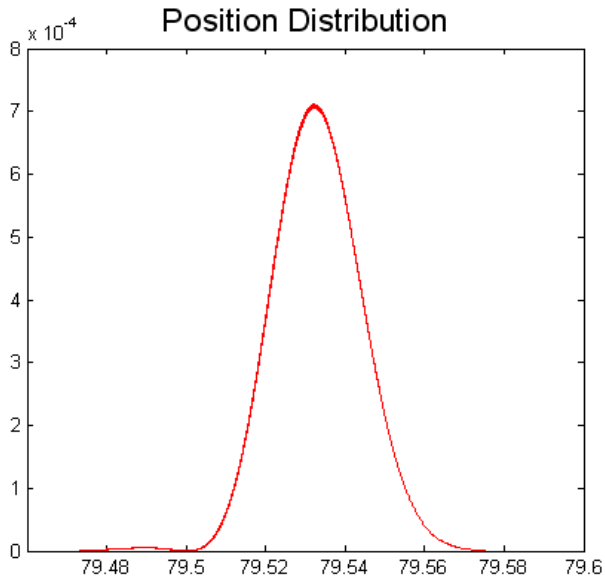

Spectra for output h:

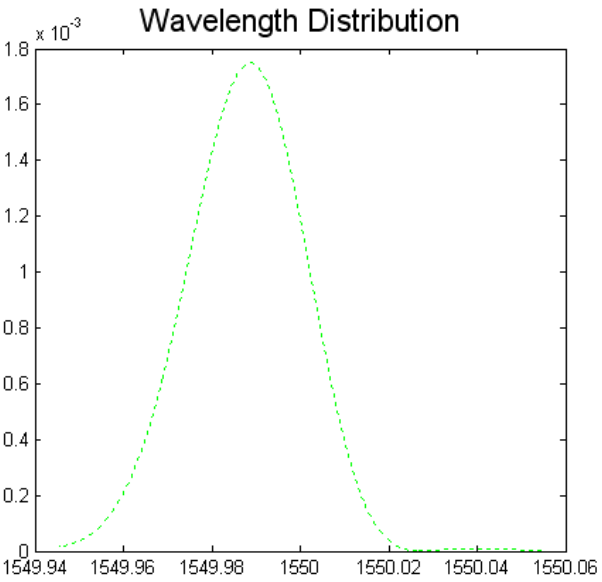

Comparison of outputs o & p:

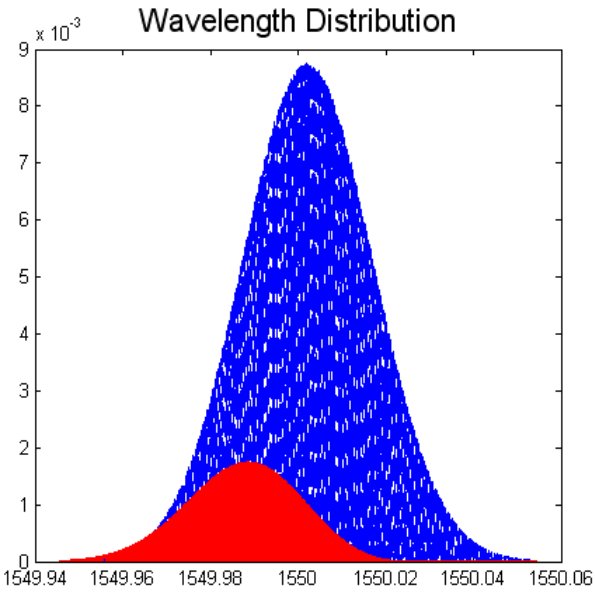

Comparison of all outputs (o & p & h & sum):

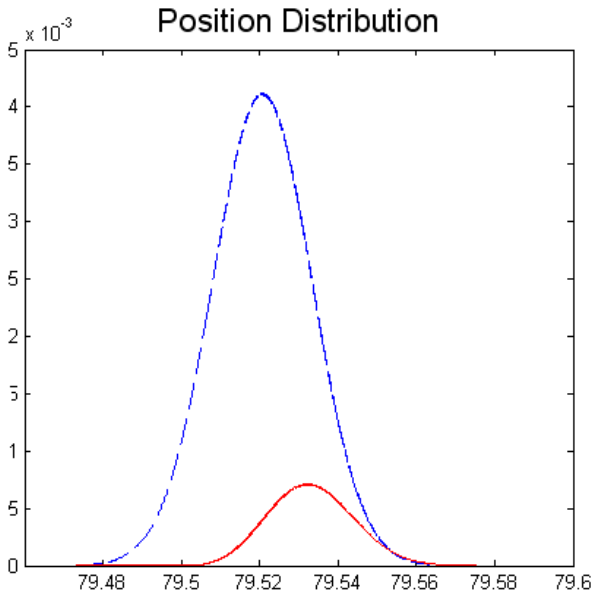

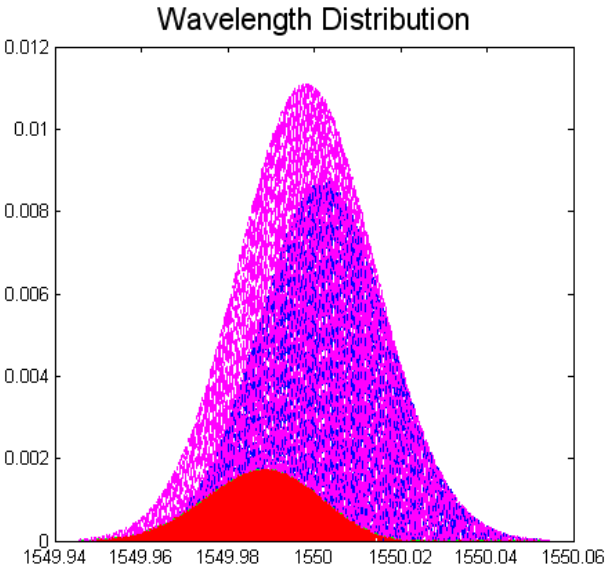

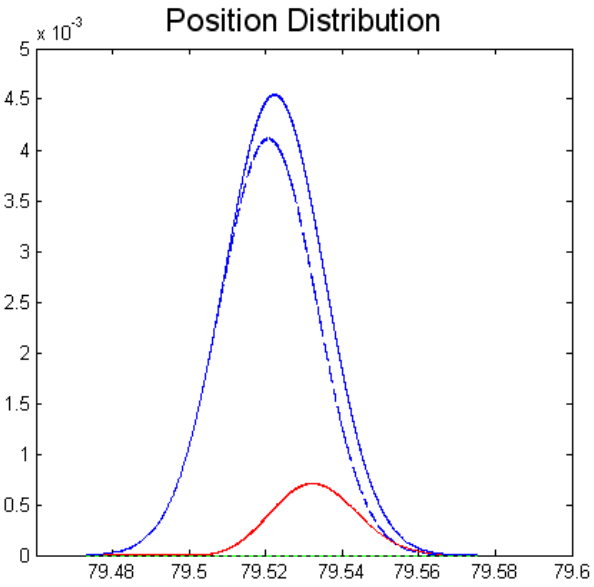

C. Results and Discussion

The effects of CD and PMD are illustrated by dint of some examples on the position, wavelength and intensity spectra. We tried to snapshot changes in terms of position, wavelength or intensity as much as possible.

In example 1.1.1($\sigma = 2.10^{-4}$, $\lambda_0 = 870\,nm$, $D_{PMD} = 0\,\frac{ps}{\sqrt{km}}$, $D_{\lambda_0} = -80\,\frac{ps}{km.nm}$, p. 34-38), wavelength positions of output modes o and p without PMD and with negative CD show an unrealistic scheme, since it is very difficult to keep $D_{PMD} = 0$ for such a long path (50 km) as we learn in earlier topics. Although example 1.1.1 is not the ideal scheme, it is a hypothetical model, because comprising PMD is absolutely necessary as well as the CD. But this try provides us with a chance to experience what if the PMD factor would not exist, and a negative CD factor would exist in a quantum cryptography communication system (thanks our MATLAB GUI program, so that we can input any arbitrary value for each parameter according to wish, and then let us see the result by pleasure). Here at outputs o and p even h, wavelength distributions are very close (almost same), while position distribution of output o is higher than position distribution of output p. These can be seen also in their comparative demonstrations. Position distribution of output h is always zero and intensity of it always oscillates between 0 and 1, since it has no connection to 2. MZ. That is why we will skip position distribution and intensity of output h in next examples. As we look at total output distributions, total wavelength distribution is naturally greater than its additive components. Additionally, total intensity is always 1, because of photon conservation. It is going to be skipped in the next examples as well. These total schemes can be achieved through λ -distribution functions due to [5].

Example 1.1.2. ($\sigma = 2.10^{-4}$, $\lambda_0 = 1312\,nm$, $D_{PMD} = 0{,}2\,\frac{ps}{\sqrt{km}}$, $D_{\lambda_0} = 0\,\frac{ps}{km.nm}$, p. 39-41) represents a possible, realistic well set-up communication system, because PMD coefficient is very low and CD coefficient is compensated totally. This example represents a greater wavelength λ_0 =1312 nm than the wavelength in former example, and can be inferred from each output (o, p, h) and total output. There is also an increment for position distributions, so that the spectra are shifted to greater x-values by about +105 m. Modulations therefore mostly depend on PMD and CD coefficients.

In example 1.1.3. ($\sigma = 2.10^{-4}$, $\lambda_0 = 1550\,nm$, $D_{PMD} = 0{,}9\,\frac{ps}{\sqrt{km}}$, $D_{\lambda_0} = 17\,\frac{ps}{km.nm}$, p. 42-44), we see a very bad condition to use a communication channel. In both of position distribution and wavelength distribution, we encounter bigger scales with bigger dispersion coefficients than in former 2 examples. However, it is clear to experience a failure and information losses in phase coding.

Example 1.2. ($\sigma = 10^{-3}$, $\lambda_0 = 870\,nm$, $D_{PMD} = 0{,}5\,\frac{ps}{\sqrt{km}}$, $D_{\lambda_0} = -80\,\frac{ps}{km.nm}$, p. 45-47). In this example we increased $\delta\lambda$, and again decreased λ_0 to 870 nm. Through a relatively high PMD value and negative CD value, in all 3 outputs Gauss curves occur for wavelength distribution as well as position distribution. And it is interesting to see that these Gauss curves full of intense oscillations. This means, in this scheme γ_{ij} has a crucial effect on oscillations.

Another example with the same σ value is 1.3.($\sigma = 10^{-3}$, $\lambda_0 = 1312\,nm$, $D_{PMD} = 0{,}6\,\frac{ps}{\sqrt{km}}$, $D_{\lambda_0} = 0\,\frac{ps}{km.nm}$, p. 47-50). This is also a realistic scheme in nature without CD and with a high PMD by $D_{PMD} = 0{,}6\,ps/\sqrt{km}$. As earlier examples above the quantities κ and ε comes into the

scene through B_{total} ($B_{total}{}^2 = \sqrt{B_{CD}{}^2 + B_{PMD}{}^2}$) . Despite the fact that D_{λ_0} is zero, the shifting amounts are affected poorly due to high D_{PMD} value. We therefore see that in position spectra, the wave packets are close together, the interfering part of the spectrum probably causes some modifications of the spectrum which are not desired cases.

Example 2.1.($\sigma = 2.10^{-4}$, $\lambda_0 = 1312\,nm$, $D_{PMD} = 0 \frac{ps}{\sqrt{km}}$, $D_{\lambda_0} = 0 \frac{ps}{km.nm}$, p. 50-53) exemplifies a perfect scheme for phase coding method in quantum cryptography, even if it looks like a utopistic scheme for today. In this example, we come across neither a PMD coefficient nor a CD coefficient. Therefore it is possible to see flawless interferences for the position spectra of output o. By reason that we chose $\Delta_d = \Delta_m$, the short-long and the long-short paths are indistinguishable. Hence, shifts can be easily shifted to create separated wave packets in space or time pulses behind both 1.MZ and 2. MZ, though fiber connection length (l_g =100 km) is pretty high. These were general information for a perfect phase coding quantum cryptography scheme. Let's take a look at position distribution of output o:

There are 2 side peaks appear since the photons travel in short arms in both interferometers or take the long arms respectively, that is, the arms with the phase shifters Δ_d and Δ_m . Thereby, these two side peaks are departed from each other by value of $\Delta_d + \Delta_m = 2$ cm. Output o shows a higher peak in the middle about 4 times higher than the two side peaks. This is because of $\Delta_d = \Delta_m$ again, as mentioned above. In this case, a constructive interference occur, since the short-long and the long-short conditions are fulfilled. On the other hand, in output p's position distribution figure, a destructive interference appears due to the phase factor of the Hadamard transformation of the beam splitter and hence no peak in the middle occurs [5, 6]. Since the pulses' peaks are total separated, phase coding quantum cryptography is realized perfectly. However, this is just a hypothetical case and not possible in real. To make this example more clear, instructive and helpful, let's take a look with and without PMD version of this example below:

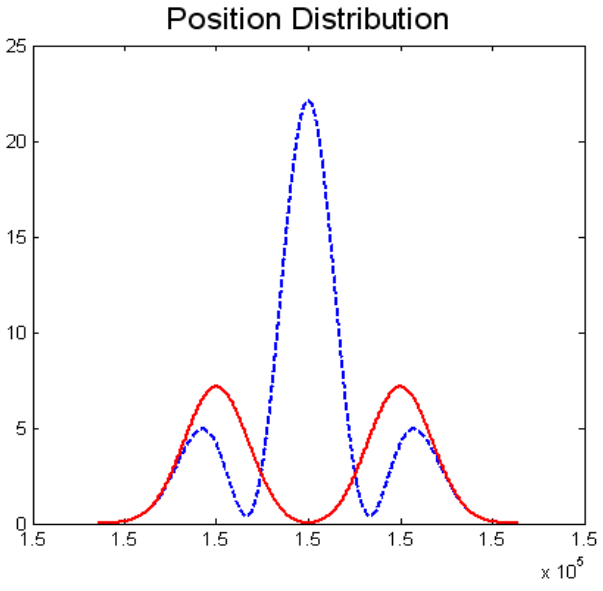

The figure on the left: σ , D_{PMD} , are changed to 3e-005 and 1 respectively, then the peaks don't get separated.

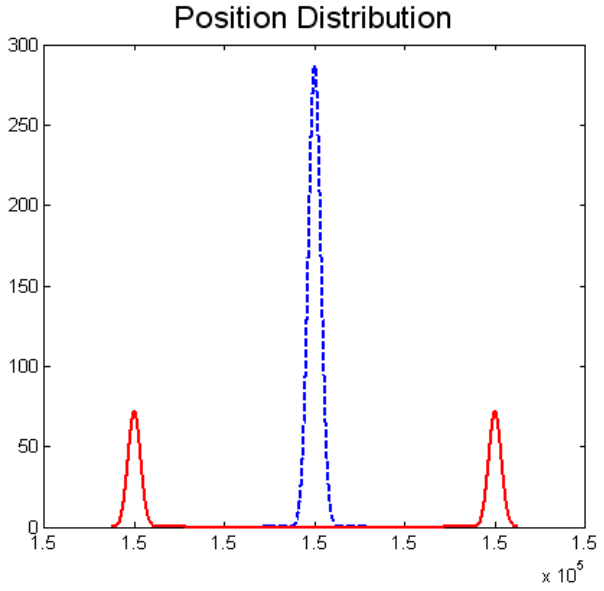

The figure on the right: σ , D_{PMD} , are chosen to 3e-004 and 0 respectively. It implies that the peaks get separated.

2.2.($\sigma = 10^{-5}$, $\lambda_0 = 1550\,nm$, $D_{PMD} = 0{,}7\frac{ps}{\sqrt{km}}$, $D_{\lambda_0} = 17\frac{ps}{km.nm}$, p. 53-55). This sub-sample includes some of the worst conditions along all examples due highness of the PMD and CD coefficients. For wavelength spectra of output o and output p, there exist Gauss curves full of intense oscillations, However, output h exhibits an empty Gauss curve. The position spectra of outputs o and p are similar to position spectra in example 1.3, so that, because of the phase shift, the interference term causes strong change between spectra.

Chapter 6

Summary and Conclusion

In this thesis, the simulations of the effects of the CD and PMD in a double Mach-Zehnder interferometer application, applied for phase coding method in quantum cryptography have been aimed to investigate. Two unbalanced Mach–Zehnder interferometers (one for Alice and one for Bob) are established one after another by a single optical fiber can be used to exchange a quantum key by the method of phase coding. As observing counts as a function of time, Bob achieves three peaks. The left one corresponds to the cases where the photons chose the short paths both in Alice's and in Bob's interferometers, while the right one corresponds to photons taking the long paths in both interferometers. Consequntly, the central peak corresponds to photons choosing the short path in Alice's interferometer and the long one in Bob's, or vice versa. If these two situations are indistinguishable, they cause interference. A quantum key can be arranged through choosing the related phase shifts at Alice's and Bob's parts [6].

Therefore, understanding of double Mach-Zehnder interferometer set-up scheme and phase coding quantum cryptography based on double Mach-Zehnder interferometer is very important, which are introduced shortly. CD and PMD occurs in dispersive media, i.e. single-mode optical fibers in our case, which are necessary for connection between interferometers. Their inner and outer structure and effects in quantum channel cause CD and PMD, which limit information transfer in quantum channel for phase coding, are given.

General meaning of dispersion and 5 kinds of dispersions have been introduced. Chromatic dispersion consists of two of them, waveguide and material dispersion. Polarization mode dispersion is also one of them. PMD and CD have been presented in detail, others have been presented by brief calculations and figures. To learn PMD, learning the term of polarization (of light) would be very useful, which has also been presented as a motivation for PMD. DGD, 1st and 2nd order PMD have been demonstrated.

To investigate interactions, differences, common components between PMD and CD would have been very useful to compare their impacts in quantum cryptography which have been done in this work.

Before exhibiting simulations, some calculations as a background have been studied with elementary parameters $\sigma, \lambda_0, D_{PMD}, D_{\lambda_0}, \kappa, \varepsilon$, which are also elementary for simulations in our GUI application. Most of calculations originate from Gaussian wave packet description. After calculations, several examples of simulations of CD and PMD in phase coding quantum cryptography have been released. Simulations rely on 4 possible cases: Spectra with PMD and with CD, spectra with PMD and without CD, spectra without PMD and with CD, spectra without PMD and without CD. Spectra have belonged to wavelength and position distribution mostly, and rarely to intensities. It has been demonstrated that without or with least values of PMD and CD coefficients, it is possible to make interferences and apply phase coding for quantum cryptography. In opposite, with high values of PMD and CD coefficients, no interference or very low amount of interference occurs.

In the Appendix part, source code of GUI application for these simulations have been released, to benefit from this work thoroughly.

Appendix: Main Parts of MATLAB GUI Source Code

```
                    ....................................

% Main figure within all components.

fh=figure('Position',[5 35 1273 700],...
    'numbertitle','off',...
    'MenuBar','none',...
    'Color',[0.6 0.6 0.5],...
    'name','Measuring with Interferometer');

axis off;

                    ....................................

% Body of the first slider (Lambda Null) along with its components.
sh1=uicontrol(fh,'Style','slider',...
    'Max',1550,'Min',870,'Value',1312,...
    'SliderStep',[0.05 0.2],...
    'Position',[15 585 15 70],...
    'BackgroundColor','white',...
    'Callback',@slider1_callback);

eth1=uicontrol(fh,'Style','edit',...
    'String',num2str(get(sh1,'Value')),...
    'Fontsize',7,...
    'Position',[5 660 50 15],...
    'Callback',@edittext1_callback);

parameter1=text('units','inch',...
    'position',[-1.63 6.32], ...
    'fontsize',10,...
    'interpreter','latex',...
    'color',[0.6 0 0],...
    'string',['$$\lambda_{0}[nm]$$']);

number_errors1=0;

                    ....................................


% Callback for the first slider
function slider1_callback(hObject,eventdata)
    set(eth1,'String',...
        num2str(get(hObject,'Value')));
end

                    ....................................
```

```
%Callback for the first text edition
function edittext1_callback(hObject,eventdata)
val1=str2double(get(hObject,'String'));
%If the value entered into the text box
%is between the min and max values of the slider,
%set the new value of the slider.
if isnumeric(val1)&&length(val1)==1&&...
        val1>=get(sh1,'Min')&&...
        val1<=get(sh1,'Max')
    set(sh1,'Value',val1);
else
    %If any incorrect input has occurred,
    %then increase 1 the error timer.
    number_errors1=number_errors1+1;
    set(hObject,'String',...
        ['Total number of incorrect inputs=',...
        num2str(number_errors1)]);
end
end
```

.....

```
% GUI Axes


ah1 = axes('Parent',fh,'units','pixels',...
           'Position',[40 50 375 350]);


set(get(ah1,'Title'),'String','Wavelength Distribution','fontsize',16)


ah2 = axes('Parent',fh,'units','pixels',...
           'Position',[460 50 375 350]);

set(get(ah2,'Title'),'String','Position Distribution','fontsize',16)

ah3 = axes('Parent',fh,'units','pixels',...
           'Position',[880 50 375 350]);

set(get(ah3,'Title'),'String','Intensity','fontsize',16)


% First push button for output o
bh1 = uicontrol(fh,'Position',[665 610 75 40],...
                'String','Output o',...
                'BackgroundColor','b',...
                'Callback',@button1_plot);
```

.....

```
% Get user input from number parameter entries.
% Calculations and substitutions of abovementioned parameters
% based on formulations.

% lambda null
lmb_0=str2double(get(eth1,'String'))*1E-9;

% mean Wavenumber k0 with [1/m]
k0=2*pi/lmb_0;

% Amplitude Sigma
sgm=str2double(get(eth2,'String'));
s2=sgm^2;

% k-coordinate - Variable  = k
k=k0*(1-3.5*sgm):k0*sgm/5000:k0*(1+3.5*sgm);
lambda_nm=1E9*2*pi./k;

% CD Coefficient
cd=str2double(get(eth4,'String'));

% c0 light velocity, c0=300000 km/s= 300000 nm/ps
c0=300000;

% kpp(=kappa) is the parameter for the CD, shaped according to CD
% coefficient cd
kpp=-(c0*lmb_0^2*cd)/4*pi;

%PMD Coefficient
pmd=str2double(get(eth3,'String'));

% eps(=epsilon) is the parameter for the pmd, shaped according to pmd
% coefficient
eps=(c0*lmb_0*pmd)/4*pi;

% Phase shift delta c
del_c=str2double(get(eth5,'String'));

% Phase shift delta d
del_d=str2double(get(eth6,'String'));

% Phase shift delta g
del_g=str2double(get(eth7,'String'));

% Phase shift delta m
del_m=str2double(get(eth8,'String'));

% Phase shift delta n
del_n=str2double(get(eth9,'String'));

% Phase shifts delta parameters
   lc=str2double(get(eth10,'String')); % length of arm c
   ld=str2double(get(eth11,'String')); % length of arm d
   lg=str2double(get(eth12,'String')); % length of arm g
   lm=str2double(get(eth13,'String')); % length of arm m
   ln=str2double(get(eth14,'String')); % length of arm n
```

```
    tc=str2double(get(eth15,'String')); % Transmission Coefficient c
    td=str2double(get(eth16,'String')); % Transmission Coefficient d
    tg=str2double(get(eth17,'String')); % Transmission Coefficient g
    tm=str2double(get(eth18,'String')); % Transmission Coefficient m
    tn=str2double(get(eth19,'String')); % Transmission Coefficient n



% Amplitude Sigma
sigma=get(sh2,'Value');
s2=sigma^2;

% k-coordinate - Variable  = k
k=k0*(1-3.5*sigma):k0*sigma/5000:k0*(1+3.5*sigma);
sh1=1E9*2*pi./k;

% Group index N_0

N_0=1.500


% Test : PMD=0
    eps2=0;


% kappacm corresponds to \delta_{cm} in the manual
    % calculations kappacm=kpp*(lg+lc+lm);
    pmdcm=sqrt((kpp*(lg+lc+lm))^2+(eps2)*(lg+lc+lm)/s2);
    pmdcn=sqrt((kpp*(lg+lc+ln))^2+(eps2)*(lg+lc+ln)/s2);
    pmddm=sqrt((kpp*(lg+ld+lm))^2+(eps2)*(lg+ld+lm)/s2);
    pmddn=sqrt((kpp*(lg+ld+ln))^2+(eps2)*(lg+ld+ln)/s2);


% Description as above
    % kappacn=kpp*(lg+lc+ln);
    gammacn=1+16*k0^4*s2^2*pmdcn^2;
    X0cn=del_g+del_c+del_n+N_0*(lg+lc+ln)+2*k0*pmdcn;




% X0cm for Calculation of domain X
    %X0cm=del_g+del_c+del_m+a*(lg+lc+lm)+2*k0*pmdcm;
    X0cm=del_g+del_c+del_m+N_0*(lg+lc+lm)+2*k0*pmdcm;


% kappadm=kpp*(lg+ld+lm);
gammadm=1+16*k0^4*s2^2*pmddm^2;
X0dm=del_g+del_d+del_m+N_0*(lg+ld+lm)+2*k0*pmddm;

% kappadn=kpp*(lg+ld+ln);
gammadn=1+16*k0^4*s2^2*pmddn^2;
X0dn=del_g+del_d+del_n+N_0*(lg+ld+ln)+2*k0*pmddn;


% gammacm corresponds to \gamma_{cm} in the manual calculations
gammacm=1+16*k0^4*s2^2*pmdcm^2;
```

```
% Determination of domain X
% The distance of X0 fell away is sqrt(gamma*log(sqrt(1000)))/(k0*sigma) in
% that of the exponent on 1/1000.
X=min([X0cm X0cn X0dm X0dn])...
-sqrt(min([gammacm gammacn gammadm gammadn])*log(sqrt(1000)))...
/(k0*sigma):((max([X0cm X0cn X0dm X0dn])...
+sqrt(max([gammacm gammacn gammadm gammadn])*log(sqrt(1000)))...
/(k0*sigma))-(min([X0cm X0cn X0dm X0dn])...
-sqrt(min([gammacm gammacn gammadm gammadn])*log(sqrt(1000)))...
/(k0*sigma)))/length(k):max([X0cm X0cn X0dm X0dn])...
+sqrt(max([gammacm gammacn gammadm gammadn])*log(sqrt(1000)))...
/(k0*sigma)*(1-1/length(k));

% Calculations:
    %
    % IMPULSE-Function alphao2=|\alpha_{o}(k)|^{2} and alphap2=|\alpha_{p}(k)|
^{2}
    % for 2 MZ with 1 input and with dispersion:
    %
    % Input Interferometer A
    %
    % Profactor
    c_alpha=(2*pi*k0^2*s2)^(-1/4);
    % Impulse distribution in the Input a in the first Mach Zehnder
    alphaInputA=c_alpha*exp(-(k/k0-1).^2/(4*s2));
    %alphaInputA2=c_alpha^2*exp(-(k/k0-1).^2/(2*s2));

    % Input Interferometer B
    %
    % Impulse distribution in Input g in the second MZ
    % of PMD extended dispersion (dependent on each fiber's square root
length!):
    % Therefore instead pmd*lg written now as (eps2 in [m^3]),
    % with eps1, to the parameter for the polarisation  mode dispersion,
    % total dispersion: pmdlx=sqrt((pmd*lx)^22 + (eps1**2)*lx/s2) ... Band T/122
    %
    %*****************************
    %
    % Input parameter for the PMD in [m^3/2]:
    %
    % epssquared has dimension [m^3]
    %
    epsquadrat=13.69*10^(-27);
    % Test : exaggerated big PMD:
    %eps2=epsquared*10^(35);
    %eps2=epsquared;
    %
    %
    %*****************************
    %
    %
```

```
% PMD effects in the interferometer arms
pmdlg=sqrt((kpp*lg)^2+(eps2)*lg/s2);
pmdld=sqrt((kpp*ld)^2+(eps2)*ld/s2);
pmdlc=sqrt((kpp*lc)^2+(eps2)*lc/s2);
pmdlm=sqrt((kpp*lm)^2+(eps2)*lm/s2);
pmdln=sqrt((kpp*ln)^2+(eps2)*ln/s2);
%
alphaInputB=(1/2)*sqrt(tg)*exp(-i*k.*(del_g+N_0*lg)...
-i*k.^2*pmdlg).*alphaInputA.*(sqrt(td)*exp(-i*k.*(del_d+N_0*ld)...
-i*k.^2*pmdld)-sqrt(tc)*exp(-i*k.*(del_c+N_0*lc)-i*k.^2*del_c));
%alphaInputB=(1/2)*sqrt(tg)*exp(-i*k.*(del_g+N_0*lg)
%-i*k.^2*kpp*lg).*alphaInputA.*(sqrt(td)*exp(-i*k.*(del_d+N_0*ld)
%-i*k.^2*kpp*ld)-sqrt(tc)*exp(-i*k.*(del_c+N_0*lc)-i*k.^2*kpp*lc));
%
% Impulse distribution at output h from the 1st MZ
alphah=(1/2)*alphaInputA.*(sqrt(td)*exp(-i*k.*(del_d+N_0*ld)...
-i*k.^2*pmdld)+sqrt(tc)*exp(-i*k.*(del_c+N_0*lc)-i*k.^2*pmdlc));
alphah2=conj(alphah).*alphah;


% Output Interferometer B
%
% Impulse distribution at output o from the 2nd MZ
alphao=(1/2)*alphaInputB.*(sqrt(tm)*exp(-i*k*(del_m+N_0*lm)...
-i*k.^2*pmdlm)-sqrt(tn)*exp(-i*k*(del_n+N_0*ln)-i*k.^2*pmdln));
% Squared value of impulse function at output o
alphao2=conj(alphao).*alphao;
% Impulse distribution at output p from the 2nd MZ
alphap=(1/2)*alphaInputB.*(sqrt(tm)*exp(-i*k*(del_m+N_0*lm)...
-i*k.^2*pmdlm)+sqrt(tn)*exp(-i*k*(del_n+N_0*ln)-i*k.^2*pmdln));
% Squared value of impulse function at output p
alphap2=conj(alphap).*alphap;

% Position function psio2=|\psi_{o}(X)|^{2} und psip2=|\psi_{p}(X)|^{2}
% for 2 MZ with 1 input und with dispersion:
%
% Output interferometer B
%
% Profactor
c_psi=sqrt(tg)*c_alpha/(4*sqrt(2*pi));

% Factors for compact script
%
%



% kappad=kpp*(ld);
gammad=1+16*k0^4*s2^2*pmdld^2;
X0d=del_d+N_0*ld+2*k0*pmdld;

% kappac=kpp*(lc);
gammac=1+16*k0^4*s2^2*pmdlc^2;
X0c=del_c+N_0*lc+2*k0*pmdlc;

% xcm corresponds to x'_{cm} in the manual calculations
xcm=X-(del_g+del_c+del_m+N_0*(lg+lc+lm));

% argumentcm corresponds to z_{cm}-arg_{cm} in the manual calculations
argumentcm=(k0*xcm+4*k0^4*s2^2*pmdcm*xcm.^2-k0^2*pmdcm)/gammacm-
atan(pmdcm*4*k0^2*s2)/2;
```

```
    % Fourier-Transformed cm-component of the Impulse function
    Jcm=sqrt(tc*tm*4*pi*k0^2*s2/sqrt(gammacm)).*exp(-k0^2*s2/gammacm*(xcm-
2*pmdcm*k0).^2).*(cos(argumentcm)+i*sin(argumentcm));

    % Description as above
    xcn=X-(del_g+del_c+del_n+N_0*(lg+lc+ln));
    argumentcn=(k0*xcn+4*k0^4*s2^2*pmdcn*xcn.^2-k0^2*pmdcn)/gammacn-
atan(pmdcn*4*k0^2*s2)/2;
    Jcn=sqrt(tc*tn*4*pi*k0^2*s2/sqrt(gammacn)).*exp(-k0^2*s2/gammacn*(xcn-
2*pmdcn*k0).^2).*(cos(argumentcn)+i*sin(argumentcn));

    xdm=X-(del_g+del_d+del_m+N_0*(lg+ld+lm));
    argumentdm=(k0*xdm+4*k0^4*s2^2*pmddm*xdm.^2-k0^2*pmddm)/gammadm-
atan(pmddm*4*k0^2*s2)/2;
    Jdm=sqrt(td*tm*4*pi*k0^2*s2/sqrt(gammadm)).*exp(-k0^2*s2/gammadm*(xdm-
2*pmddm*k0).^2).*(cos(argumentdm)+i*sin(argumentdm));

    xdn=X-(del_g+del_d+del_n+N_0*(lg+ld+ln));
    argumentdn=(k0*xdn+4*k0^4*s2^2*pmddn*xdn.^2-k0^2*pmddn)/gammadn-
atan(pmddn*4*k0^2*s2)/2;
    Jdn=sqrt(td*tn*4*pi*k0^2*s2/sqrt(gammadn)).*exp(-k0^2*s2/gammadn*(xdn-
2*pmddn*k0).^2).*(cos(argumentdn)+i*sin(argumentdn));

    xd=X-(del_d+N_0*ld);
    argumentd=(k0*xd+4*k0^4*s2^2*pmdld*xd.^2-k0^2*pmdld)/gammad-
atan(pmdld*4*k0^2*s2)/2;
    Jd=sqrt(td*4*pi*k0^2*s2/sqrt(gammad)).*exp(-k0^2*s2/gammad*(xd-
2*pmdld*k0).^2).*(cos(argumentd)+i*sin(argumentd));

    xc=X-(del_c+N_0*lc);
    argumentc=(k0*xc+4*k0^4*s2^2*pmdlc*xc.^2-k0^2*pmdlc)/gammac-
atan(pmdlc*4*k0^2*s2)/2;
    Jc=sqrt(tc*4*pi*k0^2*s2/sqrt(gammac)).*exp(-k0^2*s2/gammac*(xc-
2*pmdlc*k0).^2).*(cos(argumentc)+i*sin(argumentc));

    % Squared value of the Input-Position function
    % psia2=sqrt(2*k0^2*s2/pi).*exp(-2*k0^2*s2*X.^2);

    % Squared value of the position function at the output h
    psih2=c_alpha^2/(8*pi)*(conj(Jd).*Jd + conj(Jc).*Jc + 2*(real(Jd).*real(Jc)
+imag(Jd).*imag(Jc)));

    % Squared value of the position function at the output o
    psio2=c_psi^2*(conj(Jcm).*Jcm + conj(Jcn).*Jcn + conj(Jdm).*Jdm +
conj(Jdn).*Jdn + ...
        2*(-(real(Jcm).*real(Jcn)+imag(Jcm).*imag(Jcn)) -...
% interference term
        (real(Jcm).*real(Jdm)+imag(Jcm).*imag(Jdm)) +...
% interference term
        (real(Jcm).*real(Jdn)+imag(Jcm).*imag(Jdn)) +...
% interference term
        (real(Jcn).*real(Jdm)+imag(Jcn).*imag(Jdm)) -...
% interference term
        (real(Jcn).*real(Jdn)+imag(Jcn).*imag(Jdn)) -...
% interference term
        (real(Jdm).*real(Jdn)+imag(Jdm).*imag(Jdn))));
% interference term

    % Squared value of the position function at the output p
    psip2=c_psi^2*(conj(Jcm).*Jcm + conj(Jcn).*Jcn + conj(Jdm).*Jdm +
conj(Jdn).*Jdn + ...
        2*((real(Jcm).*real(Jcn)+imag(Jcm).*imag(Jcn)) -...
% interference term
        (real(Jcm).*real(Jdm)+imag(Jcm).*imag(Jdm)) -...
```

```
% interference term
        (real(Jcm).*real(Jdn)+imag(Jcm).*imag(Jdn)) -...
% interference term
        (real(Jcn).*real(Jdm)+imag(Jcn).*imag(Jdm)) -...
% interference term
        (real(Jcn).*real(Jdn)+imag(Jcn).*imag(Jdn)) +...
% interference term
        (real(Jdm).*real(Jdn)+imag(Jdm).*imag(Jdn))));
% interference term

    % Calculation of the intensities I_{o} and I_{p} of the impulse functionen
    %
    delAdc=0:pi/k0*10^-2:10*2*pi/k0;%del_d-del_c+N_0*(ld-lc);%

    %delBdc=b*(ld-lc);%-1E-12:1E-16:0;%
    delBpmddc=sqrt((kpp*(ld-lc))^2+(eps2)*abs(ld-lc)/s2);%-1E-12:1E-16:0;%
    delAmn=del_m-del_n+N_0*(lm-ln);

    %delBmn=b*(lm-ln);
    delBpmdmn=sqrt((kpp*(lm-ln))^2+(eps2)*abs(lm-ln)/s2);

    % Interference term for the arms c und d
    IFTdc=sqrt(tc*td)./(2*(1+4*k0^4*s2^2*delBpmddc.^2).^(1/4)...
        ).*exp((-k0^2*s2/2*(delAdc+2*k0*delBpmddc).^2)./(1+...
        4*k0^4*s2^2*delBpmddc.^2)).*cos(atan(2*k0^2*s2*delBpmddc...
        )/2-(k0^4*s2^2*delBpmddc.*delAdc.^2-k0^2*delBpmddc-...
        k0*delAdc)./(1+4*k0^4*s2^2*delBpmddc.^2));

    % Intensity of the impulse function in output g
    Ig=tg*(td+tc)/4-IFTdc;

    % Intensity of the impulse function in output h
    Ih=(td+tc)/4+IFTdc;


    % Interference term for the arms m und n
    IFTmn=sqrt(tm*tn)./(2*(1+4*k0^4*s2^2*delBpmdmn.^2).^(1/4)).*exp((...
        -k0^2*s2/2*(delAmn+2*k0*delBpmdmn).^2)./(1+...
        4*k0^4*s2^2*delBpmdmn.^2)).*cos(atan(2*k0^2*s2*delBpmdmn)...
        /2-(k0^4*s2^2*delBpmdmn.*delAmn.^2-k0^2*delBpmdmn-k0*delAmn)./...
       (1+4*k0^4*s2^2*delBpmdmn.^2));

   % Interference terms  only for cd + mn as above
       IFTdcmn1=sqrt(td*tc*tm*tn)./(2*(1+4*k0^4*s2^2*(delBpmddc+...
        delBpmdmn).^2).^(1/4)).*exp((-k0^2*s2/2*((delAdc+delAmn)
+2*k0*(delBpmddc+...
        delBpmdmn)).^2)./(1+4*k0^4*s2^2*(delBpmddc+delBpmdmn).^2)).*cos(...
        atan(2*k0^2*s2*(delBpmddc+delBpmdmn))/2-(k0^4*s2^2*(delBpmddc+...
        delBpmdmn).*(delAdc+delAmn).^2-k0^2*(delBpmddc+delBpmdmn)...
        -k0*(delAdc+delAmn))./(1+4*k0^4*s2^2*(delBpmddc+delBpmdmn).^2));

% Interference terms  only for cd - mn as above
IFTdcmn2=sqrt(td*tc*tm*tn)./(2*(1+4*k0^4*s2^2*(delBpmddc-delBpmdmn).^2).^(...
1/4)).*exp((-k0^2*s2/2*((delAdc-delAmn)+2*k0*(delBpmddc-delBpmdmn)).^...
2)./(1+4*k0^4*s2^2*(delBpmddc-delBpmdmn).^2)).*cos(atan(...
2*k0^2*s2*(delBpmddc-delBpmdmn))/2-(k0^4*s2^2*(delBpmddc-...
delBpmdmn).*(delAdc-delAmn).^2-k0^2*(delBpmddc-delBpmdmn)-...
k0*(delAdc-delAmn))./(1+4*k0^4*s2^2*(delBpmddc-delBpmdmn).^2));

% Intensity of the impulse function in output o
Io=tg/4*((td+tc)*(tm+tn)/4-(td+tc)*IFTmn-(tm+tn)*IFTdc+(IFTdcmn1+IFTdcmn2));
% Intensity of the impulse function in output p
Ip=tg/4*((td+tc)*(tm+tn)/4+(td+tc)*IFTmn-(tm+tn)*IFTdc-(IFTdcmn1+IFTdcmn2));
```

```
% Plots for output o
function button1_plot(hObject,eventdata)



% Plot Wavelength distribution of output o
plot(ah1,lambda_nm,alphao2,'--b','LineWidth',2);

% Plot Position distribution of output o
plot(ah2,X,psio2,'--b','LineWidth',2);

% Plot Intensity output o
plot(ah3,delAdc,Io,'--b','LineWidth',2);

set(get(ah1,'Title'),'String','Wavelength Distribution','fontsize',16)
set(get(ah2,'Title'),'String','Position Distribution','fontsize',16)
set(get(ah3,'Title'),'String','Intensity','fontsize',16)



end


end
```

Bibliography

[1] K. C. Kao and G. A. Hockham, Dielectric-fiber surface waveguides for optical frequencies, Proc. Inst. Elect. Eng., **113**, 1151-1158 (1966)

[2] Kasap, S.O., Optoelectronics and Photonics. New Jersey: Prentice-Hall, Inc. (2001)

[3] N. Gisin, G. Ribordy, W. Tittel, H. Zbinden, Rev. Mod. Phys. **74**, 158 (2002)

[4] B.E.A. Saleh, M.C. Teich, Fundamentals of Photonics, John Wiley & Sons, Inc., ISBN 0-471-83965-5, (1991)

[5] M. Suda, Quantum Interferometry in Phase Space, 1st edn. (Springer-Verlag, Berlin, Heidelberg, New York, 2006)

[6] M. Suda, T. Herbst, A. Poppe, Eur. Phys. J., D **42**, 139-145 (2007)

[7] D. Eberlein, Messverfahren für optische Netze, Funkschau,**22/97**, 50ff, (1998)

[8] E.-G. Neumann, Single-Mode Fibers: Fundamentals, Springer Series in Optical Sciences, 57, Springer, Berlin, (1988)

[9] P. G. Doyle, J. L. Snell, Random walks and electric networks, Carus Mathematical Monographs, **22**, Mathematical Association of America,MR92081,ISBN 978-0-88385-024-4, (1984)

[10]J. N. Damask, Polarization Optics in Telecommunications, Springer, New York, (2004)

[11] Allen, Christopher, P. K. Kondamuri, D. L. Richards, D. C. Hague. “Analysis and Comparison of Measured DGD Data on Buried Single-Mode Fibers.” Symposium on Optical Fiber Measurements, Boulder, CO, **195-198**, (Sept. 24-26, 2002)

[12] N. Gisin, J. P. Pellaux, J. P. Von Der Weid, Symposium on Optical Fiber Measurements, pp 119-122, 1990

[13] N. Gisin, J. P. Pellaux, J. P. Von Der Weid, J. Lightwave Tech. **9**, 821, 1991

[14] Y. Namihira et. al., J. Lightwave Tech. **1**, 329, 1989

[15] Y. Namihira et. al., J. Optical Communication **12**, 1-8, 1991

[16] Li Xu, Polarization Mode Dispersion Analysis Via Spectral Polarimetry and High-Order Correlations, PhD Thesis, Purdue University, W. Lafeyette, Indiana, (August 2006)

[17] H. Büllow, System outage probability due to first- and second-order PMD, IEEE Photon. Technol. Lett., **10**, 696-698 (1998)

[18] G. J. Foschini, L. E. Nelson, R. M. Jopson, H. Kogelnik, Statistics of second-order PMD depolarization, J. Lightwave Tech. **19**, 1882-1886 (2001)

[19] H. Miao, C. Yang, Scheme for feed-forward polarization mode dispersion compensation, App. Optics, **43/7**, 1577-1582 (2004)

[20] http://www.porta-optica.org, Chromatic Dispersion, Information Society and Media.